

# ROLE OF PEROXISOMES IN PHYSIOLOGY AND PATHOLOGY OF OSSIFICATION AND BONE METABOLISM

GUOFENG QIAN



INAUGURAL DISSERTATION  
submitted to the Faculty of Medicine  
in partial fulfillment of the requirements  
for the PhD-degree  
of the Faculties of Veterinary Medicine and Medicine  
of the Justus Liebig University Giessen



*édition scientifique*  
**VVB LAUFERSWEILER VERLAG**

**Das Werk ist in allen seinen Teilen urheberrechtlich geschützt.**

Jede Verwertung ist ohne schriftliche Zustimmung des Autors oder des Verlages unzulässig. Das gilt insbesondere für Vervielfältigungen, Übersetzungen, Mikroverfilmungen und die Einspeicherung in und Verarbeitung durch elektronische Systeme.

1. Auflage 2010

All rights reserved. No part of this publication may be reproduced, stored in a retrieval system, or transmitted, in any form or by any means, electronic, mechanical, photocopying, recording, or otherwise, without the prior written permission of the Author or the Publishers.

1<sup>st</sup> Edition 2010

© 2010 by VVB LAUFERSWEILER VERLAG, Giessen  
Printed in Germany



*édition scientifique*  
**VVB LAUFERSWEILER VERLAG**

STAUFENBERGRING 15, D-35396 GIESSEN  
Tel: 0641-5599888 Fax: 0641-5599890  
email: [redaktion@doktorverlag.de](mailto:redaktion@doktorverlag.de)

[www.doktorverlag.de](http://www.doktorverlag.de)

# **Role of peroxisomes in physiology and pathology of ossification and bone metabolism**

Inaugural Dissertation  
submitted to  
the Faculty of Medicine  
in partial fulfillment of the requirements  
for the PhD-degree  
of the Faculties of Veterinary Medicine and Medicine  
of the Justus Liebig University Giessen

By  
**Qian, Guofeng**  
of  
Zhejiang, China

Giessen 2010

From the Institute for Anatomy and Cell Biology II  
of the Faculty of Medicine of the Justus Liebig University of Giessen  
Director / Chairperson: Prof. Dr. Eveline Baumgart-Vogt

First Supervisor and Committee Member: Prof. Dr. Eveline Baumgart-Vogt

Second Supervisor and Committee Member: Prof. Dr. Kalervo Hiltunen (Oulu)

Examination chair and Committee Member: Prof. Dr. Klaus T. Preissner

Committee Member: Prof. Dr. Martin Bergmann

## **Declaration**

"I declare that I have completed this dissertation single-handedly without the unauthorized help of a second party and only with the assistance acknowledged therein. I have appropriately acknowledged and referenced all text passages that are derived literally from or are based on the content of published or unpublished work of others, and all information that relates to verbal communications. I have abided by the principles of good scientific conduct laid down in the charter of the Justus Liebig University of Giessen in carrying out the investigations described in the dissertation."

Date: 20<sup>th</sup> December 2010

Place: Giessen, Germany

Guofeng Qian

# Table of contents

1	Introduction .....	1
1.1	Discovery of peroxisomes .....	1
1.2	Biogenesis of peroxisomes .....	2
1.2.1	Peroxisomal matrix import .....	2
1.2.2	Peroxisomal membrane import .....	4
1.2.3	Peroxisome growth and division .....	5
1.3	Metabolic functions of peroxisomes .....	7
1.3.1	Peroxisomal $\beta$ -oxidation of fatty acids and fatty acid derivatives .....	7
1.3.2	Biosynthesis of etherphospholipids and cholesterol in peroxisomes... 10	
1.3.2.1	Etherphospholipid synthesis .....	10
1.3.2.2	Cholesterol synthesis .....	11
1.3.3	Metabolism of reactive oxygen and nitrogen species (ROS and RNS) in peroxisomes..... 11	
1.4	Peroxisomal disorders .....	14
1.5	Animal models for peroxisomal biogenesis disorders (PEX2, PEX5, PEX7, PEX11 $\beta$ and PEX13 knockout mice)..... 16	
1.5.1	Animal models for Zellweger syndrome .....	16
1.5.2	The animal model for Rhizomelic chondrodysplasia punctata .....	17
1.6	Bone, Cartilage and Ossification .....	17
1.7	Signaling pathways involved in bone metabolism .....	19
1.7.1	Wnt signaling and bone .....	19
1.7.2	ROS metabolism and bone .....	21
1.7.3	Nuclear receptor signaling and bone .....	22
1.8	Peroxisomes in the skeleton .....	23
2	Aims of this study .....	24
3	Materials and Methods .....	26
3.1	Materials .....	26
3.1.1	Experimental animals .....	26
3.1.2	Laboratory instruments .....	27
3.1.3	General materials and culture media .....	28
3.1.4	Proteins and enzymes..... 28	
3.1.5	Chemicals and drugs .....	29
3.1.6	Kits..... 30	
3.1.7	Buffers and solutions .....	30
3.1.8	Primers .....	32
3.1.9	Antibodies .....	32

3.2 Methods.....	36
3.2.1 Alcian Blue/Alizarin Red staining of cartilage and bone in mice .....	36
3.2.2 Scanning of wildtype and PEX11 $\beta$ KO mice with flat-panel volumetric computed tomography.....	36
3.2.2.1 FpvCT and Scan Parameters .....	36
3.2.2.2 Calibration device.....	37
3.2.2.3 Image reconstruction.....	38
3.2.2.4 Image visualization .....	39
3.2.3 Perfusion fixation of mice and processing of mouse tissues for paraffin embedding and sectioning.....	39
3.2.4 Indirect immunofluorescence on bone or cartilage sections .....	41
3.2.5 Isolation and culture of primary osteoblasts.....	41
3.2.6 Treatments with PPAR agonists and antagonists in osteoblasts .....	43
3.2.7 Indirect immunofluorescence on primary osteoblasts .....	43
3.2.8 Analysis of peroxisome abundance in osteoblasts .....	44
3.2.9 Analysis of proliferation activity of osteoblasts at different time points .....	45
3.2.10 Mineralization analysis .....	45
3.2.11 RNA expression analysis by semiquantitative RT-PCR .....	46
3.2.11.1 RNA isolation .....	46
3.2.11.2 DNase I digestion .....	46
3.2.11.3 Reverse transcription .....	47
3.2.11.4 Primer design.....	47
3.2.12 Western Blot analysis .....	48
3.2.12.1 Isolation of proteins from osteoblasts .....	48
3.2.12.1.1 Isolation of whole cell lysates from osteoblasts .....	48
3.2.12.1.2 Isolation of nuclear proteins from osteoblasts .....	49
3.2.12.1.3 Isolation of enriched peroxisomal fractions from osteoblasts .....	49
3.2.12.2 Preparation of Western blots .....	50
3.2.13 Statistical Analysis .....	51
<b>4 Results .....</b>	<b>52</b>
4.1 Characterization of the peroxisomal compartment in cartilage and bone.....	52
4.1.1 Peroxisomes are present with heterogeneous abundance in different cell types of the skeleton .....	52
4.1.2 Matrix proteins for ROS and lipid metabolism also exhibit a heterogeneous distribution in peroxisomes of cartilage and bone .....	53

4.1.3 Peroxisome numerical abundance is inverse proportional to osteoblast proliferation and parallels osteoblast differentiation.....	56
4.1.4 The heterogeneity of the peroxisome compartment is preserved during osteoblast differentiation.....	60
4.1.5 Both PPAR $\alpha$ and PPAR $\gamma$ are involved in regulating peroxisomal functions in osteoblasts.....	66
<b>4.2 Effect of PEX11<math>\beta</math> deficiency on the skeleton, osteoblast maturation and function .....</b>	<b>70</b>
4.2.1 Mice with deficient peroxisome proliferation exhibit ossification defects and growth retardation .....	70
4.2.2 PEX11 $\beta$ KO mice exhibit substantially lower bone volume and mass .	71
4.2.3 Histological analysis revealed reduced ossification and mineralization in PEX11 $\beta$ KO mice.....	73
4.2.4 The peroxisomal numerical abundance is reduced and the protein composition altered in PEX11 $\beta$ KO mice.....	76
4.2.5 Osteoblast- secretory proteins are reduced in primary osteoblast cultures of PEX11 $\beta$ KO mice.....	79
4.2.6 In addition to catalase also other antioxidant enzymes were enhanced in PEX11 $\beta$ KO mice.....	81
4.2.7 PEX11 $\beta$ deficiency diminished Canonical Wnt signaling activity and increased PPAR $\gamma$ abundance .....	84
<b>5 Discussion .....</b>	<b>88</b>
5.1 Part 1.....	88
5.1.1 Peroxisomes are ubiquitous, however, heterogeneous in different cell types of the skeleton .....	88
5.1.2 The abundance of peroxisomal enzymes is differently affected by osteoblast maturation and seems to be regulated by PPAR $\alpha$ .....	91
5.1.3 Treatment with PPAR $\alpha$ or PPAR $\gamma$ agonists alters the enzyme composition of the peroxisomal compartment in osteoblasts.....	93
5.2 Part 2.....	95
5.2.1 Oxidative stress and lipid peroxidation might contribute to the impairment of bone ossification in PEX11 $\beta$ KO mice .....	96
<b>6 Summary .....</b>	<b>102</b>
<b>7 Zusammenfassung .....</b>	<b>104</b>
<b>8 References .....</b>	<b>106</b>
<b>9 Index of abbreviations.....</b>	<b>120</b>
<b>10 Acknowledgement .....</b>	<b>121</b>
<b>11 Curriculum Vitae .....</b>	<b>123</b>

# **1 Introduction**

## **1.1 Discovery of peroxisomes**

Peroxisomes were first described as “microbodies” by electron microscopy in proximal tubular epithelial cells of the mouse kidney and characterized as single membrane-bound organelles, containing a fine granular matrix (Rhodin, 1954). Later in 1956, these “microbodies” were also discovered in rat liver cells (Bernhard and Rouiller, 1956). After a decade, the separation of the distinct cell organelles by glycogen or sucrose-density gradient centrifugation in combination with morphological characterization of those fractions led to the identification of these “microbodies” as the cell organelles containing H<sub>2</sub>O<sub>2</sub>-producing oxidases and H<sub>2</sub>O<sub>2</sub>-degrading catalase (Baudhuin et al., 1965; Baudhuin et al., 1964). Therefore, De Duve coined the term “peroxisome” for this organelle (De Duve and Baudhuin, 1966), due to the functional involvement of most (at that time) known enzymes in hydrogen peroxide metabolism. A specific cytochemical staining for peroxisomes in light and electron microscopy was developed with the introduction of the alkaline 3, 3'- diaminobenzidine (DAB) reaction for catalase (Fahimi, 1968, 1969; Hirai, 1969; Novikoff and Goldfischer, 1969). Using this technique, Hruban and colleagues reported that peroxisomes are ubiquitous eukaryotic organelles (Hruban et al., 1972). Moreover, the absence of DAB-positive peroxisomes in patients with Zellweger syndrome - a devastating peroxisomal biogenesis disorder was noted by Goldfischer and colleagues (Goldfischer et al., 1973), further highlighting the specificity of DAB staining.

The important role of peroxisomes in lipid metabolism was revealed when the  $\beta$ -oxidation system for fatty acid degradation (Cooper and Beevers, 1969; Lazarow and De Duve, 1976) and the metabolic pathways for the biosynthesis of ether lipid and cholesterol (Hajra et al., 1979; Keller et al., 1985) were discovered in this organelle. In recent years, several other enzymes involved in scavenging ROS have also been described in these organelles, such as Cu/Zn-superoxide dismutase, Mn-superoxide dismutase, glutathione S-transferase and peroxiredoxin I and V (Antonenkov et al., 2009; Immenschuh and Baumgart-Vogt, 2005; Schrader and Fahimi, 2004). Furthermore, the involvement of peroxisomes in the regulation of lipid- and ROS- homeostasis is extensively discussed (Karnati and Baumgart-Vogt, 2008; Masters and Crane, 1984).

## ***1.2 Biogenesis of peroxisomes***

### ***1.2.1 Peroxisomal matrix import***

Peroxisomes contain no DNA or ribosomes and thus have no means to produce proteins. Therefore all of their proteins are synthesized on free ribosomes in the cytoplasm and are imported posttranslationally into the organelle (Lazarow and Fujiki, 1985). Two peroxisomal targeting signals (PTSs), PTS1 and PTS2 have been described, which are necessary for peroxisomal protein import (Eckert and Erdmann, 2003; Subramani, 1993). PTS1, is a carboxyl-terminal tripeptide with the consensus sequence (S/C/A) (K/R/H) (L/M) and targets proteins to the peroxisome in all eukaryotic organisms examined from yeast to man. PTS1-dependent protein import is mediated by a shuttling receptor, the peroxin Pex5p (see Fig1), that recognizes the PTS1 tripeptide in the cytoplasm and mediates the import of PTS1-containing proteins into the peroxisome (Dammai and

Subramani, 2001). Recent analysis of sequence variability in the PTS1 motif revealed that, in addition to the known C-terminal tripeptide, at least nine residues directly upstream are important for signal recognition in the PTS1-Pex5p receptor complex (Neuberger et al., 2003). A small subset of peroxisomal matrix proteins is targeted by the PTS2 motif, which consists of a degenerate nine-residue signal located internally or near the amino terminus. The consensus consequence for the PTS2 is: (R/K) (L/V/I) X5 (H/Q) (L/A) (Rachubinski and Subramani, 1995). The import of PTS2 proteins into peroxisomes is mediated by the hydrophilic cytoplasmic receptor Pex7p, which is also dependent on the long

isoform of Pex5p (Ghys et al., 2002; Mukai et al., 2002).

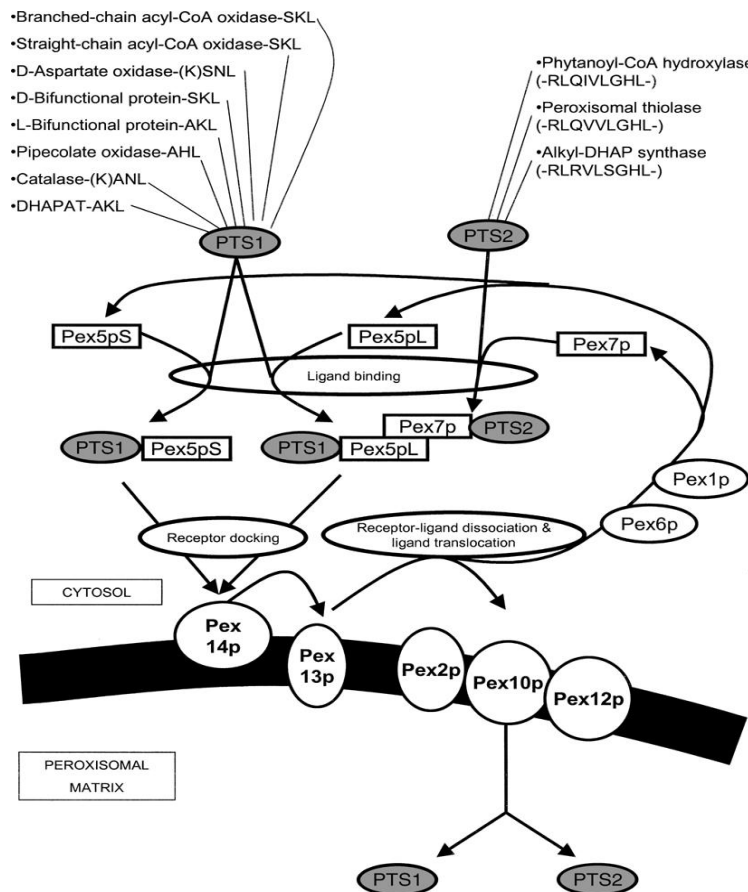


**Fig1.** The model of peroxisomal matrix import according to Wanders RJ (Wanders, 2004a). The short form of Pex5p (Pex5pS) is capable of targeting PTS1-proteins to the peroxisomal docking machinery. At the membrane, Pex14p is the first binding partner. In contrast, Pex5pL is needed for PTS2-import together with Pex7p as the PTS2-receptor. In the absence of Pex5pL, the Pex7p/PTS2-protein complex is unable to dock at the peroxisomal membrane. After binding of the receptor-cargo complex to Pex14p and subsequently to Pex13p, the complexes dissociate and the PTS1- and PTS2-proteins (cargo) translocate across the peroxisomal membrane, a process dependent on Pex2p, Pex10p, and Pex12p. The receptors Pex5pS, Pex5pL, and Pex7p recycle back to the cytoplasm. Pex1p and Pex6p are supposed to be involved in the latter process.

complexes dissociate and the PTS1- and PTS2-proteins (cargo) translocate across the peroxisomal membrane, a process dependent on Pex2p, Pex10p, and Pex12p. The receptors Pex5pS, Pex5pL, and Pex7p recycle back to the cytoplasm. Pex1p and Pex6p are supposed to be involved in the latter process.

Most of the identified peroxins (Pex proteins=Pex...p), the proteins involved in the biogenesis of peroxisomes, participate in the import of peroxisomal matrix proteins and contribute to the formation of the docking (such as Pex14p and Pex13p) and translocation machinery at the peroxisomal membranes (Sacksteder and Gould, 2000). It is assumed that the targeting receptors (e.g. Pex5p and Pex7p) accompany their cargo inside the peroxisomes and recycle back to the cytoplasm. Only few peroxins are involved in membrane biogenesis of the organelle (see 1.2.2) or in peroxisome division and proliferation (see 1.2.3). An overview on the machinery of peroxisomal matrix protein import is given in Fig 1.

### **1.2.2. Peroxisomal membrane import**

In most *pex* mutants (PEX5 and PEX13 knockout mice) (Baes et al., 1997; Maxwell et al., 2003), in which the import of PTS1 and PTS2 containing peroxisomal matrix proteins is abolished, peroxisomal membrane proteins (PMPs) can be found correctly inserted in peroxisomal membrane remnants, known as 'ghosts' (Santos et al., 1988). Thus, the import of peroxisomal membrane is independent from the import of matrix proteins (Gould et al., 1996; Santos et al., 1988).

So far, only three of the 32 peroxins identified (Pex3p, Pex16p and Pex19p) have been shown to be involved in peroxisomal membrane protein import. When any of these proteins are absent or mutated in cells, the peroxisomal ghosts disappear. Pex19p, a farnesylated protein, binds nascent PMPs in the cytoplasm and targets them to the peroxisomal membrane (Jones et al., 2004; Kashiwayama et al., 2005). Pex3p, an integral membrane protein, acts as a docking receptor for incoming complexes of Pex19p and its PMP cargoes (Fang et al., 2004; Ghaedi et al., 2000; Sacksteder et al., 2000). Pex16p is thought to

serve as a receptor for Pex3p or as a component of the membrane translocator (Fang et al., 2004; Honsho et al., 2002; Matsuzaki and Fujiki, 2008). However, to date it is not known how PMPs are exactly imported into peroxisomal membrane precursors. Heiland and Erdmann propose that this process might depend on the class of the PMP to be imported (Heiland and Erdmann, 2005). They suggest that at least two distinct classes of PMPs.

The first, class I PMPs, are synthesized on free ribosomes in the cytoplasm, where they are recognized by Pex19p that directs them to the peroxisomal membrane. The membrane association of the Pex19p receptor-cargo complex is mediated by Pex3p in the peroxisomal membrane precursors. However, how the insertion of peroxisomal membrane protein takes place still remains to be investigated.

Insertion of class II PMPs into the precursors is independent of Pex19p. Accumulating evidences suggest that class II PMPs might be targeted to the ER prior to their transport to peroxisomes (Heiland and Erdmann, 2005). But, how these proteins enter and leave the ER and their final destination in the peroxisome membrane is still unknown. Other authors also suggest that peroxisomal membrane might be synthesized *de novo* (Terlecky and Fransen, 2000).

### **1.2.3 Peroxisome growth and division**

Of the many PEX genes and products (peroxins) required for peroxisome biogenesis, only PEX11 has been shown to have a conserved role in peroxisome division (Erdmann and Blobel, 1995; Li et al., 2002a; Li and Gould, 2002; Marshall et al., 1995; Passreiter et al., 1998; Schrader et al., 1998). Overexpression of PEX11 promotes peroxisome elongation and subsequent

division, whereas loss of PEX11 results in reduced peroxisome abundance (Li et al., 2002b; Marshall et al., 1995; Schrader et al., 1998). These results indicate that PEX11 proteins may be implicated in the regulation of peroxisome growth in size and number and, thus, in peroxisomal division. Until now, three PEX11 genes in mammals have been identified and characterized, the PEX11 $\alpha$  gene, the PEX11 $\beta$  gene and the PEX11 $\gamma$  gene (Abe and Fujiki, 1998; Abe et al., 1998; Li et al., 2002a; Passreiter et al., 1998; Schrader et al., 1998). Studies in human and rat revealed that PEX11 $\beta$  has the ability to promote peroxisome proliferation in the absence of extracellular stimuli (Schrader et al., 1998). It was suggested that PEX11 $\alpha$  may regulate peroxisome abundance in response to extracellular stimuli, such as the peroxisome proliferator clofibrate and di-(2-ethylhexyl)-phthalate (Passreiter et al., 1998). However, Li and colleagues demonstrated that peroxisome proliferation occurs also in the liver of PEX11 $\alpha$  knockout mice after treatment with these drugs (Li et al., 2002a). PEX11 $\gamma$  differs from PEX11 $\alpha$  and PEX11 $\beta$  since its overexpression induces peroxisome clustering, but not peroxisome proliferation, and its expression is altered neither by classical peroxisome proliferators nor by the loss of PEX11 $\alpha$  or PEX11 $\beta$  (Li et al., 2002a).

Other proteins involved in peroxisome division are members of the dynamin family of large GTPases, which have been implicated in tubulation and fission events of cellular membranes (Danino and Hinshaw, 2001; McNiven, 1998). The dynamin-related protein Vps1p mediates peroxisome division in *S. cerevisiae* (Hoepfner et al., 2001). In contrast, the dynamin-like protein DLP1 has been shown to be required for peroxisome fission in mammalian cells (Koch et al., 2003; Li and Gould, 2003). In addition, Koch and co-workers showed that the expression of a dominant-negative DLP1 mutant deficient in GTP hydrolysis

(K38A) inhibited peroxisomal division (Koch et al., 2003). Li and Gould reported that one function of PEX11 $\beta$  is to recruit DLP1 to the peroxisome membrane, at sites where PEX11 $\beta$  itself is sequestered away from other peroxisomal membrane proteins (Li and Gould, 2003). It has been suggested that the role of DLP1 at this site may be to act as a 'pinchase' to release the daughter organelle. Recently, Koch and co-workers suggested that PEX11 $\beta$  should be involved in the elongation/tubulation of peroxisomes, whereas DLP1 should mediate peroxisome fission (Koch et al., 2004). However, this hypothesis is not supported by findings in the liver of PEX11 $\beta$  knockout mice, in which clusters of elongated tubular peroxisomes were described on the ultrastructural level (Li et al., 2002b). Therefore, the exact mechanism of peroxisome division is still an unresolved cell biological issue.

### ***1.3 Metabolic functions of peroxisomes***

#### ***1.3.1 Peroxisomal $\beta$ -oxidation of fatty acids and fatty acid derivatives***

The fatty acid  $\beta$ -oxidation system in peroxisomes was first discovered in plant cells (Cooper and Beevers, 1969) and thereafter in animal cells (Lazarow and De Duve, 1976). The peroxisomal fatty acid  $\beta$ -oxidation machinery resembles the one in mitochondria with exception of its first step, in which acyl-CoA oxidases are involved in peroxisomes in comparison to acyl-CoA dehydrogenases in mitochondria. Additionally, in contrast to mitochondria, peroxisomal  $\beta$ -oxidation has a much broader substrate specificity and oxidizes a range of fatty acids that cannot be metabolized in mitochondria. Peroxisomal substrates include very long-chain fatty acid (VLCFA), long branched chain and dicarboxylic fatty acids, eicosanoids (such as prostaglandins and leukotrienes), PUFAs involved in

signaling and apoptosis, and bile acid intermediates (Karnati and Baumgart-Vogt, 2008; Mannaerts and Van Veldhoven, 1993; Wanders, 2004b).

The four steps of peroxisomal  $\beta$ -oxidation for an acyl-CoA ester are: 1) oxidation to a 2-*trans*-enoyl-CoA compound, 2+3) hydration of the formed 2-*trans*-enoyl-CoA and dehydrogenation of 3-hydroxyacyl-CoA, and 4) thiolitic cleavage of the 3-oxoacyl-CoA. These steps are catalyzed by three different enzyme classes in peroxisomes: 1) acyl-CoA-oxidases, 2) multifunctional proteins and 3) thiolases.

Peroxisomes contain two different  $\beta$ -oxidation systems, pathway I comprising the enzymes acyl-CoA oxidase I, multifunctional protein 1 and thiolase A/B as well as pathway II comprising acyl-CoA oxidases (2+3), multifunctional protein 2 and the SCPx thiolase (Nenicu et al., 2007; Wanders, 2004b) (Fig2). The first acyl-CoA oxidase discovered was Palmitoyl-CoA oxidase, now called ACOX1, which is specific for straight-chain fatty acids (such as VLCFA) and eicosanoids (Baumgart et al., 1996). The two other acyl-CoA oxidases are respectively the trihydroxycoprostanoyl-CoA oxidase (ACOX2) and the pristanoyl-CoA oxidase (ACOX3), reacting with the CoA-esters of bile acid intermediates and 2-methyl branched-chain fatty acids, such as pristanoyl-CoA. In comparison to the situation in rodents, in which these different acyl-CoA oxidases are present, humans harbor only two enzymes involved in the oxidation of distinct lipid derivatives: 1) a straight-chain acyl-CoA oxidase (ACOX1) and 2) a branched-chain acyl-CoA oxidase (ACOX2), involved in the degradation of 3-methyl-branched fatty acids and bile acid intermediates -dihydroxycholestanoic acid (DHCA) and trihydroxycholestanoic acid (THCA) (Baumgart et al., 1996).

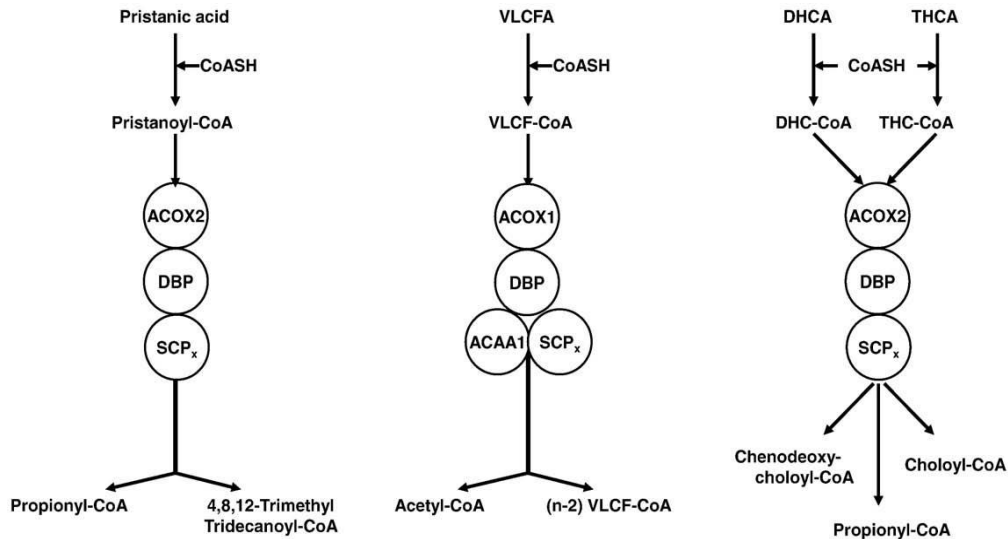


**Fig2.** Enzymology of the peroxisomal  $\beta$ -oxidation systems involved in the oxidation of pristanic acid, VLCFA and DHCA/THCA (Wanders et al.).

The enoyl-CoA-esters of VLCFA, pristanic acid, DHCA, and THCA are further metabolized by multifunctional protein (MFPs), harboring both enoyl-CoA hydratase and 3-hydroxyacyl-CoA dehydrogenase activity. At present, two distinct proteins (MFP1 and MFP2) have been described that are involved in the second and third steps of peroxisomal  $\beta$ -oxidation. Both MFP1 and MFP2 can act on straight chain compounds, whereas only MFP2 is involved in the degradation of compounds containing a 2-methyl branch, such as pristanic acid and bile acid intermediates (Dieuaide-Noubhani et al., 1997; Van Veldhoven).

The thiolytic cleavage is done by either a straight-chain 3-oxoacyl-CoA thiolase (ACAA1) or the sterol carrier protein X (SCP<sub>x</sub>), a 58 kDa protein with thiolase activity (Seedorf et al., 1994). SCP<sub>x</sub> reacts with the 3-keto-acyl-CoA-esters of pristanic acid, DHCA and THCA, whereas ACAA1 only accepts the 3-keto-acyl-CoA-esters of VLCFA (Seedorf et al., 1994).

### ***1.3.2 Biosynthesis of etherphospholipids and cholesterol in peroxisomes***

#### ***1.3.2.1 Etherphospholipid synthesis***

Ether phospholipids play a vital role in biophysical properties of membranes and are important ROS trappers, protecting membranes against damaging effects of lipid peroxidation (Karnati and Baumgart-Vogt, 2008). The vinyl ether bond is especially important for ROS trapping, which is introduced in peroxisomes (Brites et al., 2004).

Biosynthesis of etherphospholipids starts in the peroxisome with the conversion of dihydroxyacetonephosphate (DHAP) to acyl-DHAP, which is catalyzed by dihydroxyacetone phosphate acyltransferase (DHAPAT), followed by alkyldihydroxyacetone phosphate synthase (ADHAPS) with alkylDHAP as product (Wanders, 2004b). Both enzymes are strictly located in peroxisomes (Singh et al., 1989; Wanders, 2004b). The importance of DHAPAT and ADHAPS for etherphospholipid biosynthesis is emphasized by the fact that patients with a genetically determined deficiency of either DHAPAT or ADHAPS lack the synthesis of etherphospholipid (Brites et al., 2004). The third step of etherphospholipid biosynthesis is located in two different organelles - peroxisomes and the endoplasmic reticulum (ER) and this reaction is catalyzed by the enzyme alkyl/acyl-DHAP: NAD (P) H oxidoreductase. Thereafter, the product alkylglycerol-3-phosphate (alkyl-G-3P) undergoes subsequent conversion into plasmalogens in the ER (Brites et al., 2004). According to the consensus nomenclature provided by the mouse Genome Informatics Database (MGI), "dihydroxyacetonephosphate (DHAP)" is now termed "glyceronephosphate (GNP)" and the enzyme names are changed accordingly, e.g. DHAPAT to GNPAT.

### **1.3.2.2 Cholesterol synthesis**

Cholesterol is another important lipid of the plasma membrane that is especially enriched in lipid rafts in which signaling receptors are embedded.

Peroxisomes play a major role in isoprenoid and cholesterol biosynthesis, since enzymes catalyzing the conversion of mevalonate to farnesyl diphosphate (FPP), such as mevalonate kinase (MVK), phosphomevalonate kinase (PMVK), mevalonate pyrophosphate decarboxylase (MPD) and isopentenyl – diphosphate delta isomerase (IDI1) are localized in peroxisomes (Kovacs et al., 2002; Kovacs et al., 2007). Furthermore, acetyl-CoA derived from peroxisomal  $\beta$ -oxidation of very long-chain fatty acids and medium-chain dicarboxylic acids is preferentially channeled to cholesterol synthesis inside the peroxisomes (Kovacs et al., 2007). In addition, Kovacs and his colleagues demonstrated that peroxisomes play a vital role in the maintenance of cholesterol homeostasis (Kovacs et al., 2004). A recent study from their group further revealed that cholesterol biosynthesis pathway abnormalities persisted in PEX2 KO mice even when the cholesterol balance was maintained (Kovacs et al., 2009).

### **1.3.3 Metabolism of reactive oxygen and nitrogen species (ROS and RNS) in peroxisomes**

In the past decades, it has been known that peroxisomes play an important role in the production and degradation of reactive oxygen species (ROS) and reactive nitrogen species (RNS).

In addition, in this organelle, lipid and ROS metabolism are intensely coupled to each other, therefore, peroxisomes might be involved in “metabolic signaling” (Karnati and Baumgart-Vogt, 2008).

***Peroxisomal enzymes producing ROS***

Mammalian peroxisomes are densely packed with enzymes that form ROS (Table 1). Most of them are FAD (or FMN)-dependent oxidases, generating H<sub>2</sub>O<sub>2</sub> during conversion of their substrates as a reaction byproduct. In addition, some observations indicate the presence of the superoxide radical O<sub>2</sub><sup>·-</sup> producing enzyme xanthine oxidoreductase (Angermuller et al., 1987) and the inducible form of nitric oxide synthase (Loughran et al., 2005) in this cell organelle.

**Table 1. Enzymes in mammalian peroxisomes that generate ROS** (Antonenkov et al., 2009)

<b>Enzyme</b>	<b>Substrate</b>	<b>ROS</b>
Palmitoyl-CoA oxidase	Long- and very long-chain fatty acids, dicarboxylic fatty acids, glutaryl-CoA	H <sub>2</sub> O <sub>2</sub>
Pristanoyl-CoA oxidase	2-Methyl-branched fatty acids	H <sub>2</sub> O <sub>2</sub>
Trihydroxycoprostanoyl-CoA	Bile acids intermediates	H <sub>2</sub> O <sub>2</sub>
Urate oxidase	Uric acid	H <sub>2</sub> O <sub>2</sub>
L- $\alpha$ -hydroxyacid oxidases	Glycolate, lactate, medium- and long chain 2-hydroxyacids	H <sub>2</sub> O <sub>2</sub>
Polyamine oxidase	<i>N</i> -acetyl spermine/spermidine	H <sub>2</sub> O <sub>2</sub>
Pipecolic acid oxidase	L-Pipecolic acid	H <sub>2</sub> O <sub>2</sub>
Sarcosine oxidase	Sarcosine, L-proline	H <sub>2</sub> O <sub>2</sub>
D-amino acid oxidase	D-isomers of neutral and basic amino acids	H <sub>2</sub> O <sub>2</sub>
D-aspartate oxidase	D-isomers of acidic amino acids	H <sub>2</sub> O <sub>2</sub>
Xanthine oxidase	Hypoxanthine, xanthine	O <sub>2</sub> <sup>·-</sup>
NO synthase	L-arginine	·NO

***Peroxisomal antioxidant defense systems***

Peroxisomes are well equipped with antioxidant defense systems composed of enzymes involved in the decomposition of  $\text{H}_2\text{O}_2$  and  $\text{O}_2^{\cdot-}$  (Table 2). Among them, catalase, the classical marker enzyme for peroxisomes, metabolizes both  $\text{H}_2\text{O}_2$  and a variety of substrates, such as ethanol, methanol, phenol and nitrites by peroxidatic activity (Oshino et al., 1973). In most mammalian cells, catalase is targeted to peroxisomes via a modified PTS1.

**Table 2. Antioxidative enzymes in mammalian peroxisomes** (Antonenkov et al., 2009)

<b>Enzyme</b>	<b>Substrate</b>
Catalase	$\text{H}_2\text{O}_2$
Peroxiredoxin I	$\text{H}_2\text{O}_2$
Peroxiredoxin V (PMP20)	$\text{H}_2\text{O}_2$
Cu/Zn-superoxide dismutase	$\text{O}_2^{\cdot-}$
Mn-superoxide dismutase	$\text{O}_2^{\cdot-}$
Epoxide hydrolase	Epoxides
Soluble glutathione S-transferase (member of kappa family)	Hydroperoxides
Membrane bound ('microsomal') glutathione S-transferase	Lipid hydroperoxides

The main metabolic functions of peroxisomes are summarized in Fig 3.

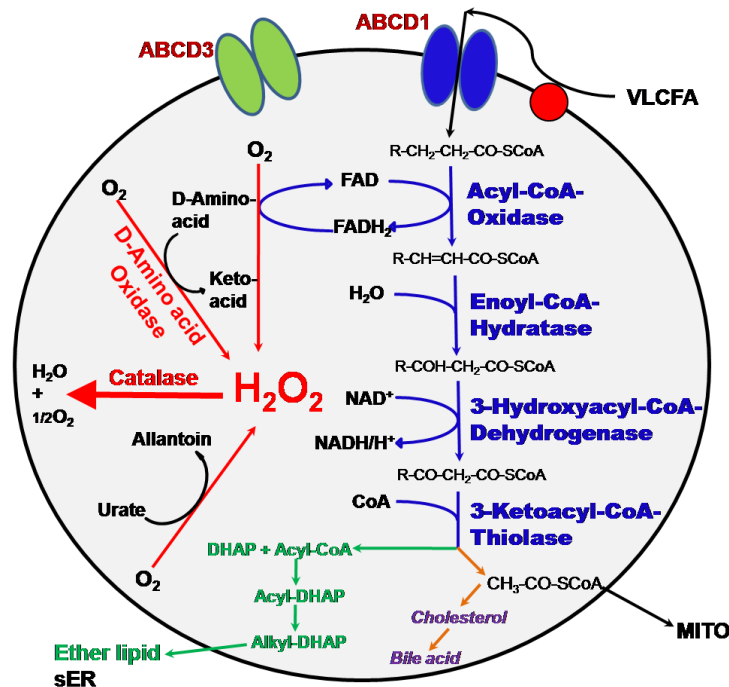


**Fig3.** This scheme depicts the general functions of peroxisomes, including  $\text{H}_2\text{O}_2$  metabolism,  $\beta$ -oxidation of distinct lipid derivatives as well as the synthesis of cholesterol and Etherlipid. This picture is provided by kind courtesy of Prof. Dr. Eveline Baumgart-Vogt.

## 1.4 Peroxisomal disorders

The vital importance of the peroxisomal compartment for human health is depicted by the devastating diseases resulting from peroxisomal deficiency. To date, approximately 20 peroxisomal diseases are known. Currently, two groups of peroxisomal disorders are distinguished from each other: (1) peroxisomal biogenesis disorders (PBDs) and (2) single peroxisomal enzyme deficiencies. PBDs are autosomal recessive diseases that arise from mutations in PEX genes, encoding proteins, called peroxins (= Pex...p), required for the normal biogenesis of peroxisomes. The most severe form of a PBD is the cerebrohepatorenal

syndrome of Zellweger (Zellweger syndrome: ZS) (Goldfischer et al., 1973), a multiple congenital anomaly syndrome, characterized by craniofacial abnormalities, eye abnormalities, neuronal migration defects, hepatomegaly, and chondrodysplasia punctata. The craniofacial features include a high forehead, hypoplastic supraorbital ridges, epicanthal folds, midface hypoplasia, and a large anterior fontanel (Steinberg et al., 2006; Wilson et al., 1986). Children with this condition fail to thrive, are growth retarded and usually die in the first year of life (Wilson et al., 1986). Another severe form of the PBDs is rhizomelic chondrodysplasia punctata (RCDP) type 1, resulting from a deficient PEX7 gene (Heymans et al., 1985). One of the major characteristics of children with RCDP type 1 is that they suffer from shortening of the long bones humerus and femur and therefore have shortened proximal limbs (Agamanolis and Novak, 1995; Braverman et al., 1997; Heymans et al., 1985; Motley et al., 1997; Purdue et al., 1999; Purdue et al., 1997; Shimozawa, 2007; Steinberg et al., 2006).

The second group of peroxisomal diseases -the single peroxisomal enzyme deficiencies are characterized by disruption of a single peroxisomal function, e.g X-linked adrenoleukodystrophy (X-ALD), a disease caused by a defect in the ALD protein, an ABC transporter for VLCFA, now called ABCD1(Moser, 1993). Patients with the severe form of this disease suffer from demyelination and progressive paralysis, adrenal insufficiency as well as male infertility due to germ cell loss and leydig cell degeneration.

## ***1.5 Animal models for peroxisomal biogenesis disorders (PEX2, PEX5, PEX7, PEX11 $\beta$ and PEX13 knockout mice)***

### ***1.5.1 Animal models for Zellweger syndrome***

The first knockout (KO) mouse described as a model for peroxisomal biogenesis disorders was the PEX5 KO mouse model (Baes et al., 1997). Subsequently, several other KO mouse models have also been developed, e.g. PEX2 (Faust and Hatten, 1997), PEX11 $\beta$  (Li et al., 2002b), PEX13 (Maxwell et al., 2003) and PEX7 (Brites et al., 2003). Mouse models of ZS, like PEX2, PEX5 and PEX13 KO mice exhibit the pathological hallmarks of ZS patients, including the neuronal migration defect, enhanced neuronal apoptosis, a developmental delay, neonatal hypotonia, and neonatal lethality (Baes et al., 1997; Faust and Hatten, 1997; Maxwell et al., 2003). These mice also show peroxisomal metabolic defects, including 1,000% increases in VLCFAs, a marker substrate of the peroxisomal  $\beta$ -oxidation pathway that cannot be oxidized in mitochondria and 90 to 99% decreases in plasmalogens, a marker product for the peroxisomal ether lipid synthesis pathway (Baes et al., 1997; Faust and Hatten, 1997; Maxwell et al., 2003). In contrast, craniofacial dysmorphism, enlarged cranial fontanelles and renal cysts are not so strongly developed in comparison to Zellweger patients.

PEX11 $\beta$  KO mice also exhibit numerous ZS pathologic features, including hypotonia, a developmental delay and growth defect as well as neuronal migration defect, even though peroxisomes are present in these animals, but exhibit a proliferation defect. Interestingly, peroxisomal import seems to be completely normal in PEX11 $\beta$  KO mice. In addition, these animals show only mild

defects in peroxisomal metabolic functions (Li et al., 2002b), challenging current models of ZS pathogenesis, such as the hypothesis of generation of pathological defects due to VLCFA accumulation or plasmalogen deficiency. PEX11 $\beta$  mice were used in this thesis to get more insights on the role of peroxisomes in ossification and bone growth.

### ***1.5.2 The animal model for Rhizomelic chondrodysplasia punctata***

A mouse model of RCDP type 1, PEX7 KO mouse, was generated and characterized by Brites and coworkers in 2003 (Brites et al., 2003). These mice also display many symptoms and pathologies, observed in the patients of RCDP type 1, but show no rhizomelia of long bone. The observed pathological alterations are the growth retardation, neuronal migration defects, and ossification impairments. Moreover, these mice exhibit peroxisomal metabolic defects related to a PEX7 deficiency, i.e. a severe depletion of plasmalogens, the impaired  $\alpha$ -oxidation of phytanic acid and an impaired  $\beta$ -oxidation of VLCFAs (Braverman et al.; Brites et al., 2003).

## ***1.6 Bone, Cartilage and Ossification***

The skeleton is composed of bones and associated ligaments, tendons, and cartilages. Bones consist of three major cell types plus a significant amount of extracellular matrix. Specific cell types in bone comprise: 1) the osteoblast, which is involved in synthesis and secretion of collagen I fibers and other organic components of the bone matrix; 2) the osteocyte, a mature bone cell, which is responsible for maintaining the bone tissue; 3) the osteoclast, which degrades bone tissue by removing its mineralized matrix and breaking up the organic bone structure. Osteoclasts and osteoblasts are instrumental in controlling the amount

of bone tissue: osteoblasts form bone (Harada and Rodan, 2003) and osteoclasts resorb bone (Boyle et al., 2003). Any abnormal interaction between osteoblasts and osteoclasts could lead to imbalance between the formation and resorption of bone, thus induce various bone-related diseases including osteoporosis.

Cartilage is an avascular tissue composed of specialized cells called chondrocytes that produce a large amount of extracellular matrix, composed of collagen fibers, abundant ground substance rich in proteoglycan, and collagen II fibers. Cartilage is classified in three types, hyaline cartilage, elastic cartilage and fibrocartilage. Hyaline cartilage is the most common variety of cartilage and it can be found in costal cartilages, articular cartilages, epiphyseal plates, and the majority of fetal skeleton that is later replaced by bone.

Ossification is a process of bone formation (Caetano-Lopes et al., 2007) and two types of ossification participate in this process. One is the intramembranous (or desmal) ossification. It is achieved by direct transformation of mesenchymal cells into osteoblasts, the skeletal cells involved in bone formation. It is the process responsible for the development of the flat bones of the cranial vault, including the cranial suture lines, some facial bones, and parts of the mandible and clavicle. The secondary ossification process is called endochondral ossification. Unlike intramembranous ossification, cartilage is present during endochondral ossification. It is an essential process during the rudimentary formation of long bones and the growth of long bones (Brighton et al., 1973; Caplan, 1988). A model for the formation and growth of long bones by endochondral ossification is depicted in figure 4 (Fig 4).

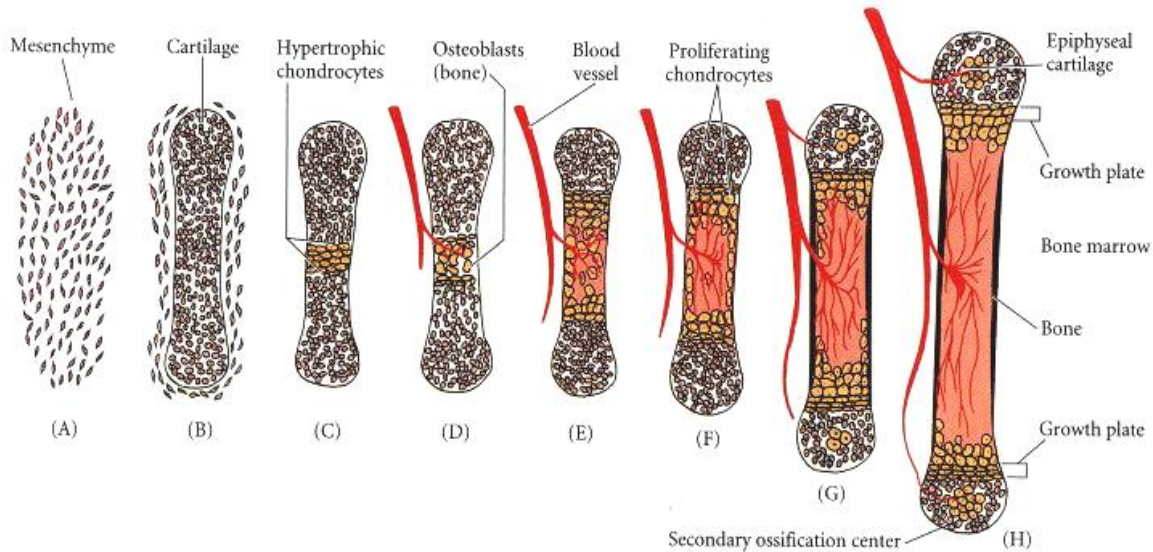


**Fig4.** Model of the formation and growth of long bones by endochondral ossification according to Horton (Gilbert, 2000). (A, B) Mesenchymal cells condense and differentiate into chondrocytes to form the cartilaginous model of the bone. (C) Chondrocytes in the center of the shaft undergo hypertrophy and apoptosis while they change and mineralize their extracellular matrix. Their deaths allow blood vessels to enter. (D, E) Blood vessels bring in mesenchymal cells that differentiate into osteoblasts, which bind to the degenerating cartilaginous matrix and deposit bone matrix. (F-H) Bone formation and growth consist of ordered arrays of proliferating, hypertrophic, and mineralizing chondrocytes. Secondary ossification centers also form as blood vessels enter near the tips of the bone.

## 1.7 Signaling pathways involved in bone metabolism

### 1.7.1 Wnt signaling and bone

Wnt proteins form a family of highly conserved, secreted signaling molecules that play a central role in many processes during embryonic development and in later stages of life. At least three distinct wnt signaling pathways have been described: the wnt/ $\beta$ -catenin pathway, the  $\text{Ca}^{2+}$ -dependent pathway and the planar cell polarity (PCP) pathway (Peters et al., 2008). In the wnt/ $\beta$ -catenin pathway, wnts binds to a receptor complex, comprising frizzled (Fz) and the low-density lipoprotein receptor-related proteins 5 or 6 (LRP5 or LRP6) (He et al., 2004; Tamai et al., 2000). Activation of this receptor complex leads to

inactivation of the glycogen synthase kinase  $3\beta$  (GSK- $3\beta$ ), which prevents phosphorylation and consecutive degradation of  $\beta$ -catenin and, thereby, results in its accumulation in the cytoplasm (Liu et al., 2002; Ruel et al., 1999). Thereafter,  $\beta$ -catenin translocates into the nucleus where it acts as a coactivator with the T-cell factor (Tcf)/ lymphoid-enhancer binding factor (Fan et al.) transcription factors and regulates the expression of wnt target genes, such as cyclin D1 (Tetsu and McCormick, 1999), axin 2 (Yan et al., 2001) and runx2 (Dong et al., 2006).

In recent years, it has been shown that Wnt/LRP5 or LRP6 signaling is a critical determinant of bone mass. Indeed, loss of function mutations in LRP5 gene leads to the osteoporosis-pseudoglioma syndrome (OPPG), a rare disease characterized by severe decreased bone formation and persistence of embryonic eye vascularization (Gong et al., 2001), whereas gain of function mutations causes the hereditary high bone mass trait in humans (Boyden et al., 2002; Little et al., 2002). Mutations in LRP6 have also been linked to changes in bone mass in humans. Members of a family in which a putative partial loss-of-function mutation in LRP6 is identified are predisposed to early cardiovascular-related death associated with dramatically elevated levels of plasma LDL and triglycerides, hypertension, diabetes, and osteoporosis (Mani et al., 2007). In addition, LRP5-deficient mice also show decreased bone formation and osteoblast proliferation (Kato et al., 2002) whereas transgenic mice that express the LRP5 G171V activating mutation in osteoblasts exhibit increased bone formation and high bone mass (Babij et al., 2003). Sclerostin was found to antagonize canonical wnt signaling by binding to Lrp5/6 (Li et al., 2005; Semenov et al., 2005). Wnt-induced transcriptional reporter activity and alkaline phosphatase

activity were effectively antagonized by sclerostin in several cell lines (Li et al., 2005; Semenov et al., 2005) and this inhibitory effect can be attenuated by the addition of anti-sclerostin antibodies (Ellies et al., 2006).

### **1.7.2 ROS metabolism and bone**

As described above, bone is a dynamic organ with a well-regulated turnover-bone formation and bone absorption. The process of bone remodeling is affected in the most frequent degenerative disease of bones – osteoporosis a disease with a low bone mass, resulting from an imbalance between bone formation and resorption (Raisz, 2005; Rodan and Martin, 2000).

Accumulating evidence suggests that bone remodelling is influenced by redox balance regulation. Almeida and coworkers have determined that female and male C57BL/6 mice lose bone strength and mass progressively between the ages of 4-31 months. These alterations are temporally linked with increased ROS levels and decreased glutathione reductase activity, as well as a corresponding increase in the phosphorylation of p53 and p66<sup>shc</sup>(Almeida et al., 2007). Consistent with this study, Chambers and colleagues show that both osteoblast number and bone formation are decreased in 2-month-old mice treated with the glutathione inhibitor buthionine sulfoximine (Jagger et al., 2005). Furthermore, these workers also show in another study that the antioxidants NAC or ascorbate, antioxidants that increase tissue glutathione levels, prevented the increased osteoclastogenesis and abolished ovariectomy-induced bone loss (Lean et al., 2003). These novel insights suggest that ROS may be one of the critical parameters determining the pathophysiology of bone loss. In addition, recent studies have provided evidences that FoxO-mediated defense against oxidative

stress in osteoblasts is indispensable for skeletal homeostasis in mice (Ambrogini et al., 2010; Rached et al., 2010).

### ***1.7.3 Nuclear receptor signaling and bone***

Recently, it has been shown that the peroxisome proliferator-activated receptor (PPAR)- $\gamma$ , a transcription factor of the ligand-activated nuclear receptor family, regulating the transcription of "peroxisomal" genes, might be involved in the bone remodelling process. Activation of this receptor by its ligands stimulates adipogenesis and inhibits osteogenesis in mesenchymal cell lines (Lecka-Czernik et al., 1999), whereas PPAR $\gamma$  insufficiency increases bone mass by stimulating osteoblastogenesis from bone marrow progenitors (Akune et al., 2004). Furthermore, activation of PPAR $\gamma$  inhibits the expression and DNA-binding activity of the transcription factor-Cbfa1 which is indispensable for osteoblast differentiation and reduces osteocalcin expression (Lin et al., 2007). The latest study from Manolagas group has shown that oxidized lipids, acting as ligands of PPAR $\gamma$  promote binding of PPAR $\gamma$  to  $\beta$ -catenin and reduce the levels of the latter, and they attenuate wnt3a stimulated proliferation and osteoblast differentiation (Almeida et al., 2009). Additionally, PPAR $\gamma$  also regulates the activation and migration of macrophages and might therefore exert an effect on bone osteoclasts as well (Mbalaviele et al., 2000; Ricote et al., 1998). Interestingly, this receptor and its other family member-PPAR $\alpha$  activate the transcription of genes of peroxisomal  $\beta$ -oxidation enzymes necessary for the degradation of the putative ligands of PPARs. However, until now no information about the effect of their ligands on peroxisomes is available in primary osteoblasts and bone or on the molecular pathologies arising from peroxisome deficiencies on skeletal tissues.

### ***1.8 Peroxisomes in the skeleton***

As mentioned above, the patients with ZS and RCDP type 1, all exhibit bone development abnormalities. In ZS, they have a high forehead, hypoplastic supraorbital ridges, midface hypoplasia, and a large anterior fontanel (Steinberg et al., 2006; Wilson et al., 1986). Whereas, the patients of RCDP type 1 suffer from shortening of the long bones humerus and femur (Agamanolis and Novak, 1995; Braverman et al., 1997; Motley et al., 1997; Purdue et al., 1999; Purdue et al., 1997; Steinberg et al., 2006). Likewise, in mouse models, a severe retardation of endochondral ossification (or intramembranous ossification) was also detected. In PEX7 KO mice, analysis of bone ossification revealed a defect in ossification of distal bone elements of the limbs as well as parts of the skull and vertebrae. However, no shortening of proximal limbs was noted in these animals (Brites et al., 2003). Additionally, PEX11 $\beta$  KO mice also exhibited a delay in the ossification of calvaria (Li et al., 2002b). Even though all distinct “peroxisomal biogenesis disorder” mouse models exhibit skeletal alterations and the absence of peroxisomes in patients with ZWS and RCDP has been already noted for such a long time, nothing is known about the molecular mechanisms resulting in the skeletal deformations in these diseases. In addition, to date, no knowledge is available on peroxisomal metabolism in bone and cartilage.

## ***2 Aims of this study***

### **Scientific basis for the goals of this study:**

It is well known that peroxisomes in different organ systems and cell types serve different metabolic functions. However, most of the knowledge on peroxisomes in the literature was acquired from studies on major metabolic organs, such as liver or kidney (Baumgart, 1997; Islinger et al., 2007; Wiese et al., 2007). Despite the fact that patients with peroxisomal diseases exhibit ossification defects, no information is available on the functions of peroxisomes in the skeleton.

Interestingly, the peroxisome proliferator-activated receptor  $\gamma$  (PPAR $\gamma$ ) was suggested to be involved in bone remodeling. Since peroxisomes regulate the abundance of lipid ligands for this receptor by their  $\beta$ -oxidation system (Karnati and Baumgart-Vogt, 2008), this feed-back loop might be an important regulator pathway in the ossification process.

In addition, children with peroxisomal diseases and corresponding knockout mice are extremely growth retarded (Baes et al., 1997). Even in a mouse model in which only peroxisome proliferation is blocked (PEX11 $\beta$  knockout mice), a severe difference in the size of the animals was noted at birth (Li et al., 2002b). However, to date, nothing is known on the pathological consequences of PEX11 $\beta$  deficiency in the skeleton.

**Therefore, the aims of this study were:**

- ❖ To localize and characterize peroxisomes in different cell types of the skeleton.
- ❖ To investigate the differences and possible functional heterogeneity of peroxisomal metabolism during osteoblast maturation.
- ❖ To analyze the effects of different PPAR agonists on peroxisomes in primary osteoblasts.
- ❖ To study the consequences of peroxisome deficiency and the pathological alterations in the skeleton of PEX11 $\beta$  deficient mice.
- ❖ To analyze the molecular pathogenesis of ossification impairment in PEX11 $\beta$  deficient mice.

## ***3 Materials and Methods***

### ***3.1 Materials***

#### ***3.1.1 Experimental animals***

Specific pathogen free (SPF) C57Bl/6J mice at the age of 40 days and pregnant mice (for delivery of newborn pups) were purchased for experimental purposes from Charles River Laboratories (Sulzfeld, Germany). They had free access to food and water and were kept under standardized environmental conditions (12h light/dark cycle, 23°C ± 1°C and 55% ± 1% relative humidity). The 40d-old mice for experiments were transported to our institute 1 day in advance, whereas the pregnant mothers were kept in the animal laboratory until newborn pups were delivered.

The PEX11 $\beta$  mouse line was kept under SPF conditions in the Central Animal Facility of Justus Liebig University. PEX11 $\beta$  knockout (KO) mice were generated by breeding of the heterozygotes and identified by genotyping of the tail DNA. The pregnancy state of heterozygous mothers was calculated according to the appearance of the vaginal plug. The morning of the presence of a vaginal plug was considered as E0.5. Pregnant mice were transported to our institute when the fetuses were at E19.

All experiments with laboratory mice were approved by the German Government Commission of Animal Care.

### 3.1.2 Laboratory instruments

Table 3. All laboratory instruments used here are listed alphabetically with notice of corresponding supplier:

Instruments	Company name
AGFA Horizon Ultra Colour Scanner	AGFA, Mortsels, Belgium
Biocell A10 water system	Milli Q-Millipore, Schwalbach, Germany
Biofuge Fresco	Heraeus, Hanau, Germany
Biofuge Pico	Heraeus, Hanau, Germany
Bio-Rad electrophoresis apparatus	Bio-Rad, Heidelberg, Germany
Dish washing machine	Miele, Gütersloh, Germany
Cary 50 Bio-UV-visible spectrophotometer	Varian, Darmstadt, Germany
Gel-Doc 2000 gel documentation system	Bio-Rad, Heidelberg, Germany
Flat-panel volumetric computed tomography	GE medical systems, Milwaukee, WI
Fraction collector Heidolph pump drive 5101	Heidolph Instruments, Schwabach, Germany
Hera cell 240 incubator	Heraeus, Hanau, Germany
Hera safe, clean bench	Heraeus, Hanau, Germany
Ice machine, Scotsman AF-100	Scotsman Ice Systems, Vernon Hills, IL, USA
iCycler PCR machine	Bio-Rad, Heidelberg, Germany
Leica DMRD fluorescence microscope	Leica, Bensheim, Germany
Leica DC 480 camera	Leica, Bensheim, Germany
Leica TP1020 embedding machine	Leica, Nussloch, Germany
Leica TCS SP2 confocal laser scanning microscope	Leica, Heidelberg, Germany
Leica SM 2000R rotation microtome	Leica, Nussloch, Germany
Microwave oven	LG, Willich, Germany
Mini-Protean 3 cell gel chamber	Bio-Rad, Heidelberg, Germany
Microtome stretching water bath	Vieth Enno, Wiesmoor, Germany
Multifuge 3 SR centrifuge	Heraeus, Hanau, Germany
pH meter	IKA, Weilheim, Germany
Pipettes	Eppendorf, Hamburg, Germany
Potter-Elvehjem homogenizer	B. Braun, Melsungen, Germany
Power supply - 200, 300 and 3000 Xi	Bio-Rad, Heidelberg, Germany
Pressure/Vacuum Autoclave FVA/3	Fedegari, Albuzzano, Italy
Pump Drive PD 5001	Heidolph Instruments, Schwabach, Germany
Sorvall Evolution RC centrifuge	Kendro, NC, USA
Smartspec™ 3000 spectrophotometer	Bio-Rad, Heidelberg, Germany
T25 basic homogenizer	IKA, Staufen, Germany
Thermo plate	Medax, Kiel, Germany
Thermo mixer HBT 130	HLC, BioTech, Bovenden, Germany
Trans-Blot SD semidry transfer cell	Bio-Rad, Heidelberg, Germany
Trimmer TM60	Reichert, Wolfratshausen, Germany
TRIO-thermoblock	Biometra, Göttingen, Germany
Ultra balance LA120 S	Sartorius, Göttingen, Germany
Ultra Turrax T25 basic homogenizer	Junke & Kunkel, Staufen, Germany
Vortex M10	VWR International, Darmstadt, Germany
Water bath shaker GFL 1083	GFL, Burgwedel, Germany

### **3.1.3 General materials and culture media**

**Table 4. General materials and culture media are listed alphabetically with notice of corresponding suppliers:**

<b>General materials and culture media</b>	<b>Company name</b>
BioMax MR-films	Kodak, Stuttgart, Germany
Cover slips	Menzel-Gläser, Braunschweig, Germany
Culture dish (35mm)	BD Biosciences, Heidelberg, Germany
Culture dish (60mm)	BD Biosciences, Heidelberg, Germany
Filter tips and canules	Braun, Melsungen, Germany
Microtome blade A35	Feather, Köln, Germany
Minimum essential Medium (MEM) $\alpha$ medium	Invitrogen, Karlsruhe, Germany
Molecular weight markers (DNA, RNA)	Fermentas, St.Leon-Rot, Germany
Multi-well cell culture plates (12 wells)	BD Biosciences, Heidelberg, Germany
Nylon meshes (100, 20 and 10 $\mu$ m)	Bückmann, Mönchengladbach, Germany
Oligo(dT)12-18 primer	Invitrogen, Heidelberg, Germany
Paraffin	Paraplast Plus, MO, USA
PVDF membranes	Millipore, Schwalbach, Germany
RT-PCR primers (see table 14)	Operon, Cologne, Germany

### **3.1.4 Proteins and enzymes**

**Table 5. Proteins and enzymes used here are listed alphabetically with notice of corresponding suppliers:**

<b>Proteins and enzymes</b>	<b>Company name</b>
Bovine serum albumin (BSA)	Roth, Karlsruhe, Germany
Collagenase 2	PAA, Cölbe, Germany
Dispase	BD Biosciences, NJ, USA
DNase I	Sigma, Steinheim, Germany
Fetal calf serum	HyClone, UT, USA
Immunostar-alkaline phosphatase	Bio-Rad, Heidelberg, Germany
Milk powder	Roth, Karlsruhe, Germany
Precision Plus protein standards, dual color	Bio-Rad, Heidelberg, Germany
Precision Plus protein standards, unstained	Bio-Rad, Heidelberg, Germany
Primary antibodies (see table 15)	Various companies see table 15
Recombinant mouse wnt-3a	R&D Systems, Wiesbaden, Germany
Secondary antibodies (see table 16)	Various companies see table 16
SuperScript II reverse transcriptase	Invitrogen, Karlsruhe, Germany
<i>Taq</i> DNA polymerase	Eppendorf, Hamburg, Germany
Trypsin	Sigma, Steinheim, Germany

### 3.1.5 Chemicals and drugs

**Table 6. Alphabetical list of used chemicals and drugs in this study with notice of corresponding suppliers:**

<b>Chemicals</b>	<b>Company name</b>
Acrylamide	Roth, Karlsruhe, Germany
Agarose LE	Roche, Grenzach-Wyhlen, Germany
Alcian Blue 8Gx	Fluka, Neu-Ulm, Germany
Alizarin Red S	Fluka, Neu-Ulm, Germany
Ascorbic acid	Sigma, Steinheim, Germany
Bradford reagent	Sigma, Steinheim, Germany
Bromophenol blue	Riedel-de-Haën, Seelze, Germany
Calcium chloride	Merck, Darmstadt, Germany
Ciprofibrate	Sigma, Steinheim, Germany
Citric acid	Merck, Darmstadt, Germany
Di-potassium hydrogen phosphate ( $K_2HPO_4$ )	Merck, Darmstadt, Germany
Dodoceny succinic anhydride (DDSA)	Plano, Wetzlar, Germany
Epoxy Resin 812	Agar, Essex, England
Ethanol	Riedel-de-Haën, Seelze, Germany
Ethidium bromide	Fluka, Neu-Ulm, Germany
Ethylene diamine tetraacetic acid (EDTA)	Fluka, Neu-Ulm, Germany
Ethylene glycol-bis (2-aminoethylether)- <i>N,N,N',N'</i> -tetraacetic acid (EGTA)	Fluka, Neu-Ulm, Germany
Formvar 1595 E	Serva, Heidelberg, Germany
Glutaraldehyde (GA)	Serva, Heidelberg, Germany
Glycine	Roth, Karlsruhe, Germany
Glycerol	Sigma, Steinheim, Germany
$\beta$ -glycerolphosphate	Sigma, Steinheim, Germany
Hydrogen peroxide ( $H_2O_2$ )	Merck, Darmstadt, Germany
4-(2-hydroxyethyl)-1-piperazineethanesulfonic acid (HEPES)	Roth, Karlsruhe, Germany
Ketavet	Bayer, Leverkusen, Germany
L-Glutamate	Cambrex BioScience, MD, USA
LR white medium grade	LR White Resin, Berkshire, England
Methylnadic anhydride (MNA)	Plano, Wetzlar, Germany
Mowiol 4-88	Polysciences, Eppelheim, Germany
3-[N-Morpholino]-propanesulfonic acid (MOPS)	Serva, Heidelberg, Germany
N-propyl-gallate	Sigma, Steinheim, Germany
Osmium tetroxide	Polysciences, Eppelheim, Germany
Paraformaldehyde (PFA)	Sigma, Steinheim, Germany
Penicillin/Streptomycin	PAN Biotech, Aidenbach, Germany
Phenylmethanesulfonyl fluoride (PMSF)	Serva, Heidelberg, Germany
1,4 Piperazine bis (2-ethanosulfonic acid) (PIPES)	Sigma, Steinheim, Germany
Ponceau S	Serva, Heidelberg, Germany
Potassiumhexacyanoferrate	Merck, Darmstadt, Germany
Potassium dihydrogen phosphate ( $KH_2PO_4$ )	Merck, Darmstadt, Germany
Potassium hydroxide (KOH)	Fluka, Neu-Ulm, Germany

Rotiphorese Gel 30	Roth, Karlsruhe, Germany
RNaseZap	Sigma, Steinheim, Germany
Sodium carbonate	Merck, Darmstadt, Germany
Sodium chloride	Roth, Karlsruhe, Germany
Sodium hydrogen carbonate	Merck, Darmstadt, Germany
Sodium hydroxide	Merck, Darmstadt, Germany
Sucrose	Merck, Darmstadt, Germany
Sodium dodecyl sulphate	Sigma, Steinheim, Germany
Tetramethylethylenediamine (TEMED)	Roth, Karlsruhe, Germany
Trishydroxymethylaminomethane (Tris)	Merck, Darmstadt, Germany
Triton X-100	Sigma, Steinheim, Germany
Troglitazone	Sigma, Steinheim, Germany
Trypan blue	Sigma, Steinheim, Germany
Tween 20	Fluka, Steinheim, Germany
Xylene	Merck, Darmstadt, Germany

### 3.1.6 Kits

**Table 7. Alphabetical list of used kits in this study with notice of corresponding suppliers:**

<b>Kits</b>	<b>Company name</b>
Avidin / Biotin-blocking kit	Vector Laboratories, Burlingame, USA
Novared Peroxidase-Substrate kit	Vector Laboratories, Burlingame, USA
PCR kit	Qiagen, Hilden, Germany
Rabbit ExtrAvidin Peroxidase-Staining kit	Sigma, Steinheim, Germany
RNeasy kit	Qiagen, Hilden, Germany
RT-PCR kit	Invitrogen, Karlsruhe, Germany

### 3.1.7 Buffers and solutions

**Table 8. Solutions for immunofluorescence in tissue sections:**

Perfusion fixative solution	4% PFA in 1X PBS (150mM NaCl, 13.1mM K <sub>2</sub> HPO <sub>4</sub> , 5mM KH <sub>2</sub> PO <sub>4</sub> ), pH 7.4
10X PBS	1.5M NaCl, 131mM K <sub>2</sub> HPO <sub>4</sub> , 50mM KH <sub>2</sub> PO <sub>4</sub> , pH 7.4
Trypsin (0.1%)	0.1g trypsin in 100ml of 1X PBS buffer, freshly prepared
TEG buffer	5mM EGTA, 0.1M Tris, pH 9.0
Blocking buffer-4% PBSA + 0,05% Tween 20	To 8g BSA add 200ml of 1X PBS and 100µl of Tween 20
Dilution buffer- 1% PBSA + 0,05% Tween 20	To 2g BSA add 200ml of 1X PBS and 100µl of Tween 20
Mowiol 4-88 solution	Overnight stirring of 16.7 % Mowiol 4-88 (w/v) + 80ml of 1X PBS, add 40ml of glycerol, stir again overnight; centrifuge at 15,000 U/min for 1h and take off the supernatant and store at -20°C
Anti-fading agent (2.5%)	2.5g N-propyl-gallate in 50ml of PBS and add 50ml of glycerol
Mounting medium	3 parts of Mowiol 4-88 + 1 part of anti-fading agent

**Table 9. Solutions for immunofluorescence in osteoblasts:**

Perfusion fixative solution	4% PFA in 1X PBS (150mM NaCl, 13.1mM K <sub>2</sub> HPO <sub>4</sub> , 5mM KH <sub>2</sub> PO <sub>4</sub> ), pH 7.4
Glycine (1%)	1g Glycine in 100ml of 1X PBS buffer
Glycine (1%) + Triton X-100 (0.3%)	1g Glycine in 100ml of 1X PBS buffer + 0.3ml Triton X-100
Blocking buffer- 1% PBSA + 0,05% Tween 20	To 2g BSA add 200ml of 1X PBS and 100µl of Tween 20
Mowiol 4-88 solution	Overnight stirring of 16.7 % Mowiol 4-88 (w/v) + 80ml of 1X PBS, add 40ml of glycerol, stir again overnight; centrifuge at 15,000 U/min for 1h and take off the supernatant and store at -20°C
Anti-fading agent (2.5%)	2.5g N-propyl-gallate in 50ml of PBS and add 50ml of glycerol
Mounting medium	3 parts of Mowiol 4-88 + 1 part of anti-fading agent

**Table 10. Solutions for isolation of proteins:**

Homogenization buffer (HMB)	To 50ml of 0.25M sucrose and 5mM MOPS (pH 7.4) add only before use 500µl 100mM EDTA + 50µl 100% ethanol + 5µl 2M DTT + 50µl 1M aminocaproic acid and 500µl cocktail of protease inhibitors
Cell lysis buffer (1X)	The stock solution (10X) is diluted into the working solution (1X), furthermore, add 1mM PMSF just prior to use

**Table 11. Solutions for SDS-PAGE:**

Resolving gel buffer A	1.5M Tris-HCl pH 8.8 + 0.4% SDS
Stacking gel buffer B	0.5M Tris-HCl pH 6.8 + 0.4% SDS
Resolving gel (12%) (for 4 SDS-PAGE gels)	8ml of 30% acrylamide + 10ml of buffer A + 2ml of ddH <sub>2</sub> O + 15µl of TEMED + 130µl of 10% APS
Stacking gel (for 4 SDS-PAGE gels)	1.25ml of 30% acrylamide + 5ml of buffer B + 5ml of DH <sub>2</sub> O + 15µl of TEMED + 130µl of 10% APS
10X Sample buffer	3.55ml ddH <sub>2</sub> O + 1.25ml 0.5M Tris-HCl, pH 6.8 + 2.5ml 50% (w/v) glycerol + 2.0ml 10% (w/v) SDS + a pinch of 0.05% bromophenol blue. Before use, add 50ml β-mercaptoethanol

**Table 12. Solutions for Western Blotting:**

10X Electrophoresis buffer	250mM Tris + 2M glycine + 1% SDS
20X Transfer buffer	Bis-Tris-HCl buffered (pH 6.4) polyacrylamide gel; NuPAGE transfer buffer, Invitrogen, Heidelberg, Germany
10X TBS	0.1M Tris + 0.15M NaCl in 1000ml of ddH <sub>2</sub> O, adjust to pH 8.0
10% Blocking buffer	10g fat free milk powder in 100ml of ddH <sub>2</sub> O
1% BSA	1g BSA in 100ml 1X TBST +0.05% Tween 20, pH 8.0
10% Goat serum solution	1ml Goat serum + 9ml 1X TBST +0.05% Tween 20, pH 8.0
1X Washing buffer (TBST)	10mM Tris/HCl, 0.15M NaCl, 0.05% Tween 20, pH 8.0
Stripping buffer (500ml)	62.5mM Tris (pH6.8), 0.2% SDS, 500ml ddH <sub>2</sub> O - 42°C water bath for 40min
Ponceau S solution	0.1% (w/v) Ponceau S in 5% (v/v) acetic acid

**Table 13. Solutions for molecular biology:**

Transfer buffer 10X (TAE)	40mM Tris base + 20mM acetic acid + 1mM EDTA, pH 7.6
RNA-loading dye (10ml)	16µl saturated aqueous bromophenol blue, 80µl 500mM EDTA (pH8.0), 720µl 37% formaldehyde, 4ml 10X gel buffer, then fill up to 10ml with ddH <sub>2</sub> O
10X RNA transfer buffer	200mM MOPS, 50mM sodium acetate, 10mM EDTA, pH 7.0
1X Formaldehyde gel	100ml 10X RNA transfer buffer + 20ml 37% formaldehyde + 880ml ddH <sub>2</sub> O

### **3.1.8 Primers**

Table 14 depicts the list of primers used in this study.

### **3.1.9 Antibodies**

Table 15 and 16 depict the overview of primary and secondary antibodies, which were used for various morphological methods and for Western blots.

Table 14. List of Primers used in this study

Genes	Forward primer (5'-3')	Reverse primer (5'-3')	Annealing Temperature ( ° C)	Length (bp)
<b>Peroxisomes</b>				
<i>ABCD1</i>	5'-GAGGGAGGTTGGGAGGCAGT-3'	5'-GGTGGGAGCTGGGGATAAGG-3'	65	465
<i>ABCD3</i>	5'-CTGGGCGTGAATGACTAGATTGG-3'	5'-AGCTGCATTTGCCAAGTACTCC-3'	64	523
<i>ACOX1</i>	5'-CTGAACAAGACAGAGGTCCACGAA-3'	5'-TGTAAGGGCCACACACTCACATCT-3'	60	565
<i>ACOX2</i>	5'-CTCTTGCACGTATGAGGGTGAGAA-3'	5'-CTGAGTATTGGCTGGGACTTCTG-3'	60	688
<i>CAT</i>	5'-ATGGTCTGGGACTTCTGGAGTCTTC-3'	5'-GTTTCCTCTCCTCCTCATTCAACAC-3'	64	833
<i>MFP1</i>	5'-ATGGCCAGATTTTCAGGAATG-3'	5'-TGCCACTTTTGTGATTTGC-3'	60	211
<i>MFP2</i>	5'-GAGCAGGATGGATTGGAAAA-3'	5'-TGACTGGTACGGTTTGGTGA-3'	60	223
<i>PEX5</i>	5'-GAGTGAAGAAGCAGTGGCTGCATAC-3'	5'-GGACAGAGACAGCTCATCCCTACAA-3'	64	508
<i>PEX11a</i>	5'-TCAGCTGCTGTCTCAGTCCCTT-3'	5'-GTACTTAGGAGGTCCTCCGAGAGGA-3'	64	420
<i>PEX11β</i>	5'-GTATGCCTGTTCCCTTCTCG-3'	5'-CTCGGTTGAGGTGACTGACA-3'	65	216
<i>PEX11γ</i>	5'-GACTCTGCTTGGTGGACACT-3'	5'-TGTCTCTCCCACTCACCTTAGGC-3'	64	682
<i>PEX13</i>	5'-GACCACGTAGTTGCAAGAGCAGAGT-3'	5'-CTGAGGCAGCTTGTGTTCTACTG-3'	65	718
<i>PEX14</i>	5'-CACCTCACTCCGAGCCATA-3'	5'-AGGATGAGGGGCAGCAGGTA -3'	60	131
<b>Osteoblasts</b>				
<i>ALP</i>	5'-GCCCTCTCAAGACATATA-3'	5'-CCATGATCACGTGATATCC-3'	55	373
<i>OPN</i>	5'-TCACCATTCGGATGAGTCTG-3'	5'-ACTTGTGGCTCTGATGTTCC-3'	58	437
<i>RUNX2</i>	5'-CCGCACGACAACCGCACCAT-3'	5'-CGCTCCGGCCCAAAATCTC-3'	62	289
<b>Signalling molecules</b>				
<i>PPARα</i>	5'-AGACCGTCACTGGGAGCTCACA-3'	5'-GGCCTGCCATCTCAGGAAAAG-3'	68	584
<i>PPARβ</i>	5'-CACCGAGTTCGCCAAGAACA-3'	5'-AGAGCCCCGCAAGATGGTGTCT-3'	60	363
<i>PPARγ</i>	5'-TCCGTAGAAGCCCGTGAAGA-3'	5'-CACCTTGGCGAACAGCTGAG-3'	60	441
<b>Loading control</b>				
<i>GAPDH</i>	5'-CACCATGGAGAAGCCGGGG-3'	5'-GACGGACACATTGGGGGTAG-3'	60	391

Table 15. List of primary antibodies used in this study

Peroxisomal antigens	Species AB raised in	Dilution (IF)	Dilution(WB)	Supplier
Catalase (CAT), mouse	Rabbit, polyclonal	1:2,000	1:10,000	Gift from Denis I. Crane, School of Biomol. Biophys. Sci., Griffith Univ., Nathan, Brisbane, Australia
Peroxisomal biogenesis factor 5 (Pex5p), mouse	Mouse, monoclonal	-	1:200	BD Transduction Laboratories, USA. Cat. no: 611594
Peroxisomal biogenesis factor 13 (Pex13p), mouse	Rabbit, polyclonal	1:2,000	1:6,000	Gift from Denis I. Crane (address see above)
Peroxisomal biogenesis factor 14 (Pex14p), mouse	Rabbit, polyclonal	1:4,000	1:20,000	Gift from Denis I. Crane (address see above)
ABC-transporter D3 (abcd3), rat	Rabbit, polyclonal	1:1,000	-	Invitrogen, Karlsruhe, Germany. Cat. no: 71-8300
ABC-transporter D3 (abcd3), mouse	Rabbit, polyclonal	-	1:100	Gift from Alfred Völkl, University of Heidelberg, Germany
"SKL" (peroxisomal targeting signal 1), mouse peptide	Rabbit, polyclonal	1:2,000	-	Gift from Denis I. Crane (address see above)
3-ketoacyl-CoA thiolase B (Thiolase B), mouse	Rabbit, polyclonal	-	1:6,000	Gift from P.Van , Catholic University Leuven, Belgium
<b>Mitochondrial antigens</b>				
Oxphos Complex III core 2 subunit (Oxphos III), human	Mouse, monoclonal	1:500	1:1,000	Invitrogen, Karlsruhe, Germany. Cat. no: A11143
Superoxide dismutase 1 (SOD1), rat	Rabbit, polyclonal	-	1:6,000	Fitzgerald Industries International, Inc, USA. Cat. no:RDI-RTSODabR
Superoxide dismutase 2 (SOD2), rat	Rabbit, polyclonal	1:5,000	1:6,000	Research Diagnostics, Inc., NJ, USA, Cat. no: RDI-RTSODMabR
<b>Osteoblast-specific antigens</b>				
Alkaline phosphatase (ALP), human	Sheep, polyclonal	1:1,000	-	Acris Antibodies GmbH, Hiddenhausen, Germany, Cat. no: BP237
Osteocalcin (BGP), mouse	Goat, polyclonal	1:100	-	Acris Antibodies GmbH, Hiddenhausen, Germany, Cat. no: BP712
Osteopontin (OPN), mouse	Mouse, monoclonal	1:600	-	Santa Cruz Biotechnology Inc., Heidelberg, Germany, Cat. no: sc-21742
Osteopontin (OPN), rat	Mouse, monoclonal	-	1:10	Developmental Studies Hybridoma Bank (DSHB), University of Iowa, Department of Biology, Iowa City, Iowa. Cat. no: MPIIIB10(1)
Runt-related transcription factor 2 (RUNX2), mouse	Rabbit, polyclonal	1:500	-	Santa Cruz Biotechnology Inc., Heidelberg, Germany, Cat. no:sc-10758
Runt-related transcription factor 2 (RUNX2), mouse	Mouse, monoclonal	1:500	1:800	MBL, Naka-ku Nagoya, Japan. Cat. D130-3
<b>Transcription factor and signaling molecules</b>				
Peroxisome proliferator-activated receptor $\alpha$ (PPAR $\alpha$ ), human	Rabbit, polyclonal	-	1:600	Santa Cruz Biotechnology Inc., Heidelberg, Germany, Cat. no:sc-9000
Peroxisome proliferator-activated receptor $\gamma$ (PPAR $\gamma$ ), human	Rabbit, polyclonal	-	1:600	Santa Cruz Biotechnology Inc., Heidelberg, Germany, Cat. no:sc-7196
$\beta$ -Catenin, mouse	Mouse, monoclonal	1:600	1:1,000	BD Transduction Laboratories™, Franklin Lakes, USA, Cat. no:610154
Forkhead box o 1 (FoxO1), human	Rabbit, polyclonal	1:600	1:1,000	New England Biolabs GmbH, Frankfurt Am main, Germany, Cat. no: 2880
Nuclear factor erythroid 2-related factor 2 (Nrf2), human	Rabbit, polyclonal	-	1:250	Santa Cruz Biotechnology Inc., Heidelberg, Germany, Cat. no:sc-13032
I $\kappa$ B- $\alpha$ , human	Rabbit, polyclonal	1:200	1:500	Santa Cruz Biotechnology Inc., Heidelberg, Germany, Cat. no:sc-847
Phospho-Glycogen synthase kinase -3 $\alpha$ / $\beta$ (p-GSK-3 $\alpha$ / $\beta$ ), human	Rabbit, polyclonal	-	1:1,000	New England Biolabs GmbH, Frankfurt Am main, Germany, Cat. no: 9331
<b>Others</b>				
Cyclin D1, human	Rabbit, polyclonal	-	1:600	Santa Cruz Biotechnology Inc., Heidelberg, Germany, Cat. no:sc-753
Heme oxygenase 1 (HO-1), rat	Rabbit, polyclonal	1:2,000	1:2,000	Assay Designs, Inc. Michigan, USA, Cat.no:SPA-895
Ki67, mouse	Rat, monoclonal	1:600	-	Dakocytomation, Denmark, Cat. no: M7249
$\alpha$ -tubulin, mouse	Mouse, monoclonal	-	1:5,000	Sigma, Steinheim, Germany. Cat. no: T5168
Glyceraldehyde 3-phosphate dehydrogenase (GAPDH), rabbit	Mouse, monoclonal	-	1:10,000	HyTest Ltd, Turku, Finland, Cat. no: 5G4

**Table 16. List of secondary antibodies in the present study**

Secondary detection system used	Host	Method	Dilution	Supplier
Anti Rabbit-IgG Alexa Fluor 488	Donkey	IF	1:600	Molecular Probes/Invitrogen, Cat. no: A21206
Anti Sheep-IgG Rhodamine Red-X	Donkey	IF	1:600	Dianova, Hamburg, Germany, Cat no: 713-295-147
Anti rat-IgG Alexa Fluor 594	Goat	IF	1:600	Molecular Probes/Invitrogen, Cat. no: A11007
Anti mouse-IgG Texas Red	Horse	IF	1:200	Vector laboratories, Inc, Burlingame, USA, Cat. no: TI-2000
Anti goat-IgG Alexa Fluor 594	Chicken	IF	1:600	Molecular Probes/Invitrogen, Cat. no: A11007
Anti mouse IgG alkaline phosphatase	Goat	WB	1:20,000	Sigma, Steinheim, Germany. Cat. no: A3562
Anti rabbit IgG alkaline phosphatase	Goat	WB	1:20,000	Sigma, Steinheim, Germany. Cat. no: A3562

## **3.2 Methods**

### **3.2.1 Alcian Blue/Alizarin Red staining of cartilage and bone in mice**

The E19 pups were anaesthetised intraperitoneally with a combination of xylazine (13µg/g b.w.) and ketamine (65µg/g b.w.). Thereafter, they were fixed in an ample volume of 96% ethanol for at least seven days. Prior to staining, skin and viscera were carefully removed. Afterwards, the mice were immersed in approximately 20ml of Alcian Blue solution and incubated for three days. Then 96% ethanol was used to rinse the preparations at least twice to remove debris. In the following step, the skeletons were cleared in 2% KOH for approximately 12h and the bones were stained in Alizarin red solution overnight. Thereafter, the skeletons remained in destaining solution for 2-3 days and any remaining loose bits of undissolved tissues were dissected out. The destaining solution was changed daily. Finally, the skeletons were passed through a series of glycerol/ethanol (each of the 20% and 50% glycerols for 1-2 days, and stored in 100% glycerol. The skeletal preparations in 100% glycerol were photographed with a canon camera.

### **3.2.2 Scanning of wildtype and PEX11β KO mice with flat-panel volumetric computed tomography**

#### **3.2.2.1 FpvCT and Scan Parameters**

Radiological analysis was performed with a flat-panel volumetric computed tomography (fpvCT) (Fig5) from General Electric company (GE), a research CT system, in conjunction with Dr. Obert from the Department of Neuroradiology at the Justus Liebig University of Giessen (Obert et al., 2005). This CT scanner uses

flat-panel detectors for radiation detection, which is the characteristic feature of a high-resolution CT system. The detectors consist of cesium iodide deposited on an amorphous silicon photosensitive array. The volume imaged with the applied acquisition protocol was 13.6cm diameter in the xy plane x 4.2cm in Z direction. In all scans, projection data of 1000 columns and 360 rows were used from the 1,024 x 1,024 detector matrix. 1000 views were acquired within a single gantry rotation protocol with a scan time of 8s at 70kV and 200mA.

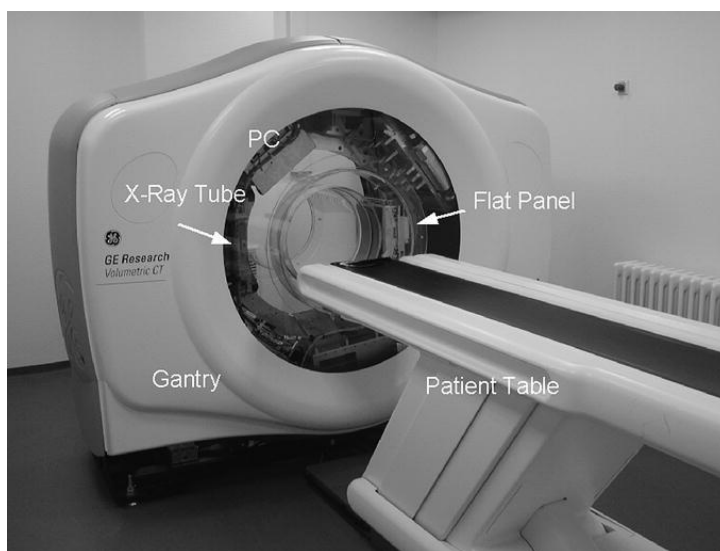


**Fig5.** The flat-panel based volumetric Computer Tomography (fpvCT).

### **3.2.2.2 Calibration device**

A small Plexiglas specimen holder was prepared, which served as holder for the mouse pups and the calibration phantom for bone density estimates. The specimen holder consisted of two 10cm x 10cm x 0.6cm Plexiglas plates with a matrix of drill holes, in which the individual bore hole had a diameter of a plastic straw. Different straws with a length of 10cm were sealed on one end with silicon paste and filled with H<sub>2</sub>O or aqueous solutions of 50, 100, 200, and 400mg K<sub>2</sub>HPO<sub>4</sub> per ml H<sub>2</sub>O. Thereafter, the ends of the straws were also closed. The

different  $K_2HPO_4$  concentrations were used to produce a calibration curve that mimicked the calcium concentration in the skeleton. Additional straws were mounted between the edge bore holes of the Plexiglas plates to produce a stable holder. The calibration straws were positioned parallel to each other defining the bottom of the holder. A thin plastic sheet was positioned above the calibration straws that formed the holder of the mouse-pup bodies. The holder was placed on the specimen holder of the fpvCT such that mice as well as the calibration straws could be imaged together. The calibration straws were positioned precisely parallel to the Z direction of the fpvCT so that cross-sections of each straw with different  $K_2HPO_4$  concentrations were visible in each sectional image of the scan.

Each mouse was scanned three times with a slightly different rotated positioning on the phantom holder so that partial volume effects could be estimated. The phantom was used not only for calibration purposes in each CT measurement, but also for a correction of the uniformity of the Z-image-plane of the VCT.

### ***3.2.2.3 Image reconstruction***

VCT image analysis was done in cooperation with Dr. Martin Obert. The data were reconstructed with a cone-beam filtered back-projection algorithm into a  $512 \times 512 \times k$  voxel matrix, where k ranged from approximately 200 to 400 depending on the length in the Z-direction of the specimen. The final 12 bit DICOM image data had isotropic voxel sizes of  $(0.100\text{mm})^3$ . A LINUX cluster with 7 dual 2.2GHz processor PCs was used to perform the reconstruction. The reconstruction time for a data volume consisting of  $512^3$  voxels was approximately 13min.

#### ***3.2.2.4 Image visualization***

Visualization of the data was performed with an Advantage Workstation, Version 4.1, GE Medical Systems, USA, a LINUX based dual 2.2GHz processor PC with 4GB RAM. Using that workstation, the volume data were visualized as maximum intensity projection (MIP). Dr. Obert developed software (IDL, Version 6.0, RSI, Boulder, CO, USA) that enabled the measurement of bone volume [mm<sup>3</sup>], bone mass [mg], and bone density [mg/mm<sup>3</sup>] of a complete mouse body. Averages were calculated of three scans for each mouse. The following steps were necessary to conduct the evaluation of each mouse scan: The 3D-data sets were transferred to an Advantage Workstation. The visualization tools of the workstation had been used to find the 3D-coordinates of a small cuboid that contained just the complete body of the scanner mouse. These coordinates were tabulated and used by the IDL program that performed a segmentation of the mouse-pup body based on Hounsfield Unit (HU) thresholding within the described cuboid. The software then automatically detected the straws with the different calibration liquids within the image data. Measurement of the HU in the areas of known concentration of bone density within the straw calibration phantoms allowed the linear conversion of HU to bone density of the mouse body, in units of mg/mm<sup>3</sup>. As result, the program returned volume, mass, and density of the complete mouse bones.

#### ***3.2.3 Perfusion fixation of mice and processing of mouse tissues for paraffin embedding and sectioning***

Five wildtype C57Bl/6J mice at the age of 40 days were anesthetized with isoflurane and subsequent intraperitoneal injection of a mixture of ketamine/xylazine. The skin was removed by median vertical incision from the

pelvis to the mandible, loosened with a scissor and fixed beside the animal on both sides with a needle. The thorax was opened sagittally through the sternum and cut laterally in the last intercoastal space. The heart was punctured with a 21 size gauge needle connected to a perfusion system with a rotating pump. After a short rinse with 0.9% NaCl to remove blood cells, perfusion fixation was carried out for 5min via the left ventricle of the heart using freshly prepared 4% paraformaldehyde in PBS, pH 7.4. Mouse femora, knee joint and vertebrae were dissected out and immersion fixed overnight in the same fixative. The femora, knee joints and vertebrae were decalcified with 10% EDTA at 4°C for 7d. Thereafter, the specimens were embedded into paraffin using a Leica TP 1020 automated vacuum infiltration tissue processor with the following steps: 90min each- 70%, 80%, 90%, 3x 100% ethanol; 2h each: 2x xylene, 2x paraffin. Paraffin blocks were cut with a Leica RM2135 rotation microtome into sections of 3-4µm thickness.

Newborn (or E19) pups were anesthetized intraperitoneally with a combination of xylazine (13µg/g b.w.) and ketamine (65µg/g b.w.). The skin was removed from the thorax by median vertical incision, loosened with a scissor and removed from the ribs. Thereafter the mouse pups were perfused through the heart with 4% freshly depolymerized paraformaldehyde in PBS, pH 7.4. After postfixation for 24h by immersion in the same fixative, the animals were cut sagittally in two halves and embedded in paraffin using the above-mentioned programme. 3-4µm sections of whole animals were cut with a Leica RM2135 rotation microtome and mounted on Superfrost Plus slides.

### ***3.2.4 Indirect immunofluorescence on bone or cartilage sections***

Prior to deparaffinization, sections were placed for a week at 37°C. Then, they were deparaffinized with xylene (3x 5min) followed by rehydration in a series of ethanol (2x 99%, 96%, 80%, 70%, 50% ethanol, 2min each step). For improved antigen retrieval and accessibility of epitopes, deparaffinized and rehydrated decalcified bone or cartilage sections from adult mice were subjected to digestion with 0.1% trypsin for 20min at 37°C and nondecalcified sections from newborn mice were microwaved in TEG buffer for 5-6min. Nonspecific binding sites were blocked with 4% BSA and 0.05% Tween 20 in PBS for 2h at room temperature (RT) and sections were incubated with primary antibodies (see Table 15) overnight at 4°C. On the following morning, the sections were rinsed carefully with PBS and thereafter incubated with the secondary antibodies (see table 16) for 2h at room temperature. Nuclei were labelled with Hoechst 33342 (2µg/ml). Negative control sections without primary antibody incubation were processed in parallel.

### ***3.2.5 Isolation and culture of primary osteoblasts***

Primary osteoblasts were isolated from E19 pups or newborn animals (P0.5). Calvariae were removed and washed with  $\alpha$ -MEM. The fibrous tissue surrounding the bone was gently scraped off with the tweezers. The calvariae were divided in two halves and the sutures were cut out. The trimmed calvariae were transferred to a 50ml Erlenmeyer flask containing 4mM EDTA and placed in a shaking water bath (37°C) for 10min, washed with PBS for 5min, and incubated a second time in 4mM EDTA at 37°C for 10min. Calvariae were then subjected to a series of collagenase digestions in a 37°C water bath with gently shaking. The first two

digests were discarded. Digests 3, 4, and 5 (15min each), which were sufficient to release all cells from small calvariae, were neutralized with  $\alpha$ -MEM, pooled, and filtered through a sterile polypropylene mesh with 200–297 $\mu\text{m}^2$  pore size into a 50ml tube. The filtrate was centrifuged for 5min at 1,000rpm, the supernatant was removed, and the cells were resuspended in  $\alpha$ -MEM containing 10% FCS and seeded into 35mm culture dishes. The next morning the medium was exchanged. Thereafter, the cells were cultivated to differentiate into osteoblasts with regular medium exchange every two days. Enhancement of mineralization was initiated from day 8 (or from day 10 in PEX11 $\beta$  experiments) by the addition of ascorbic acid (50 $\mu\text{g}/\text{ml}$ ) and  $\beta$ -glycerolphosphate (10mM). The identity of these cells as osteoblasts was confirmed by immunostaining for osteocalcin as a specific cell marker. The purity of the osteoblast cultures was higher than 95% (Fig6).

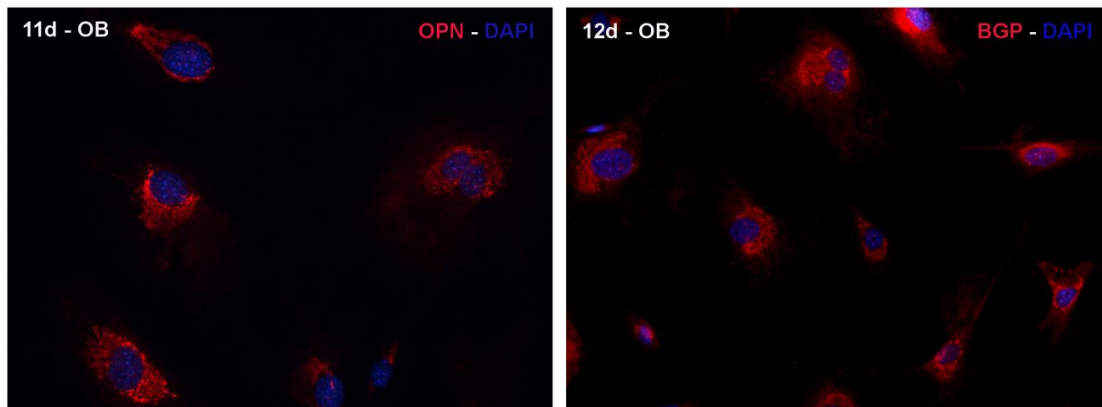


**Fig6.** Primary osteoblasts were labelled with the bone marker antibodies against osteopontin (OPN) or osteocalcin (BGP) to examine the purity of the osteoblast culture. The purity of the osteoblast cultures was higher than 95%.

### **3.2.6 Treatments with PPAR agonists and antagonists in osteoblasts**

For treatments with PPAR $\alpha$  or PPAR $\gamma$  agonists, osteoblasts were precultivated in 35mm dishes for 3 days. On day 4, they were trypsinized and reseeded onto 60mm culture dishes at a density of  $2.5 \times 10^4$  cells/cm<sup>2</sup>. Cells were grown for 24h and thereafter treated for 6 days, with the PPAR $\alpha$  agonist -ciprofibrate (100 $\mu$ M and 500 $\mu$ M). Similarly, osteoblasts were also treated with the PPAR $\gamma$  agonist - troglitazone (2 $\mu$ M and 10 $\mu$ M) for 6 days.

### **3.2.7 Indirect immunofluorescence on primary osteoblasts**

Primary osteoblasts grown on poly-L-lysine-coated coverslips were rinsed with PBS (pH 7.4) and fixed with 4% paraformaldehyde (PFA) in PBS for 20min at RT. After fixation, cells were washed three times with PBS. Thereafter, they were incubated for 10min in PBS containing 1% glycine and for an additional 10min in PBS containing 1% glycine and 0.3% Triton X-100 for permeabilization. After washing with PBS, cells were incubated for blocking of nonspecific protein binding sites for 30min in PBS containing 1% BSA and 0.05% Tween 20. After blocking, the coverslips were incubated with primary antibodies overnight at 4°C in a moist chamber, followed by extensively washing with PBS (3 $\times$  5min) and the incubation with secondary antibodies for 1h at RT. Nuclei were counterstained with Hoechst 33342 (2 $\mu$ g/ml). The high quality of immunofluorescence staining for the localization of specific proteins in distinct subcellular compartments (catalase and Pex14p for peroxisomes; SOD2 for mitochondria; Runx2 in nuclei) is shown in Fig7.

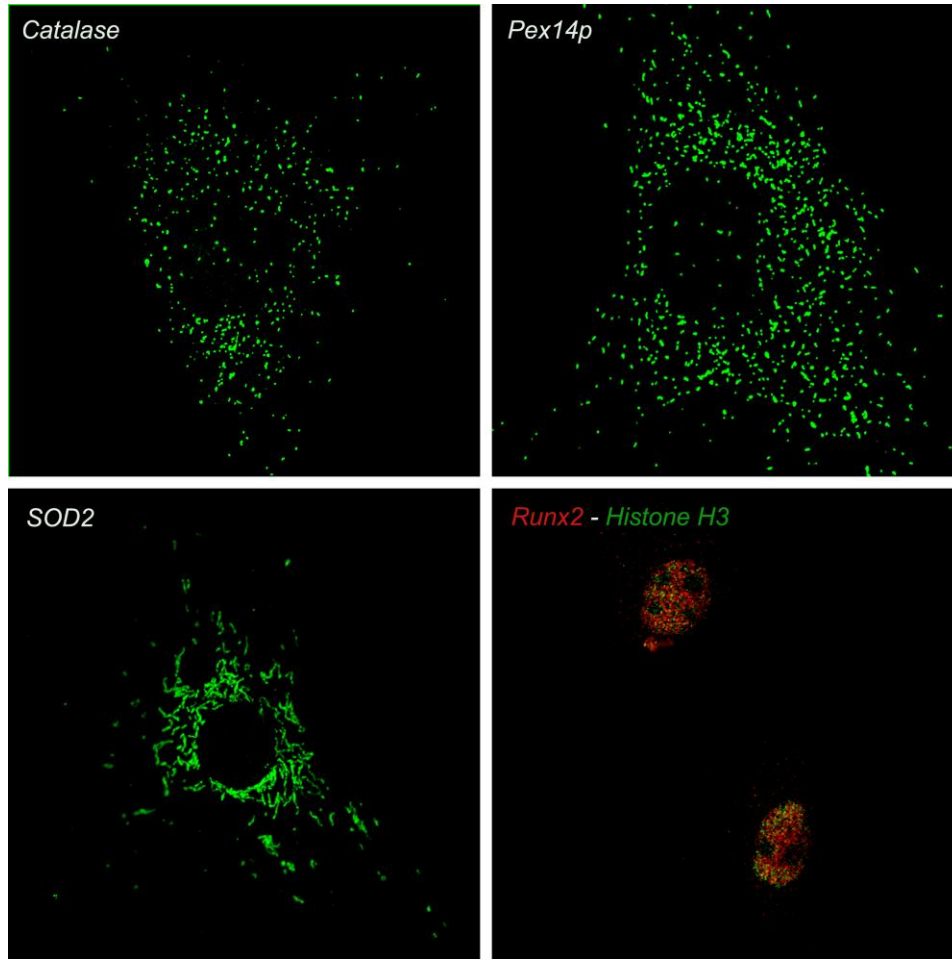


**Fig7.** Primary osteoblasts were labelled with different marker antibodies against catalase, pex14p, SOD2, Runx2 and Histone H3.

### ***3.2.8 Analysis of peroxisome abundance in osteoblasts***

Osteoblasts were stained after various time points of cultivation (3, 7, 11 and 15d) with a rabbit anti-mouse Pex14p antibody and a donkey anti-rabbit Alexa Fluor 488 secondary antibody for analysis of peroxisome abundance. For each time point, pictures from 50 osteoblasts were taken by confocal laser scanning microscopy (CLSM) with a Leica TCS SP2 using a 63× objective and setting at Airy1. The number of peroxisomes per  $\mu\text{m}^2$  was counted automatically in each

cell by using the Image-Pro Plus software (Media Cybernetics, USA). All different experiments were performed three times.

### ***3.2.9 Analysis of proliferation activity of osteoblasts at different time points***

To quantify osteoblast proliferation at different time points in cell cultures (3, 7, 11 and 15d), the expression of Ki67 was used as a marker for S, G2, and M phases. Osteoblasts were stained with the rat anti-mouse Ki67 antibody and a goat anti-rat Alexa Fluor 594 secondary antibody. Ki67 positive cells in comparison to the number of Hoechst 33342 positive nuclei were quantified with regular fluorescence microscopy using a 10× objective. For each time point, the number of Ki67 positive cells was counted in 10 different areas and each area contained approximately 100-150 cells. All counting experiments were performed three times.

### ***3.2.10 Mineralization analysis***

Osteoblasts were cultured at a density of  $1.0 \times 10^4$  cells/cm<sup>2</sup>. Differentiation was initiated on day 8 by the addition of ascorbic acid (50µg/ml) and β-glycerolphosphate (10mM). Mineralization analysis was performed at different time points in cell cultures (7, 15 and 23d). Briefly, cells were rinsed with PBS (pH 7.4) twice and incubated with 95% ethanol for 15min at RT. Thereafter, the cells were washed three times with distilled water and incubated in 0.1% Alizarin Red-S in Tris-HCl (pH 8.3) for 40 min at 37°C. After washing with distilled water (3× 5min), the stained cells in culture dishes were air-dried at RT. Finally, the different culture dishes were scanned with an ESPON perfection 1660 photo scanner.

### **3.2.11 RNA expression analysis by semiquantitative RT-PCR**

#### **3.2.11.1 RNA isolation**

Total RNA was isolated from primary osteoblasts using the RNeasy Mini Kit from Qiagen. Homogenization of cells in RLT buffer was performed either with an Ultra Turrax T25 basic homogenizer for 30sec or the lysate was pipetted directly into a QIAshredder spin column placed in a 2ml collection tube, and centrifuged for 2min at full speed. RNA extraction was carried out with the Qiagen RNeasy Mini kit according to the manufacturer's protocol (<http://www.qiagen.com/products/rnastabilizationpurification/rneasysystem/rneasymini.aspx>). The isolated RNA was redissolved in RNase free water and stored at -80°C for further use. The quantity and integrity of the isolated RNA was assessed by optical density measurements, obtaining the ratio of absorbance values at 260 and 280nm using a Bio-Rad spectrophotometer. The integrity of the RNA was analyzed by visualization of ethidium bromide-stained intact 28S, 18S and 5S ribosomal RNA bands in 1% denaturing formaldehyde agarose gels. For the consecutive RT-PCR experiments, the RNA samples with best quality were used.

#### **3.2.11.2 DNase I digestion**

Prior to reverse transcription, a DNase I digestion was performed to remove residual chromosomal DNA in the RNA preparation. One µg of the RNA sample was added to the DNase digestion mixture and incubated for 15min at RT. The DNase I was inactivated by the addition of 1µl of 25mM EDTA solution to the reaction mixture and heating for 10min at 65°C. Thereafter, the RNA sample was stored at -80°C for further experiments or was directly used for the subsequent reverse transcription reaction.

**Preparation of RNA samples for DNase digestion prior to RT-PCR**

RNA sample	1µg
10X DNase I reaction buffer	1µl
DNase I, amplification grade, 1U/µl	1µl
DEPC-treated water	to 10µl

**3.2.11.3 Reverse transcription**

Total RNA (0.5 - 1µg) was reverse-transcribed into cDNA using 0.5µg oligo (dT) 12-18 primers and 10mM dNTP mixtures as described in the protocol below.

Oligo(dT)12-18 (500µg/ml)	1µl
RNA (1µg)	~ 10µl
dNTP mixture (10mM each)	1µl
Sterile distilled water	to 12µl

For denaturation, the RNA mixture was heated to 65°C for 5min and thereafter immediately chilled on ice. Then, 4µl of 5X first strand buffer, 2µl of 0.1M DTT and 1µl of RNaseOUT™ (40U/µl) were added to the reaction mixture.

The reaction mixture was mixed gently and incubated at 42°C for 2min. Finally, 1µl of SuperScript™ II Reverse Transcriptase (200U) was added and the complete solution was incubated at 42°C for 50min for reverse transcription. The reaction was inactivated by heating at 70°C for 15min.

**3.2.11.4 Primer design**

All primers used in this study are described in table 14. For primer design, all corresponding complete cDNA sequences of mRNAs to be analyzed were downloaded from the *Nucleotide Database* of the NCBI (<http://www.ncbi.nlm.nih.gov/nucleotide/>). For a standard PCR, 20-22bp long primer sequences were selected with the *Primer3* online software (<http://frodo.wi.mit.edu>). The AT and GC content was set between 40%-60% and the difference in the melting

temperature ( $T_m$ ) between the forward and reverse primers was kept in a range of 2-4°C.

Intron-spanning primers were designed to prevent amplification of genomic DNA. The specificity of each primer was confirmed by BLAST searches against the EST and non-redundant mouse transcriptome databases (<http://www.ncbi.nlm.nih.gov/blast/Blast.cgi>). Only primers which in the BLAST search gave no matching results at their 3' ends were selected. All primers were ordered online from Operon (<https://www.operon.com>). Each primer pair was tested and the PCR conditions optimized in a gradient PCR from 55°C-70°C on a BioRad iCycler.

### **3.2.12 Western Blot analysis**

#### **3.2.12.1 Isolation of proteins from osteoblasts**

##### **3.2.12.1.1 Isolation of whole cell lysates from osteoblasts**

Whole cell lysates were obtained in two ways: 1) Primary osteoblasts were rinsed with PBS and suspended with 10 volume of cold lysis buffer (50mM Tris-HCl, pH 7.2, 250mM NaCl, 0.1% NP-40, 2mM EDTA, 10% glycerol) containing appropriate protease inhibitors. Incubation was done on a rotating shaker for 30min at 4°C. Thereafter, the solution was sonicated briefly (up to 10s). Finally, the tube was centrifuged at 12,000g for 10min at 4°C and the supernatant was collected for subsequent experiments. 2) Primary osteoblasts were washed with PBS to remove residual media. Thereafter, 400µl of 1x lysis buffer from Cell Signaling Technology Corp. was added per 10cm cell culture dish. The cells in the culture dishes were incubated on ice for 5min. In the following step, they were scraped off with a rubber cell scraper and sonicated briefly. Finally, they

were spun for 10min at 14,000g in a cold (4°C) microfuge and the supernatants were collected for further use.

### ***3.2.12.1.2 Isolation of nuclear proteins from osteoblasts***

After washing with ice-cold PBS, the cells were suspended with cold low salt buffer A (10mM HEPES/KOH, pH 7.9, 10mM KCl, 0.1mM EDTA, 0.1mM EGTA, 1mM  $\beta$ -mercaptoethanol) containing 10% protease inhibitor mix M (SERVA, Heidelberg, Germany). After incubation on ice for 10min, 10 $\mu$ l of 10% NP-40 was added and cells were lysed by gentle vortexing. The homogenate was centrifuged for 10s at 16,000g in a microfuge. The supernatant representing the cytosolic fraction was collected and the pellet containing the cell nuclei was washed 4 additional times in buffer A by centrifugation at 16,000g for 10s. Thereafter, the nuclear pellet was dissolved in high salt buffer C (20mM HEPES/KOH, pH 7.9, 400mM NaCl, 1mM EDTA, 1mM EGTA, 1mM  $\beta$ -Mercaptoethanol, and 10% protease inhibitor mix M). The tubes were incubated for 15min on ice, and centrifuged for 10min at 16,000g at 4°C. The supernatant representing the nuclear extract was collected.

### ***3.2.12.1.3 Isolation of enriched peroxisomal fractions from osteoblasts***

Primary osteoblasts were harvested and homogenized with a single stroke (2min, 1000rpm) using a Potter-Elvehjem homogenizer (Potter-S; B. Braun, Melsungen, Germany) in homogenization medium (HM: 5mM MOPS, pH 7.4, 250mM sucrose, 1mM EDTA, 0.1% [v/v] ethanol, 0.2mM dithiothreitol, 1mM 6-aminocaproic acid) supplemented with 10% protease inhibitor mix M. The homogenate was centrifuged at 500g for 10min. The resulting supernatant (S1a) was kept on ice, and the pellet was resuspended in HM and recentrifuged at

500g for 10min, resulting in the supernatant (S1b) and the pellet (P1) with unbroken cells and nuclei. The pooled supernatant S1 (S1a + S1b) was further subjected to centrifugation at 1,900g for 10min, the supernatant (S2a) was collected and kept on ice, and the pellet was dissolved in HM and recentrifuged at 1,900g for 10min, resulting in the supernatant (S2b) and the pellet (P2) with large mitochondria. The pooled supernatant S2 (S2a + S2b) was centrifuged at 50,000g for 20min to yield the enriched peroxisomal fraction (pellet) and the supernatant (S3a). The enriched peroxisomal pellet was resuspended in HM and recentrifuged at 50,000g for 20min, yielding the enriched peroxisomal fraction (P3) and the supernatant (S3b). The supernatant S3a plus S3b were combined (S3). Fractions S2, P2, S3, and P3 were analyzed by Western blotting. The enriched peroxisomal fraction is a mixed organelle fraction, also known as light mitochondrial fraction (LM) or D-fraction, containing a high amount of peroxisomes with medium size as well as small mitochondria, lysosomes, and a lower amount of microsomal vesicles.

### ***3.2.12.2 Preparation of Western blots***

Protein concentrations of the samples were determined with the Bradford method using BSA as a standard (Bradford, 1976). The protein samples (7-30 $\mu$ g) were separated on 12% SDS polyacrylamide gels and transferred onto polyvinylidene fluoride (PVDF) membranes. Nonspecific protein-binding sites were blocked with Tris-buffered saline (TBS) containing 10% nonfat milk powder and 0.05% Tween-20 for 1h. The blots were incubated overnight at 4°C or for 1h at RT with primary antibodies. Following the primary antibody incubation, the membranes were washed 3 times and thereafter directly incubated for 1h at RT with alkaline phosphatase-conjugated secondary antibodies. Alkaline

phosphatase activity was detected using the Immun-Star™ AP substrate from Bio-Rad (Munich, Germany) and exposure of the blots to Kodak Biomax MR Films. Blots were scanned with an AGFA scanner. All Western blot analyses were performed three times.

### ***3.2.13 Statistical Analysis***

For statistical evaluation, data were compared using One-way ANOVA test and  $P < 0.05$  was considered as significant. Data are presented as the mean  $\pm$  SEM.

## **4 Results**

Even though children with peroxisomal diseases exhibit severe ossification defects, to date nothing is known about the function of peroxisomes in different cell types of the skeleton. Therefore, in the first part of this section, this cell compartment was characterized in different cell types of the skeleton during intramembranous and endochondral ossification processes. In addition, these results were completed with studies in differentiating primary osteoblast cultures and the analysis of functional alterations after treatment with peroxisome proliferator activated receptor (PPAR) agonists.

In the second part of the result section, studies on PEX11 $\beta$  KO mice were performed to investigate the molecular pathogenesis of ossification defects observed in children with peroxisomal diseases. The PEX11 $\beta$  KO mouse model proved to be an ideal animal model for studying the consequences of peroxisome proliferation deficiency in different cell types of the skeleton.

### ***4.1 Characterization of the peroxisomal compartment in cartilage and bone***

#### ***4.1.1 Peroxisomes are present with heterogeneous abundance in different cell types of the skeleton***

Immunostaining preparations on paraffin-embedded sections for the localization of the peroxisomal biogenesis marker Pex14p revealed the presence of peroxisomes in all cell types of the skeleton (Fig8a-b, Fig9a-b, Fig10a and Fig11a). Peroxisomes could already be detected as individual organelles by regular fluorescence microscopy (Fig8), but were resolved much better by using

confocal laser scanning microscopy, especially in hypertrophic chondrocytes and osteoblasts (Fig9, Fig11). Clear differences were noted in the number of Pex14p-positive particles and the intensities of individual signal. Pex14p-positive peroxisomes were most abundant in hypertrophic chondrocytes (Fig8a-b, Fig9a-b). Peroxisomes in proliferating chondrocytes were less numerous and chondrocytes of reserve zone only contained very few peroxisomes (Fig8a-b, Fig9a-b). In addition to hypertrophic chondrocytes, osteoblasts were also intensively labelled for Pex14p, whereas only a weak staining was observed in osteocytes (Fig10a, Fig11a).

#### ***4.1.2 Matrix proteins for ROS and lipid metabolism also exhibit a heterogeneous distribution in peroxisomes of cartilage and bone***

Most knowledge on peroxisomal metabolic pathways has been obtained from results of experiments in liver and kidney. In these organs, peroxisomes are rich in enzymes involved in ROS and lipid metabolism. Therefore, antibodies against the H<sub>2</sub>O<sub>2</sub>-decomposing enzyme catalase and against the major lipid transporter ABCD3, formerly called PMP70, were used for labelling of peroxisomal metabolic pathways in different cell types of the skeleton. The ROS metabolizing enzyme-catalase was distributed in a similar pattern as Pex14p with the staining intensities, showing a continuous increase from chondrocytes of the reserve zone to hypertrophic chondrocytes (Fig8c-d, Fig9c-d). Osteoblasts also showed strong catalase immunoreactivity (Fig10b, Fig11b). In contrast, the peroxisomal ABC transporter ABCD3 was strongly enriched in hypertrophic chondrocytes (Fig8e-f, Fig9e-f). Other chondrocytes were only very weakly stained for ABCD3 or remained negative.

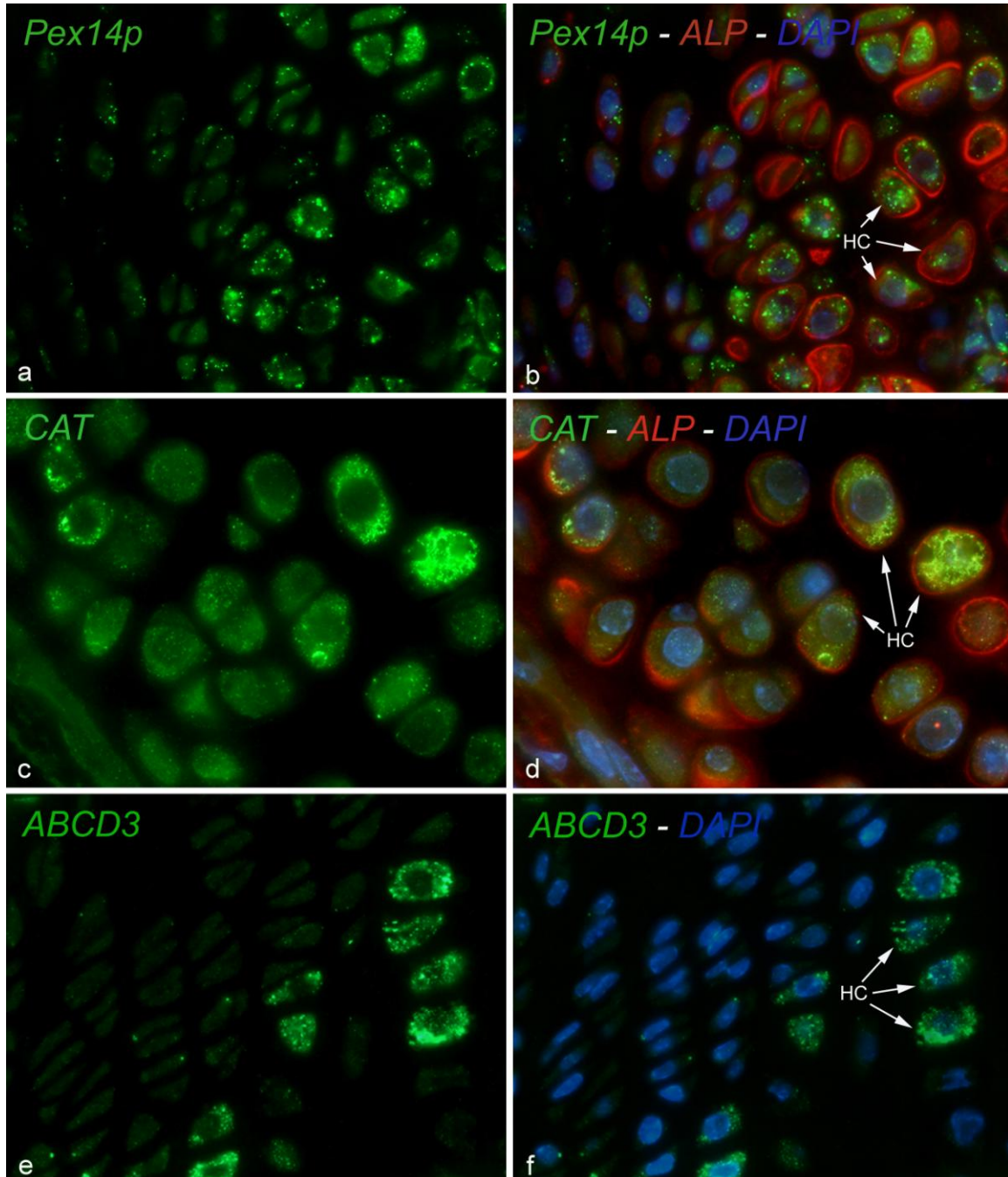


**Fig8. Detection of peroxisomes in distinct cell types of the skeleton by immunostainings for peroxisomal marker proteins using regular fluorescence microscopy. Stainings in a-d: vertebrae; e-f: femur growth plate.** Staining for the peroxisomal biogenesis protein Pex14p revealed a higher intensity in hypertrophic chondrocytes (**a, b**). The peroxisomal metabolic enzyme catalase exhibited the same pattern as Pex14p (**c, d**). In contrast, the ABC transporter-ABCD3 was only enriched in hypertrophic chondrocyte (**e, f**). HC: hypertrophic chondrocytes.

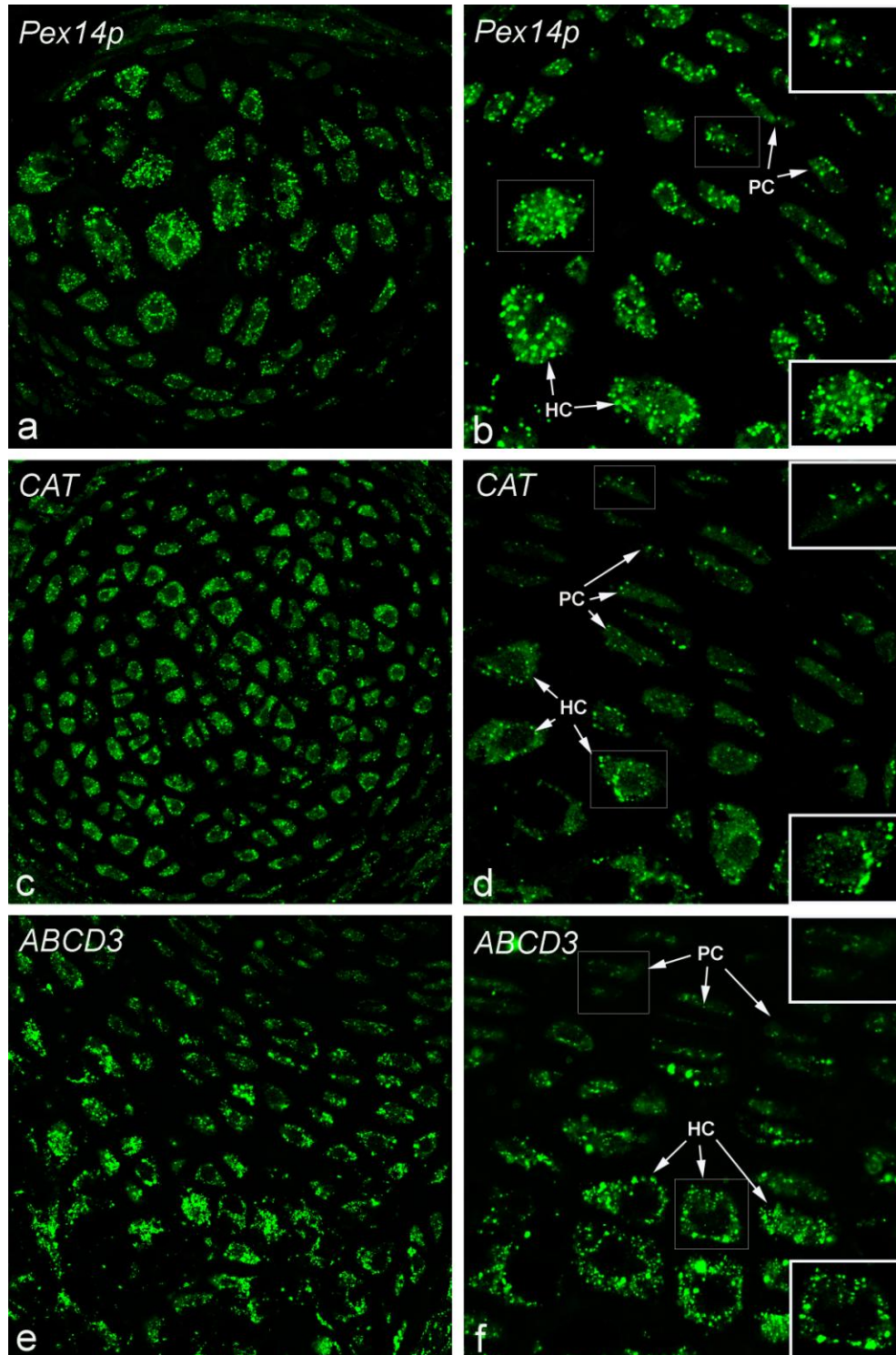


**Fig9. Immunofluorescence detection of peroxisomal proteins in distinct cell types of the embryonic skeleton by confocal laser scanning microscopy.** Staining with antibodies against peroxisomal marker proteins—Pex14p, catalase and ABCD3 revealed that peroxisomes were abundant in hypertrophic chondrocytes in comparison to proliferative chondrocytes in embryonic ribs (a-f). PC: proliferative chondrocytes; HC: hypertrophic chondrocytes.

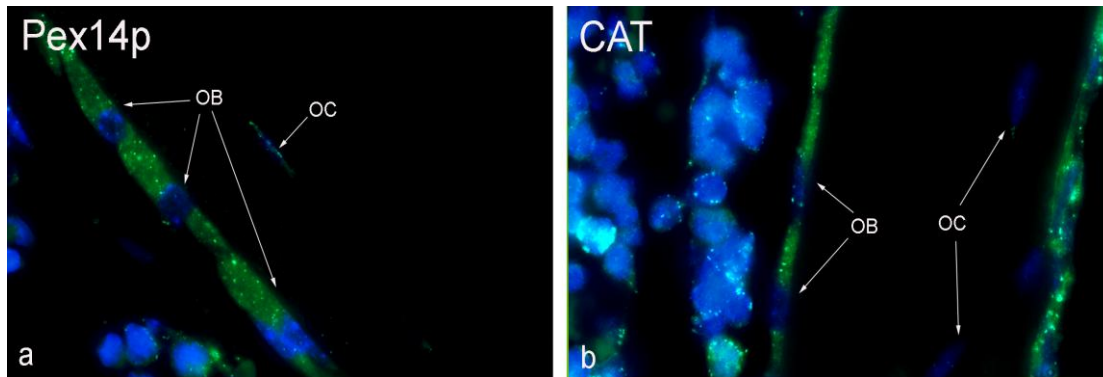


**Fig10. Distribution of peroxisomes in different cell types of a mouse vertebra by regular fluorescence microscopy.** Stainings for the peroxisomal membrane protein Pex14p and the metabolic enzyme catalase in a mouse vertebra (**a,b**). OB: osteoblasts; OC: osteocytes.

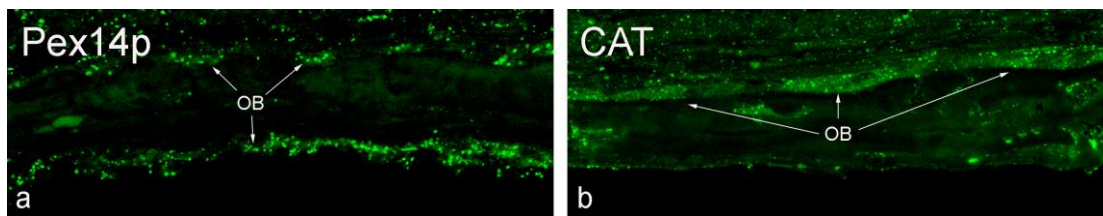
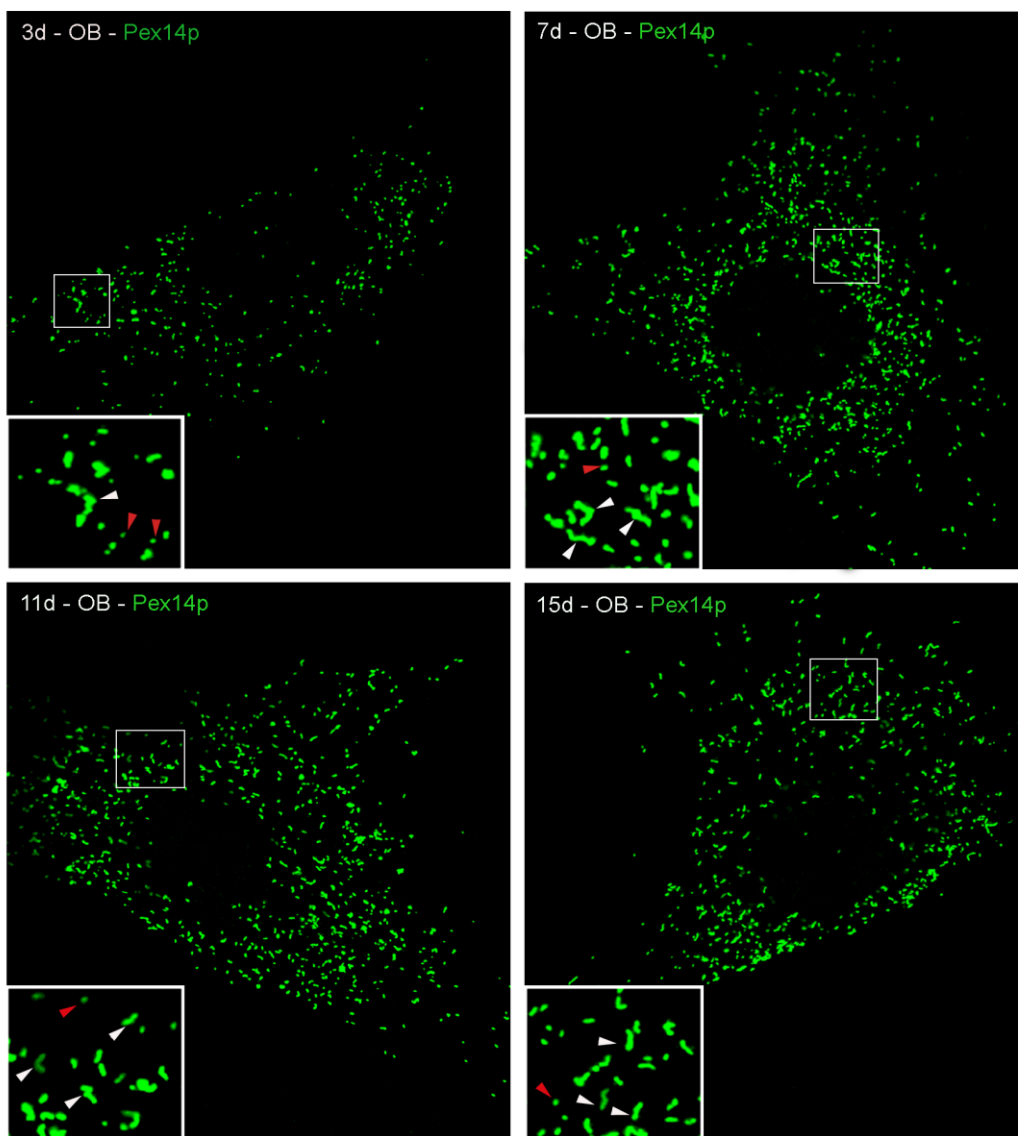


**Fig11. Localization of peroxisomal proteins in the calvaria of a mouse embryo by confocal laser scanning microscopy.** Positive immunoreactivity for Pex14p and catalase was observed in the calvaria of a mouse embryo, showing a higher intensity in osteoblasts in comparison to osteocytes (**a, b**). OB: osteoblasts.

#### ***4.1.3 Peroxisome numerical abundance is inverse proportional to osteoblast proliferation and parallels osteoblast differentiation***

As known from **4.1.1**, the peroxisomal biogenesis protein, Pex14p is the best marker to analyze peroxisome numerical abundance. Immunofluorescence analysis for this protein in primary osteoblasts of different time points revealed that peroxisome abundance was significantly altered during osteoblast differentiation (time points of analyses: 3d, 7d, 11d and 15d) (Fig12). In the early osteoblasts (3d), the number of peroxisomes was lowest ( $0.189 \pm 0.037/\mu\text{m}^2$ ). Furthermore, most peroxisomes were spherical and only

few tubular peroxisomes could be observed at this stage. In comparison to early osteoblasts, osteoblasts in cultures of later time points showed a higher number of peroxisomes (Fig12). Osteoblasts at day 7 exhibited a 30% increase in peroxisome number compared with 3d osteoblasts (7d:0.244±0.036/μm<sup>2</sup>). Moreover, more tubular peroxisomes were detected from this stage (7d, 11d and 15d).



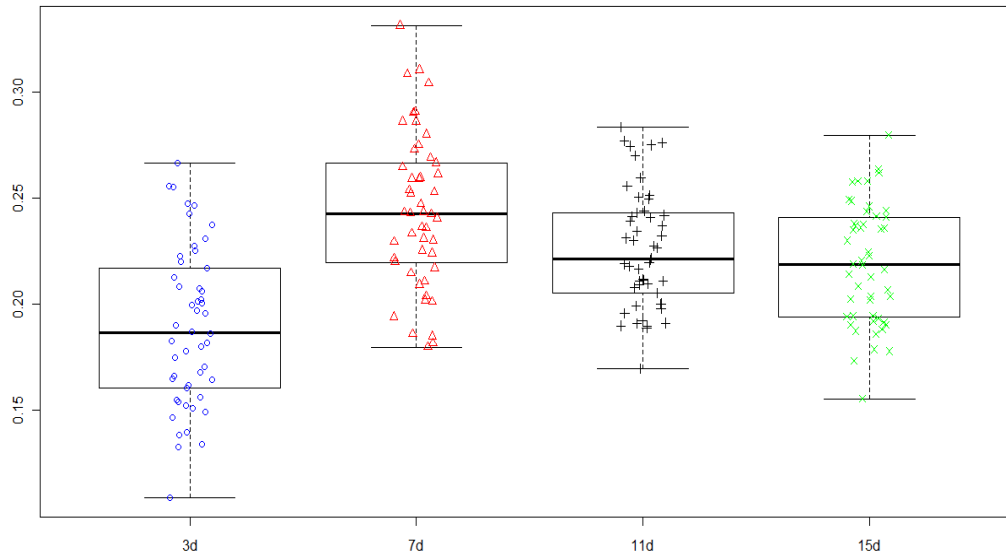


**Fig12. Morphometric analysis of the numerical abundance of peroxisomes at various time points.** Osteoblasts were harvested at various time points (3d, 7d, 11d and 15d) and stained for Pex14p to analyze the peroxisome abundance. The morphometric analysis of Pex14p-positive particles revealed that the numerical abundance of peroxisomes was lowest at day3. Peroxisomes were present in a highest amount at day 7 and thereafter maintained a high level. Statistical analysis was performed to check for significant alterations of the peroxisome abundance at different time points. Compared to 3d osteoblasts, osteoblasts contained a significantly higher numerical abundance of peroxisomes at day7, day 11 and day 15 with P value of less than 0.001. A significantly higher peroxisomal abundance was also noted in 7d osteoblasts in comparison to 11d and 15d osteoblasts ( $P < 0.01$ ). However, no difference between 11d and 15d osteoblasts was observed ( $P > 0.05$ ). Red arrow head: spherical peroxisomes; white arrow head: tubular peroxisomes.

To relate the alteration of the peroxisomal compartment to osteoblast proliferation, we analyzed the Ki67 protein expression, a marker of late G1, S, G2, and M phases, often used to detect cell proliferation. Immunofluorescence preparations for Ki67 revealed that osteoblasts had the highest proliferation rate at day 3 ( $0.630 \pm 0.048$ ). Thereafter, the proliferation rate decreased (Fig13) (7d:  $0.276 \pm 0.020$ ; 11d:  $0.233 \pm 0.023$ ; 15d:  $0.227 \pm 0.011$ ). Taken together, our data indicate that peroxisome proliferation is inversely proportional to osteoblast proliferation and is occurring during osteoblast differentiation.

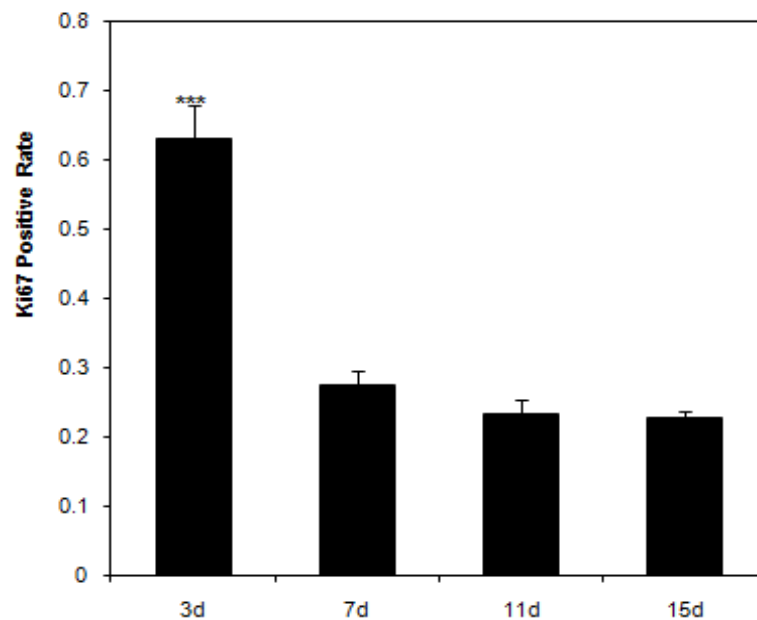
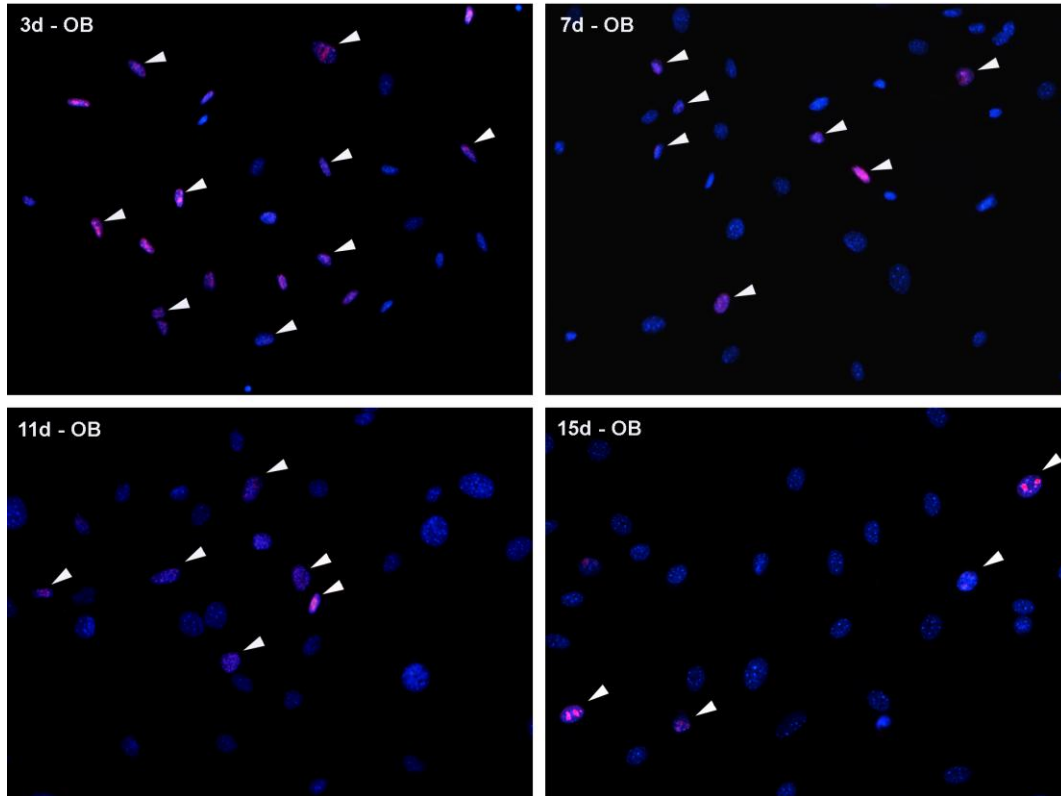


**Fig13. Detections of osteoblast proliferation rates at different time points.** To determine osteoblast proliferation rates at different time points, we analyzed the expression of the Ki67 protein. Staining for Ki67 antibody revealed that osteoblasts exhibited the highest proliferative rate at 3d, and then decreased. Compared to 3d osteoblasts, proliferation rates were much lower at day 7, day 11 and day 15. P values were less than 0.001. White arrow head: Ki67-positive osteoblasts.

#### ***4.1.4 The heterogeneity of the peroxisome compartment is preserved during osteoblast differentiation***

Using semiquantitative RT-PCR, the expression levels of mRNAs encoding peroxisomal proteins were determined in primary osteoblasts. Calculation of differences in mRNA expression levels were done by normalizing the RT-PCR band intensities of related genes to the band intensity of GAPDH of the same cDNA preparation. Messenger RNAs for catalase, PEX14, MFP2 and ABCD3 were present at very low amounts in the early osteoblasts (3d). Their levels reached a maximum at day 7 or day 11 (compared with 3d osteoblasts, catalase: 2.2-fold induction; PEX14:1.5-fold induction; MFP2: 1.3-fold induction; ABCD3: 1.2-fold induction) and decreased at day 15 again (Fig14). Similarly, the mRNA levels of MFP1, PEX11 $\beta$ , OPN and RUNX2 were also present at lower levels initially (3d) in comparison to the later stages (Fig14). By contrast, PEX11 $\alpha$ , PPAR $\alpha$  and ABCD1 mRNA levels were upregulated continuously in a time-dependent manner. In comparison to 3d osteoblasts, the expression levels for PEX11 $\alpha$ , PPAR $\alpha$  and ABCD1 increased about 1.2-fold, 1.5-fold and 1.3-fold at day 15, respectively (Fig14). Interestingly, the mRNA level of the first enzyme of peroxisomal  $\beta$ -oxidation ACOX2 was higher at day 3 compared with 11d and 15d osteoblasts (Fig13). In addition, the expression level of PPAR $\gamma$  was reduced in a time-dependent manner and the level at day 15 exhibited a 35% decrease compared with 3d osteoblasts (Fig14). The mRNAs for other genes, such as ALP, PEX5, PEX13, ACOX1 and PPAR $\beta$  were not altered during these stages (Fig14).

To confirm the morphological and the RT-PCR results obtained from primary osteoblasts, Western blot analyses were performed using distinct subcellular fractions obtained by differential centrifugation from homogenized osteoblast

preparations. The highest abundance of Pex14p, the marker for peroxisomal membranes, was found in pellet 3, which corresponds to the enriched peroxisomal fraction, containing medium sized peroxisomes and small mitochondria. The amount of Pex14p was lower in pellet 2, which contains mostly large mitochondria and large peroxisomes. OPN, a bone marker protein, was present at higher amounts in pellet 2, where in addition to heavy mitochondria, apparently also Golgi apparatus and large secretory vesicles are present. In contrast, the highest level of the complex III of the respiratory chain (Oxphos III core 2), was observed in pellet 2 (heavy mitochondria), followed by pellet 3 (light mitochondria) (Fig15A). Due to enrichment of different organelles in distinct pellets, the corresponding subcellular fractions were used to detect different marker proteins at various time points of primary osteoblast cultures. Western blot analyses revealed that peroxisomal metabolic enzymes, such as catalase and thiolase exhibited the lowest levels at the early stage (3d), and subsequently reached their maximum expression at day 7 (Fig15B), corroborating the mRNA results. In comparison to the mRNA levels, however, peroxisomal matrix proteins decreased again thereafter (Fig15B). By contrast, the lower levels of peroxisomal membrane proteins (ABCD3, Pex13p and Pex14p) were also found at day 3 and thereafter increased at day 7 (Fig15B). In addition, mitochondrial complex III of the respiratory chain was enhanced in a time-dependent manner (Fig15B) and the mitochondrial antioxidant protein SOD2 exhibited the highest abundance at day 11 (Fig15B). Moreover, a clear increase in the production of OPN was observed from day 7 to 15, suggesting differentiation of osteoblast into bone matrix synthesizing and secreting cells (Fig15B).

PPAR $\alpha$ , the nuclear receptor responsible for peroxisome proliferation, was present at low levels in nuclear fractions of 3d osteoblasts and most of the PPAR $\alpha$  protein was located in the cytoplasmic fraction (Fig15C). During osteoblast differentiation (7d-11d), a significant increase of PPAR $\alpha$  level in the nuclear fraction was observed (Fig15C), reflecting the PPAR $\alpha$  translocation into the nucleus for transcriptional activation. A shift of the PPAR $\alpha$  protein to the cytoplasm was noted at day 15, fitting well to the lower abundance of peroxisomal thiolase, a PPAR $\alpha$ -dependent gene of the peroxisomal  $\beta$ -oxidation pathway 1 (Fig15C).

To investigate the effect of calcium mineralization supplements in medium, ascorbic acid (50 $\mu$ g/ml) and  $\beta$ -glycerolphosphate (10mM) was added to the primary osteoblast cultures after day 7. Interestingly, the addition of these compounds into the culture exerted significant effects on peroxisomal thiolase and Pex14p expression at day 15 (Fig16). A significant increase of cytoplasmic Pex5p expression was also noted at day 15 (Fig16). Additionally, the addition of differentiation medium into the culture also resulted in the alteration of protein expression of OPN, showing low level of OPN expression at day 15 in comparison to day 7 (Fig16). Moreover, mineralization nodule staining showed that 15d osteoblasts incubated with differentiation medium had formed primary mineralization areas (Fig17), indicating maturation of these osteoblasts.

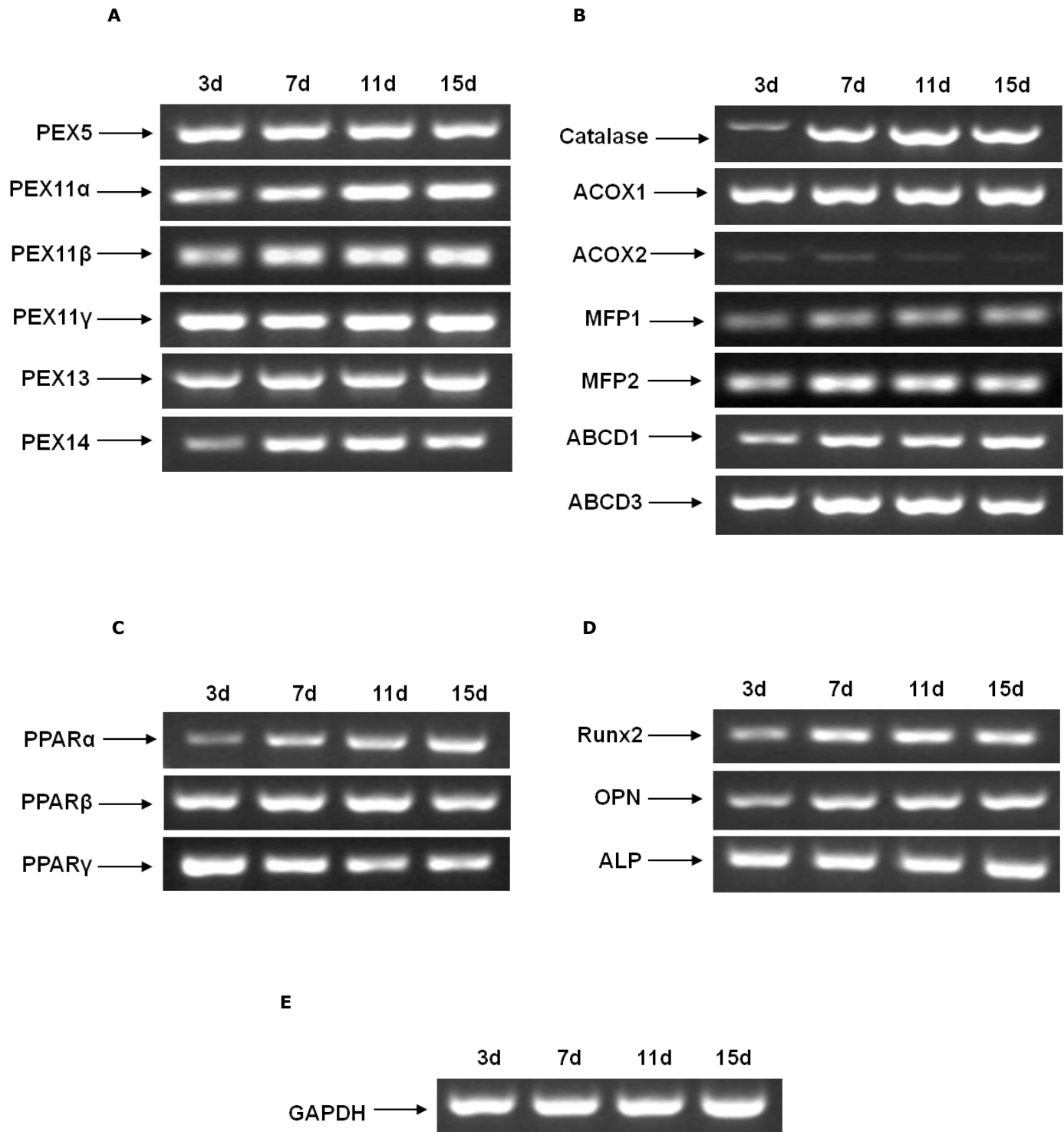
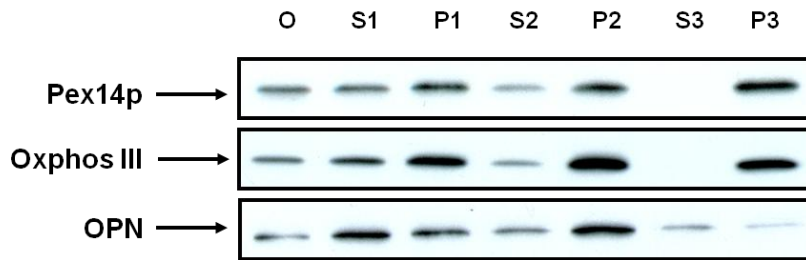
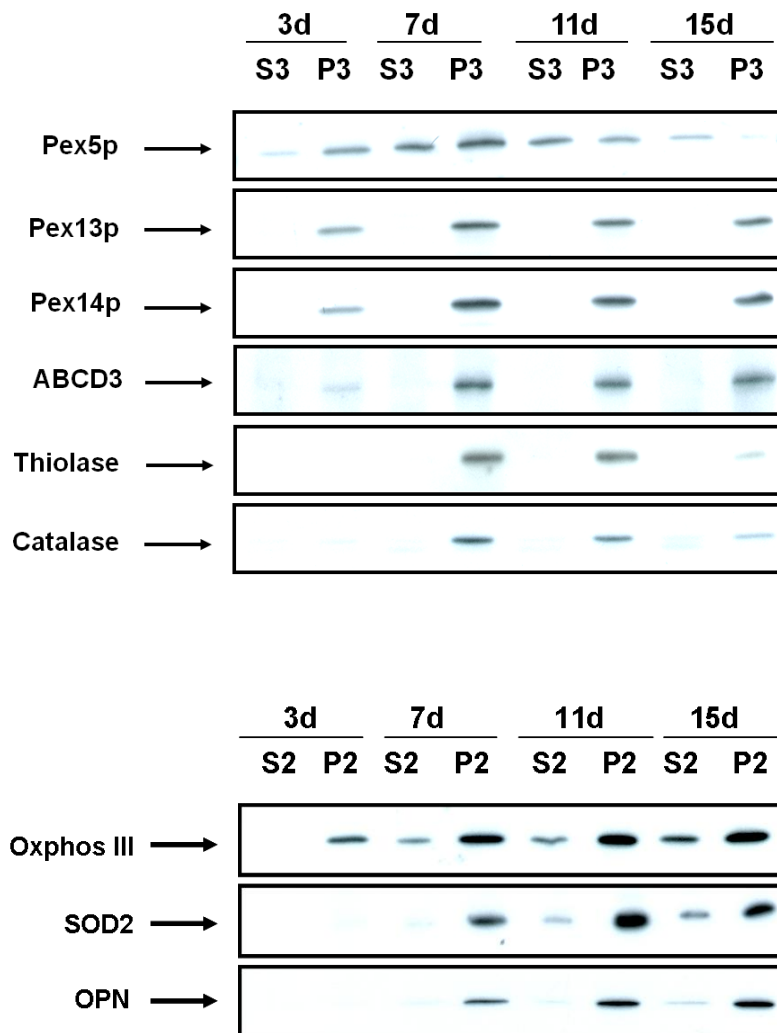


**Fig14. Semiquantitative RT-PCR analysis was performed on cDNAs prepared from total RNA of distinct time points of osteoblasts.**

A



B



C



**Fig15. Western blot analyses of organelle fractions from primary osteoblasts were preformed.** (A) Distinct pellets got by different centrifuge speeds were used to detect different marker proteins, such as peroxisomal marker protein-Pex14p, mitochondrial protein-oxphos III core 2 and a bone marker protein- OPN. (B) Western blot analyses revealed that the levels of peroxisomal metabolic enzymes were not parallel to peroxisome abundance during osteoblast differentiation. Mitochondrial proteins and OPN were increased during osteoblast growth. (C) Nuclear enriched proteins were isolated to investigate the PPARα expression at different stages of osteoblasts.

**S1, P1, S2, P2, S3, and P3:** all the details can be found in the method.

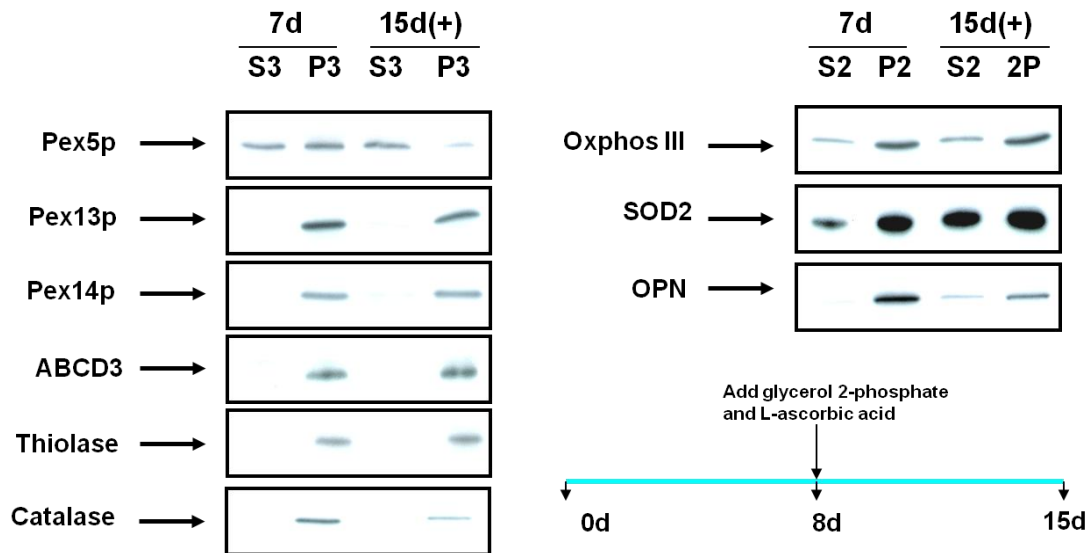


**Fig16. The addition of ascorbic acid (50µg/ml) and β-glycerolphosphate (10mM) was added to stimulate the osteoblastic differentiation.** Under this condition, the expression levels of all peroxisomal marker proteins, mitochondrial proteins and OPN were investigated.

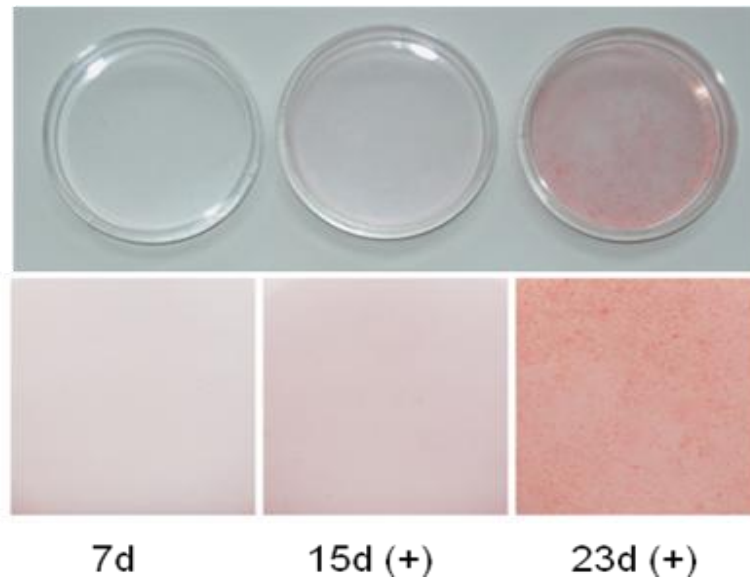


**Fig17. Mineralization staining was performed to detect the synthesized matrix at various stages of osteoblast differentiation.** The differentiation medium was added to the culture from day 8.

#### ***4.1.5 Both PPAR $\alpha$ and PPAR $\gamma$ are involved in regulating peroxisomal functions in osteoblasts***

Based on the evidence that treatment with ciprofibrate leads to proliferation of peroxisomes and induction of peroxisomal  $\beta$ -oxidation enzymes in H4IIEC3 rat hepatoma cells, we examined whether ciprofibrate can induce the similar effect in primary osteoblast cultures as well. Indeed, treatment with ciprofibrate induced catalase and Pex14p expression in osteoblast homogenates, suggesting peroxisome proliferation (Fig18A). Moreover, treatment with this PPAR $\alpha$  agonist also induced the catalase expression in individual peroxisomes of pellet 3 (Fig18B). Additionally, the Pex13 protein was also enhanced when treated with the higher concentration of ciprofibrate (500 $\mu$ M) (Fig18B). In contrast, the expression level of ABCD3 was significantly reduced in a dose-dependent manner (Fig18B). Furthermore, thiolase expression was induced, suggesting a positive

effect of the PPAR $\alpha$  activator on the function of peroxisomal  $\beta$ -oxidation (Fig18B). Consistent with previous report in which the PPAR $\alpha/\delta$  agonists upregulate osteoblast differentiation and induce bone formation (Still et al., 2008), the abundance of OPN protein was also elevated after treatment with ciprofibrate (Fig18C).

To determine whether the PPAR $\gamma$  agonist troglitazone is also involved in the regulation of peroxisomal abundance and peroxisomal metabolism, osteoblasts were incubated with different concentrations of troglitazone for 6 days. After incubation with troglitazone, a dose-dependent induction of catalase expression occurred that was much more pronounced as the one after ciprofibrate treatment, suggesting a stronger effect of PPAR $\gamma$  on antioxidant enzyme expression than PPAR $\alpha$  (Fig19A, B). Troglitazone treatment also exhibited a slight upregulation of Pex14 protein in osteoblast homogenates (Fig19A), which was similar to the result obtained from ciprofibrate treatment. In contrast, hardly any effect on the abundance of the peroxisomal membrane protein Pex13p and the enzyme of peroxisomal  $\beta$ -oxidation thiolase was noted in enriched peroxisomal fractions (Fig19B). Interestingly, the expression of the ABC transporter ABCD3 was increased in a dose-dependent manner (Fig19B). Contrarily, the marker of osteoblastic maturation -OPN was remarkably decreased (Fig19C), indicating an inhibitory effect of the PPAR $\gamma$  agonist on osteoblast differentiation. In addition, troglitazone also had an effect on abundance of the mitochondrial complex III, leading to a significant increase, especially with 10 $\mu$ M troglitazone (Fig19C). This result indicates that PPAR $\gamma$  activators are also important for the regulation of mitochondrial functions in osteoblasts.

Interestingly, even though peroxisomal matrix proteins were up-regulated, the expression level of Pex5p was decreased, especially after troglitazone treatment (Fig18B and 19B).

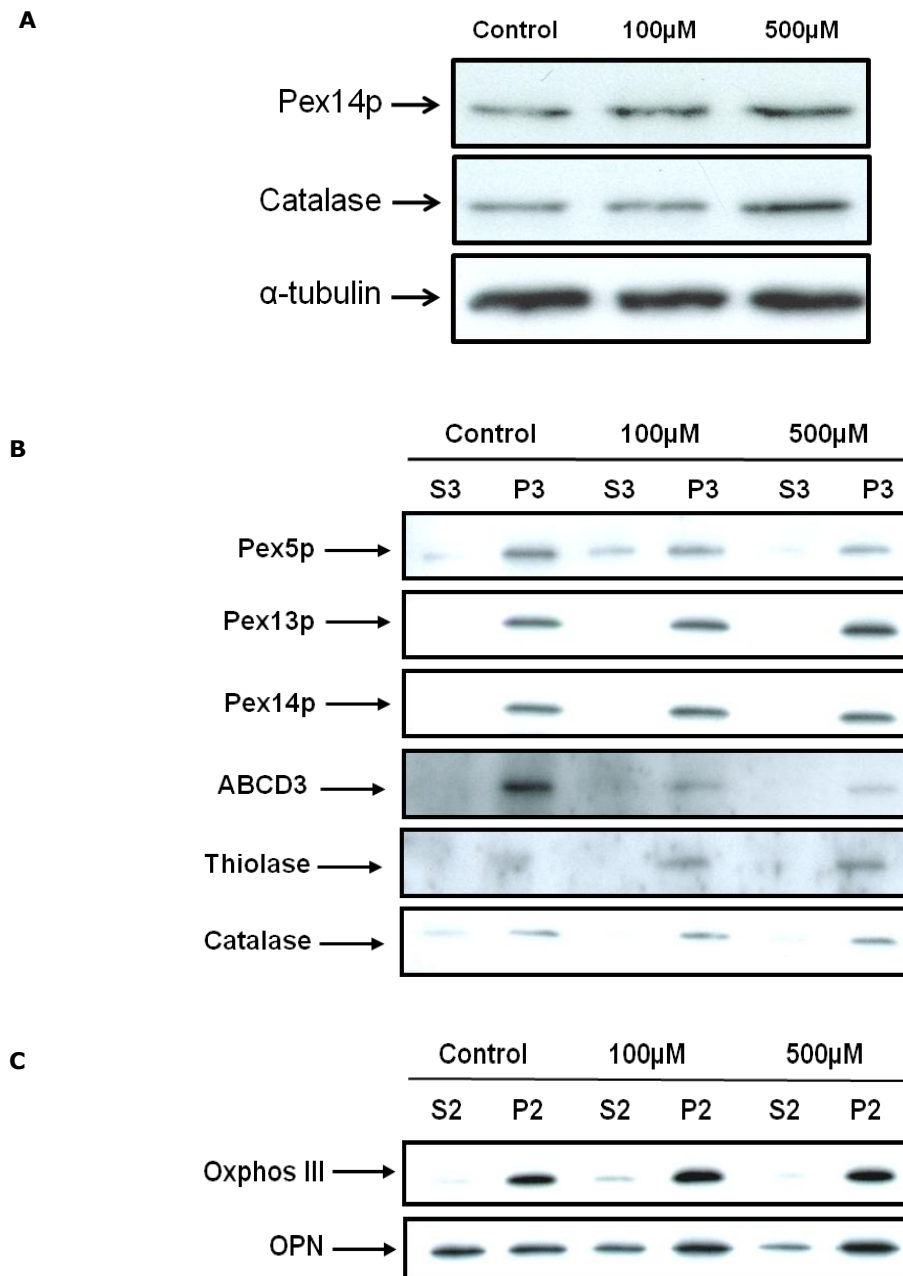


**Fig18. Comparative western blot analyses to examine all peroxisomal marker proteins, OPN and mitochondrial protein as treated with ciprofibrate.** Incubated with ciprofibrate for 6 days, the whole cell lysate (**A**) or enriched organelle fractions (**B, C**) were isolated to detect the expressions of different proteins, such as peroxisomal proteins, mitochondrial protein and OPN.

**Control:** only culture medium; **100μM:** 100μM ciprofibrate; **500μM:** 500μM ciprofibrate

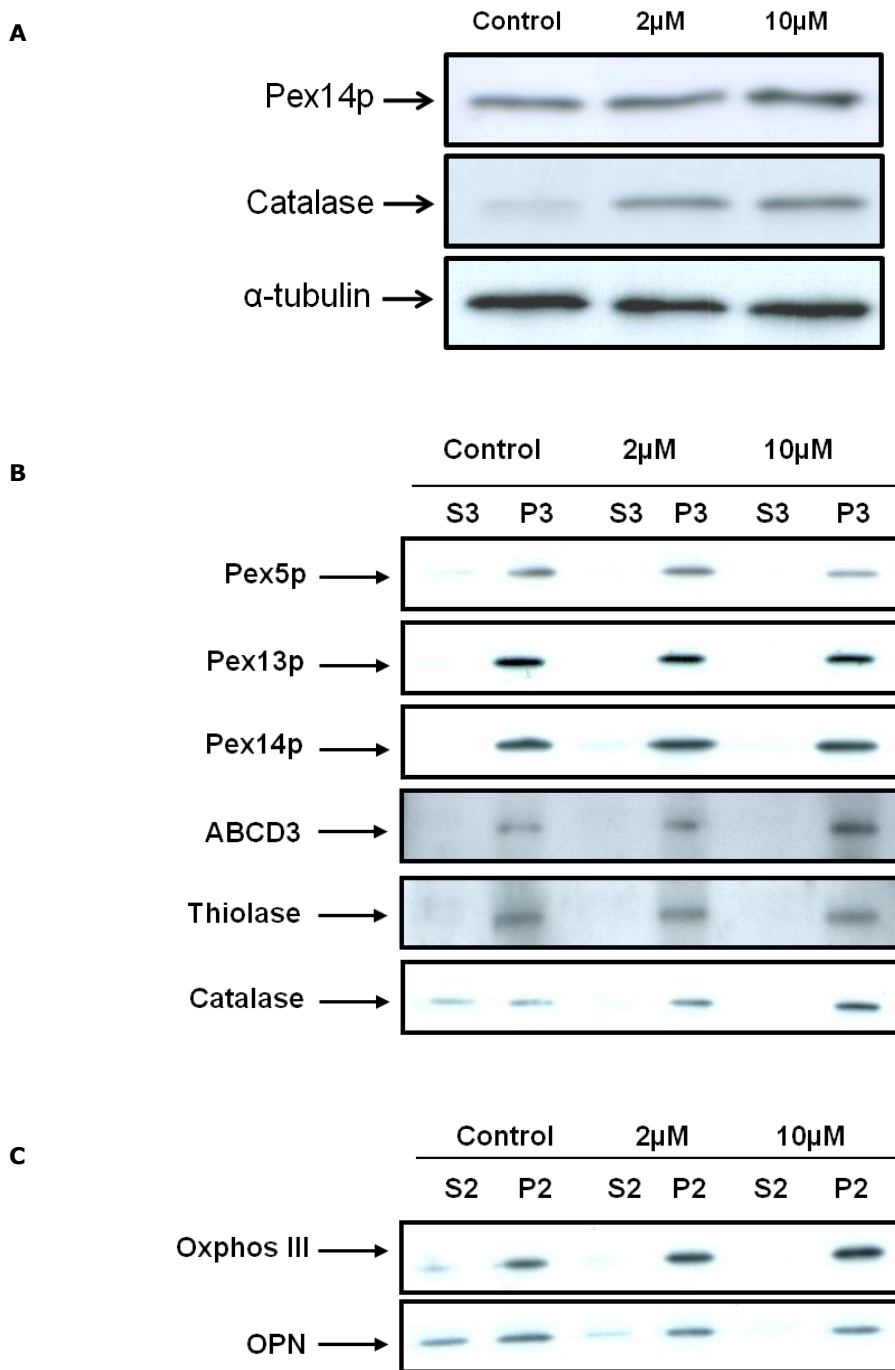


**Fig19. Comparative western blot analyses to investigate all peroxisomal marker proteins, OPN and mitochondrial proteins as treated with troglitazone.** The levels of all proteins, including peroxisomal proteins, mitochondrial protein and OPN were investigated as treatment with troglitazone for 6 days. **A:** the whole cell lysate; **B, C:** enriched peroxisomal fractions. **Control:** only culture medium; **2μM:** 2μM troglitazone; **10μM:** 10μM troglitazone

## ***4.2 Effect of PEX11 $\beta$ deficiency on the skeleton, osteoblast maturation and function***

PEX11 $\beta$  KO mice were generated by disrupting the Exons 1 to 3 of the mouse gene in conjunction with my supervisor Prof. Baumgart-Vogt. These mice show a clear Zellweger phenotype, despite only minor alterations in very long-chain fatty acids (Li et al., 2002b). Until now, no studies on the skeleton have been performed with these mice.

### ***4.2.1 Mice with deficient peroxisome proliferation exhibit ossification defects and growth retardation***

PEX11 $\beta$  KO fetuses at E19 were undersized, and exhibited a 60% reduction of body weight (WT:  $0.96 \pm 0.16$ g; PEX11 $\beta$  KO:  $0.70 \pm 0.08$ g). Therefore, a more detailed analysis was pursued to resolve the alteration in the skeleton due to peroxisome deficiency. For this purpose, the skeletons of E19 WT and PEX11 $\beta$  KO mice were stained for visualization of bone and cartilage. Alizarin red and Alcian blue staining revealed significant alterations of ossification in PEX11 $\beta$  KO pups (Fig20). In comparison to the skull of WT mice at this age, the skull of PEX11 $\beta$  KO pups showed less ossification, suggesting a defect in intramembranous ossification. In the axial skeleton, defects in ossification were evident in the sacral and coccygeal vertebrae of PEX11 $\beta$  KO pups. Additionally, the fore- and hindlimbs of PEX11 $\beta$  KO mice showed impaired ossification as well, indicating endochondral ossification problems. Moreover, defects in ossification were noted in the sternum of PEX11 $\beta$  KO animals. Take together, these results suggest that both intramembranous and endochondral ossifications are affected in PEX11 $\beta$  KO mice.

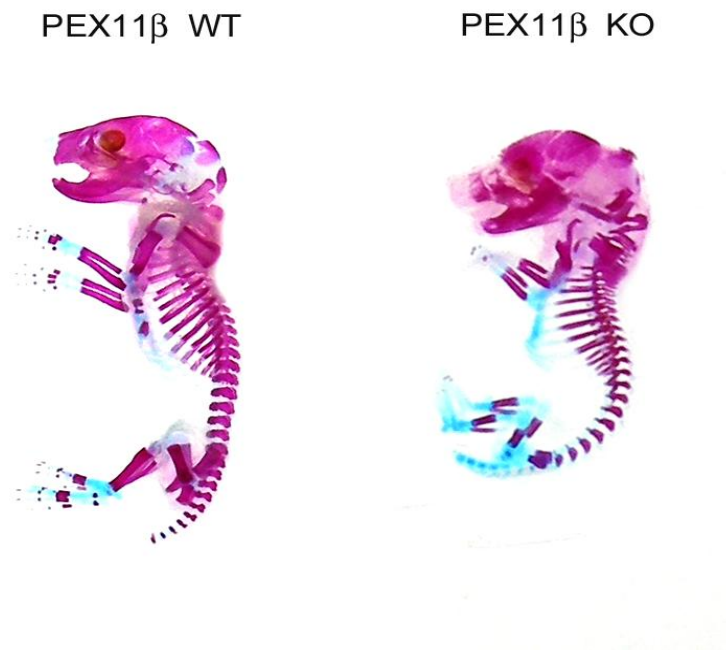


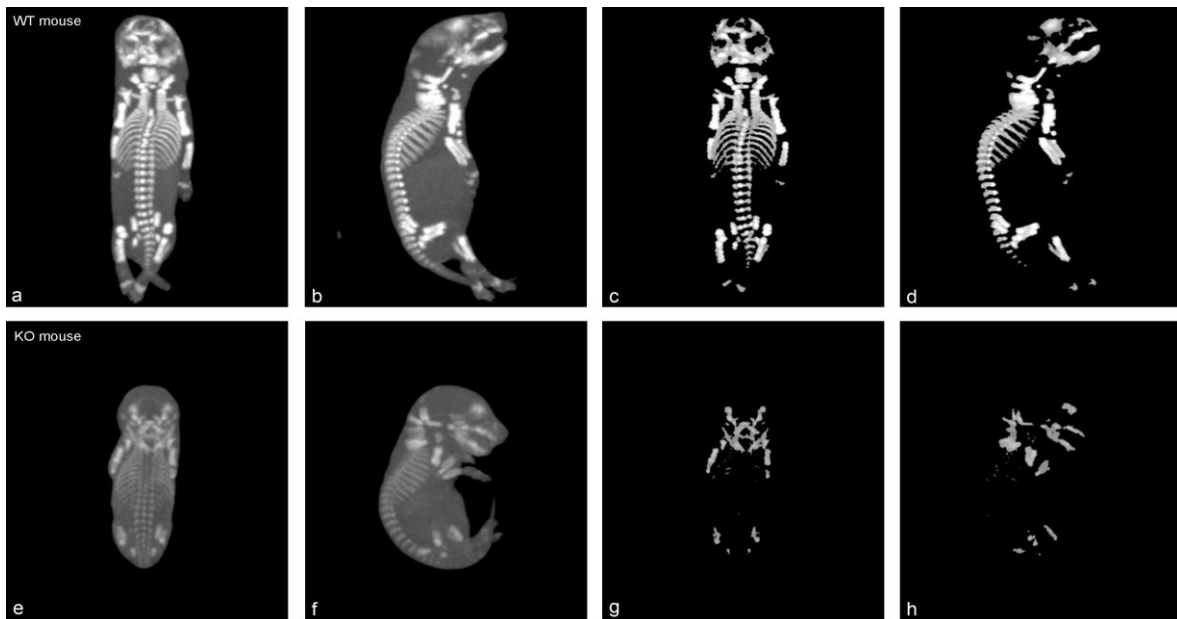
**Fig20. Alizarin Red and Alcian Blue staining of the skeletons from control and PEX11β KO mice.** Skeleton stainings revealed the impaired ossification of distal bone elements of the limbs, sacral and coccygeal vertebrae as well as parts of the skull and the sternum in PEX11β KO mice.

#### **4.2.2 PEX11β KO mice exhibit substantially lower bone volume and mass**

Flat-panel based volumetric Computer Tomography (fpvCT) is a new noninvasive 3-dimensional (3D) imaging technology, which can monitor the skeleton of mice *in vivo* (Obert et al., 2005). Therefore, in this study both WT and PEX11β KO mice were scanned with this technique. The results revealed a significant lower bone mass in PEX11β KO mice. In comparison to WT littermates of the same age, both intramembranous (calvaria) and endochondral ossifications (vertebrae and limbs) were strongly impaired (Fig21A), corroborating the result obtained from skeleton stainings. Quantitative morphometric analysis of the skeleton revealed that PEX11β KO pups possessed a 70% reduction in total bone volume (WT:  $1043.2 \pm 136.88 \text{mm}^3$ ; PEX11β KO:  $613.08 \pm 60.58 \text{mm}^3$ ) and a 123% decrease in bone mass (WT:  $28.04 \pm 4.27 \text{mg}$ ;

PEX11 $\beta$  KO: 12.6 $\pm$ 1.25mg), as well as a 31% decreased whole-body bone mineral density (WT: 26.82 $\pm$ 0.88mg/mm<sup>3</sup>; PEX11 $\beta$  KO: 20.52 $\pm$ 0.63mg/mm<sup>3</sup>), demonstrating the impaired ossification in PEX11 $\beta$  KO mice (Fig21B).

**A**



**B**

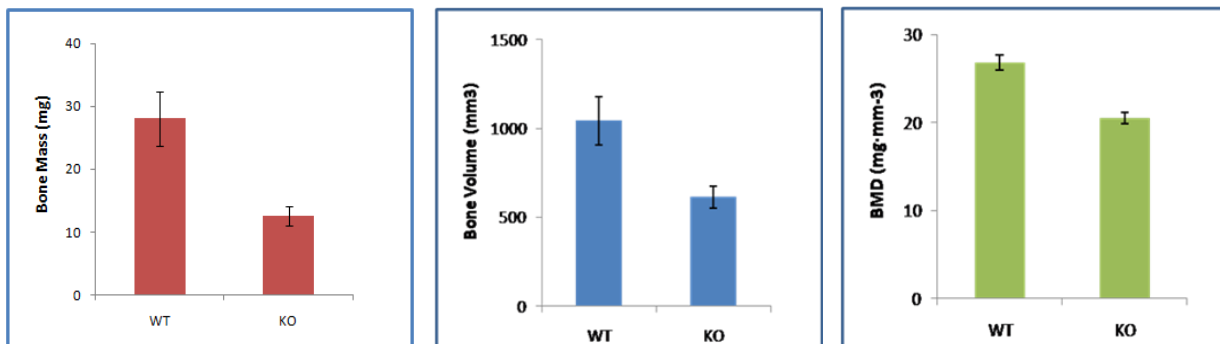


**Fig21. WT and PEX11 $\beta$  KO mice were scanned by flat panel volume computer tomography (fpvCT). (A)** Pictures are presented with two different windows of Hounsfield Units (a, b, e, and f: 0 to 500 HU; c, d, g and h: 200 to 500 HU). Large differences were observed in WT and PEX11 $\beta$  KO mice. **(B)** FpvCT analyses revealed the substantially lower total bone volume and mass, as well as a decrease in whole-body bone mineral density in PEX11 $\beta$  KO animals (WT: n=7; KO: n=5).

### ***4.2.3 Histological analysis revealed reduced ossification and mineralization in PEX11 $\beta$ KO mice***

Different mouse models for peroxisomal biogenesis disorders, like the PEX2, PEX5, and PEX7 mice, exhibit a severe retardation in growth and ossification. To examine whether these alterations also take place in PEX11 $\beta$  KO mice, immunofluorescence analysis for osteopontin (OPN) was performed. OPN is a cell secreted adhesive bone glycoprophosphoprotein with arginine-glycine-aspartic acid (RGD) cell-binding sequence, which plays a role in bone matrix organization and /or stability. Our results showed that OPN-positive ossification centers were significantly decreased in vertebrae of PEX11 $\beta$  KO mice, suggesting a reduced endochondral ossification process in comparison to age-matched littermates (Fig22a, b). Moreover, as shown in Fig22c and d, the abundance of OPN protein was remarkably decreased in proliferative and calcified zones of the epiphyseal growth plate, revealing the disturbance of endochondral ossification. In addition, Alizarin Red S staining exhibited an impaired mineralization for the limb and vertebrae of PEX11 $\beta$  KO mice (Fig23). Alizarin Red S is an anthraquinone derivative, which can be used to identify calcium in tissue sections. In PEX11 $\beta$  KO animals, calcium deposits were significantly reduced compared with WT mice (Fig23), indicating that the mineralization in the ossification process was affected in this animal, corroborating the fpvCT results. In sum, these data further suggest that PEX11 $\beta$  might play a role in the regulation of ossification and mineralization.

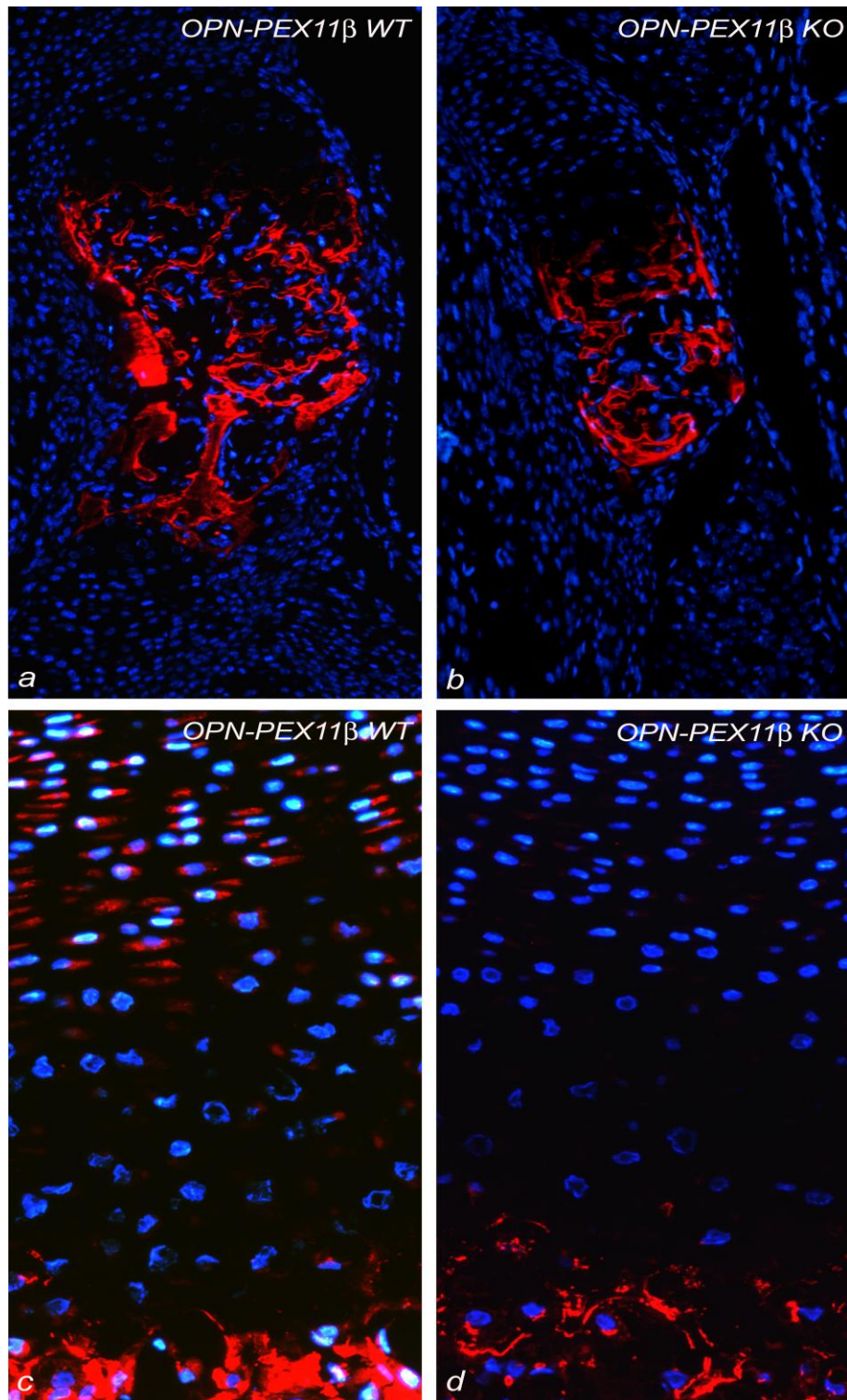


**Fig22.** An antibody against OPN was used to examine the alterations of endochondral ossification in WT and PEX11 $\beta$  KO mice. WT: a+c; PEX11 $\beta$  KO: b+d. **Fig a+b:** Overview on endochondral ossification of vertebrae with OPN staining. **Fig c+d:** Higher magnification view of the epiphyseal growth plate in the limb.

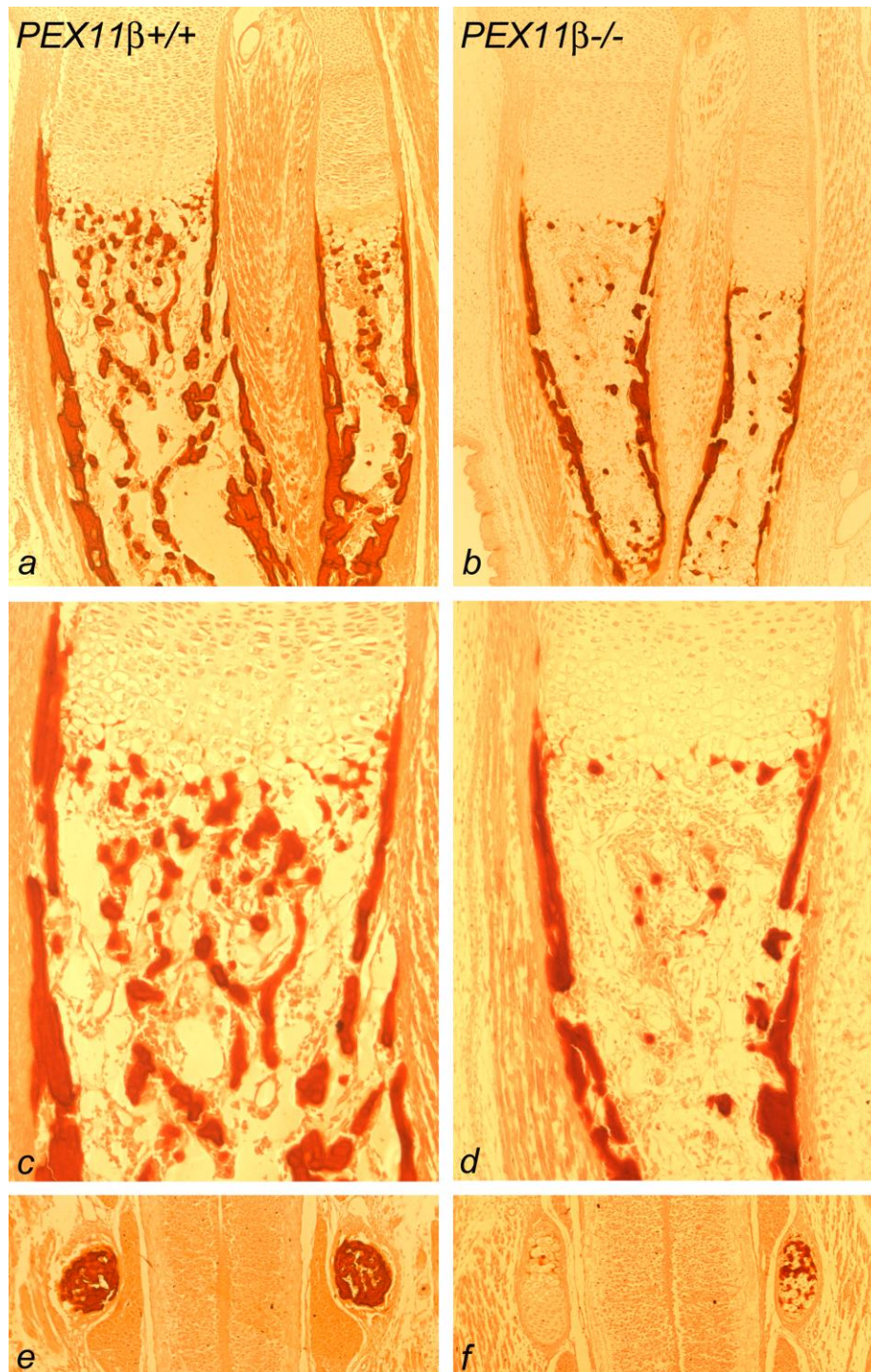


**Fig23. Alizarin Red staining was performed to investigate the mineralization. WT: a+c+e; PEX11 $\beta$  KO: b+d+f. Fig a+b:** Overview on the mineralization of the tibia and fibula. **Fig c+d:** Higher magnification view of the same areas in the tibia. **Fig e+f:** Differences of the mineralization in arches of lumbar vertebrae.

#### ***4.2.4 The peroxisomal numerical abundance is reduced and the protein composition altered in PEX11 $\beta$ KO mice***

Mouse models of Zellweger syndrome (PEX2, PEX5 and PEX13 knock-outs) display a number of cellular abnormalities. Chief among these is the inability to import peroxisomal matrix enzymes, leading to the mistargetting of peroxisomal enzyme into the cytoplasm and the disruption of all metabolic pathways in peroxisomes with all its secondary consequences. To determine whether similar phenomena are also present in PEX11 $\beta$  KO mice, both immunofluorescence preparations and Western blot analyses with antibodies against peroxisomal matrix proteins were done. The results revealed that enzyme import was unaffected in PEX11 $\beta$  KO osteoblasts as shown in Fig24+25 by the detection of the peroxisomal matrix enzyme catalase, demonstrating that the peroxisomal matrix protein import pathway is functional in osteoblasts lacking PEX11 $\beta$  (Fig24,25B). The specific organelle staining pattern indicates that peroxisomal matrix proteins are not mislocalized into the cytoplasm as in PEX2, PEX5 and PEX13 knockout animals. In addition, the responsible import receptor for PTS1-containing proteins Pex5p was increased, especially on the surface of the organelles (Fig25B). Due to the dual localization of this receptor in the cytoplasm and on the peroxisomal surface, positive bands with different intensities are obtained from Western blot analyses in S3 and P3, depending on its subcellular distribution. However, the knockout of PEX11 $\beta$  induced a reduction of peroxisome number together with a concomitant increase of peroxisome elongation as shown in IF preparations for Pex14p (Fig24). Whereas, the overall amount of Pex14p was not altered in the whole cell lysate or in the enriched peroxisomal fraction compared with WT osteoblasts (Fig25A, B). The reduction of

the peroxisomal numerical abundance was also observed in stainings for other peroxisomal membrane proteins, such as ABCD3 (Fig24). In addition, western blots revealed that catalase, the major peroxisomal antioxidant enzyme was increased in PEX11 $\beta$  KO osteoblasts (Fig25A, B), suggesting that these cells might be under oxidative stress. The higher content of catalase in individual peroxisomes was reflected by a significant induction of the catalase protein band in the enriched peroxisomal fractions (P3) (Fig25B) as well as in more intensive and larger fluorescence signals representing individual peroxisomes in IF preparations (Fig24). Finally, a decrease was noted for the ABCD3 and thiolase levels in PEX11 $\beta$  KO osteoblasts, suggesting an altered capacity in peroxisomal  $\beta$ -oxidation (Fig25B).

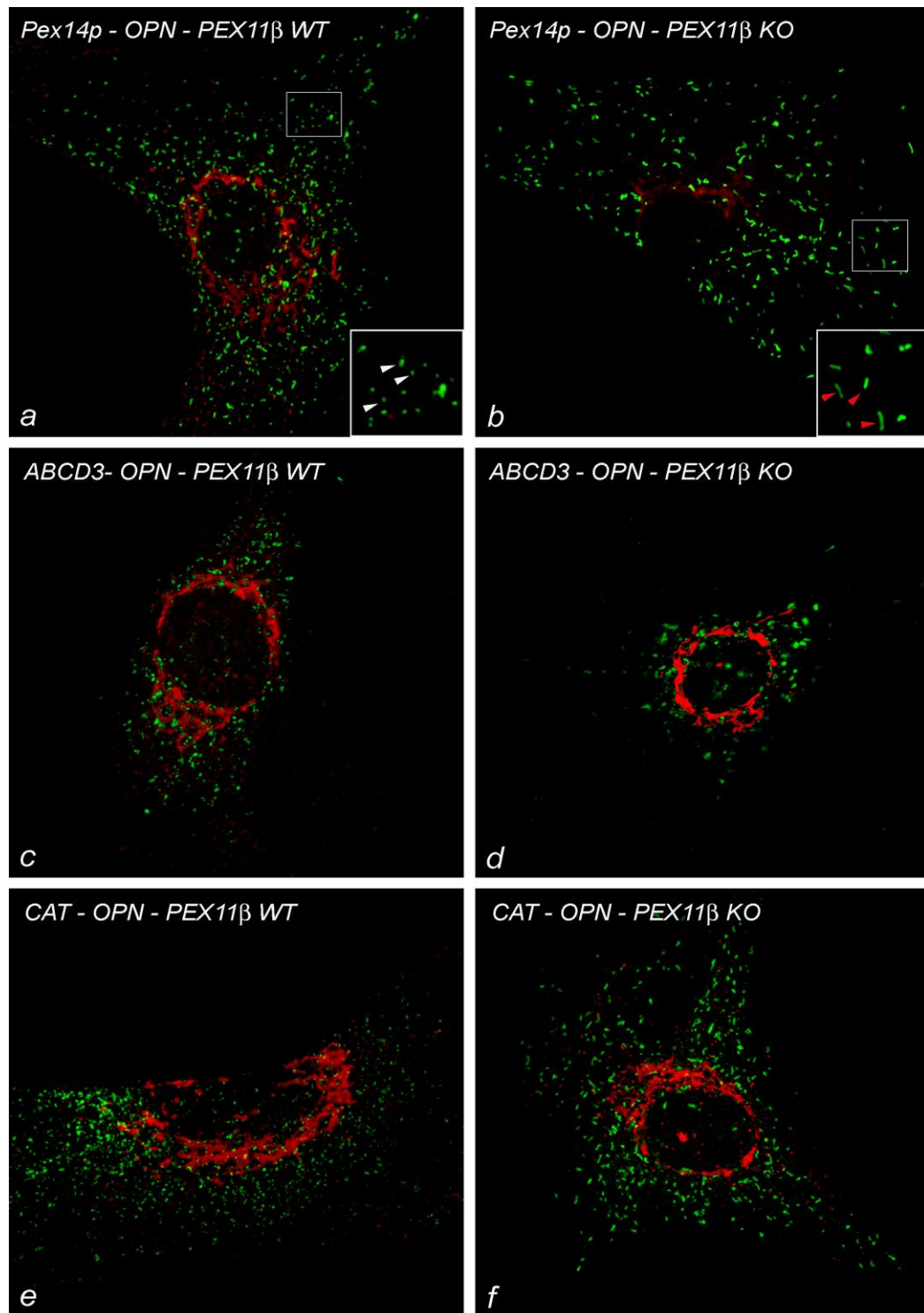


**Fig24.** Double-immunofluorescence preparations revealed a decrease in numerical abundance of peroxisomes and an increase in tubular elongation of these organelles in PEX11 $\beta$  KO osteoblasts. The purity of the osteoblast preparation was assessed by double staining with OPN. White arrow head: spherical peroxisomes; Red arrow head: tubular peroxisomes.

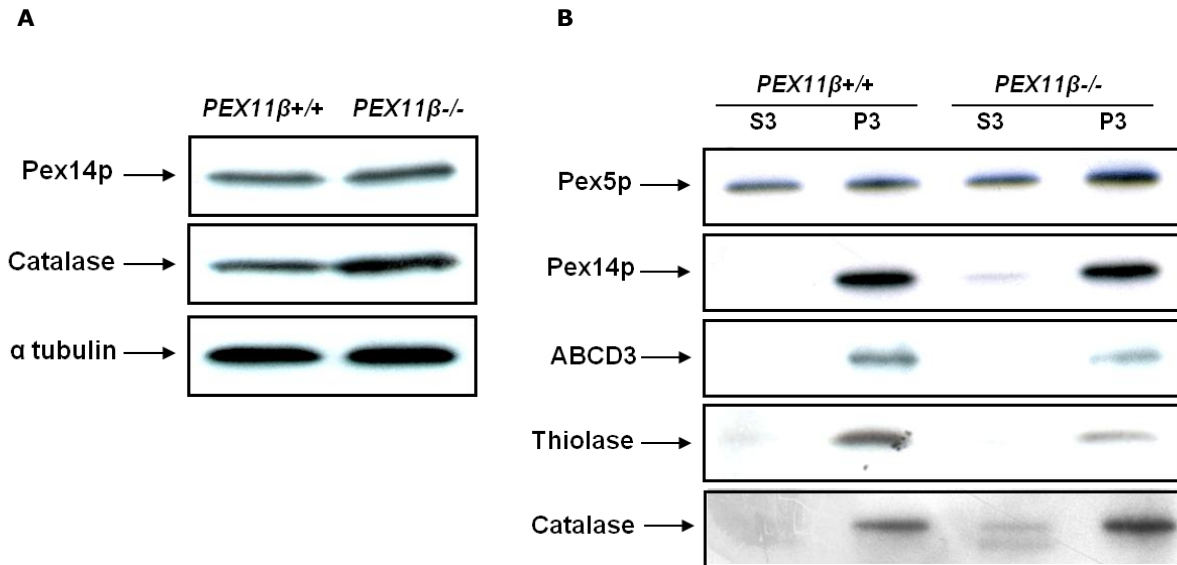


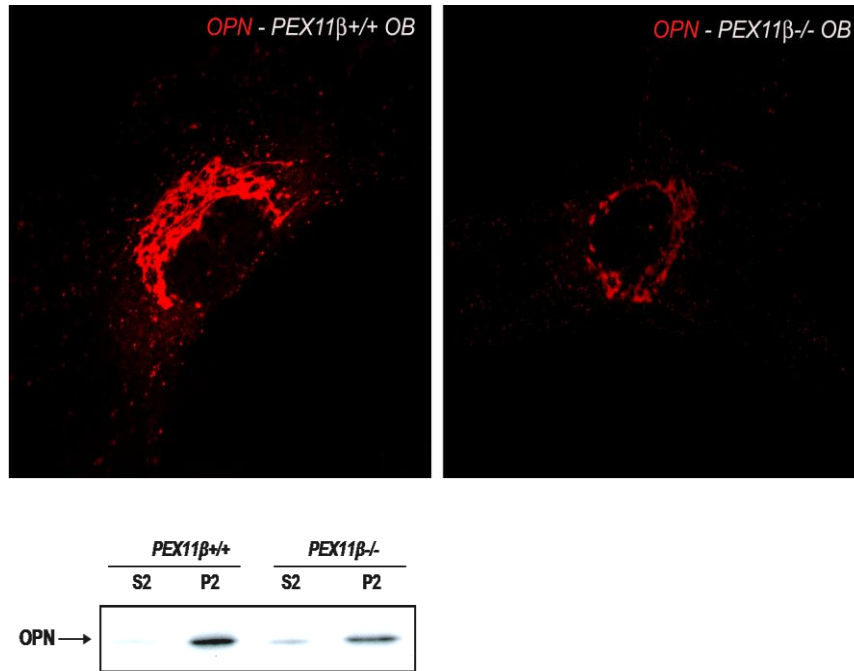
**Fig25.** Western blot analyses for peroxisomal proteins were performed with the whole cell lysates (homogenates) and enriched peroxisomal fractions versus the 50,000g supernatant (S3), containing microsomes and the cytoplasmic proteins (**A**, **B**). The high quality of the isolated enriched peroxisomal preparations is indicated by the low leakage of matrix proteins into the S3 fractions (empty in WT S3). Due to stronger tubulation and longer organelles with concomitant width reduction, breakage into small organelles occurs during the homogenization procedure, leading to the occurrence of these small sized organelles also in S3 (faint bands). Heterogeneity and relative differences of peroxisomal protein alterations are obvious in *PEX11β* KO osteoblasts.

**A:** the whole cell lysate; **B:** enriched peroxisomal fractions.

#### **4.2.5 Osteoblast- secretory proteins are reduced in primary osteoblast cultures of *PEX11β* KO mice**

OPN and osteocalcin (BGP) are typical osteoblast marker proteins. OPN is the marker for osteoblast maturation in the middle stage of their differentiation and BGP is a late marker for mature osteoblasts. Here as shown in IF preparations for OPN and BGP, *PEX11β* KO osteoblasts in primary cultures are less mature in comparison to WT osteoblasts (Fig26). Both proteins were stained much weaker in *PEX11β* KO osteoblasts, suggesting that *PEX11β* KO osteoblasts produce less bone matrix proteins (Fig26). These results were also corroborated in Western blots, which showed less levels of OPN in enriched organelle fractions (Fig26A).

A



B

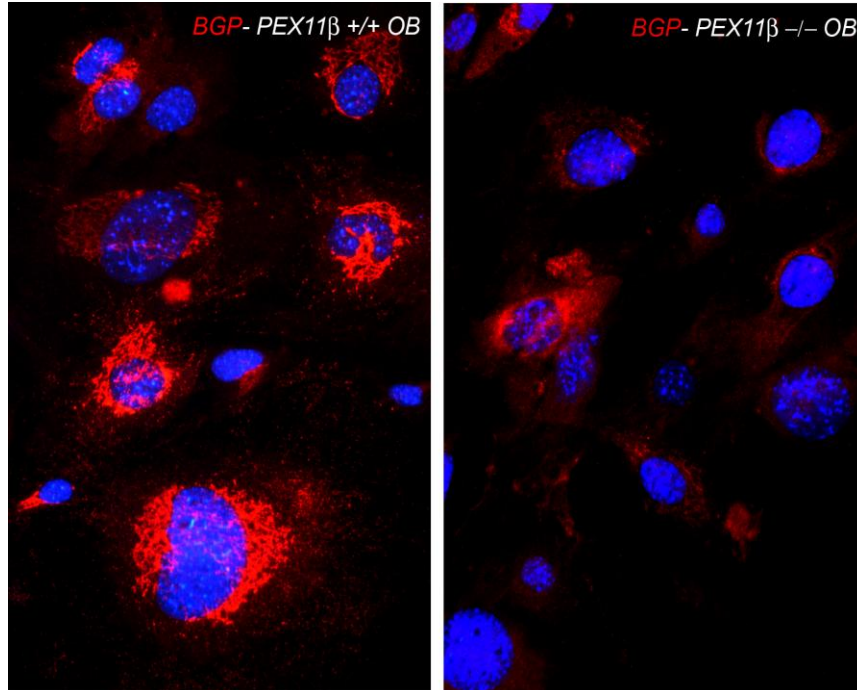


**Fig26.** (A) Immunofluorescence preparation and western blot analysis revealed a decrease in the level of OPN in PEX11 $\beta$  KO osteoblast. (B) In immunofluorescence preparations for osteocalcin in primary osteoblasts, a strong downregulation of the osteocalcin protein was also noted.

#### ***4.2.6 In addition to catalase also other antioxidant enzymes were enhanced in PEX11 $\beta$ KO mice***

The catalase upregulation in primary PEX11 $\beta$  KO osteoblasts could also be corroborated in bone sections. As shown in Fig27B, the abundance of the catalase protein was also upregulated in osteoblasts of calvaria. Besides catalase in peroxisomes, other major enzymes generally altered under oxidative stress are SOD1 in the cytoplasm, SOD2 in mitochondria and HO-1 in the ER. Indeed, SOD2 abundance was elevated (Fig27D, 28A, B), which might be induced by higher mitochondrial respiratory activity as shown by an increase of complex III in KO osteoblasts (Fig27A, 28B). SOD2 was significantly stronger increased than complex III, suggesting a release of ROS by the respiratory chain and a compensatory SOD2 increase (Fig28B). In addition to SOD2, also the SOD1 was upregulated, indicating a complex upregulation of antioxidant enzymes (Fig28A). Another enzyme HO-1, which is an important regulator for ROS metabolism, was also enhanced in PEX11 $\beta$  KO osteoblasts, suggesting the accumulation of ROS in these animals (Fig27C, 28A). Due to the indication for oxidative stress, lipid peroxidation was analyzed with an antibody against 4-hydroxynonenal (4-HNE) lysine adducts, depicting increased bands in PEX11 $\beta$  KO osteoblasts (Fig29A). In addition, oxidized DNA damage was also analyzed with an antibody against 8-hydroxy-2'-deoxyguanosine (8-OHdG), showing a strong nuclear labelling in the osteoblasts of calveria of PEX11 $\beta$  KO mouse (Fig29B). These data suggest that ROS causes oxidative damage to lipids and DNA in PEX11 $\beta$  deficient mice.

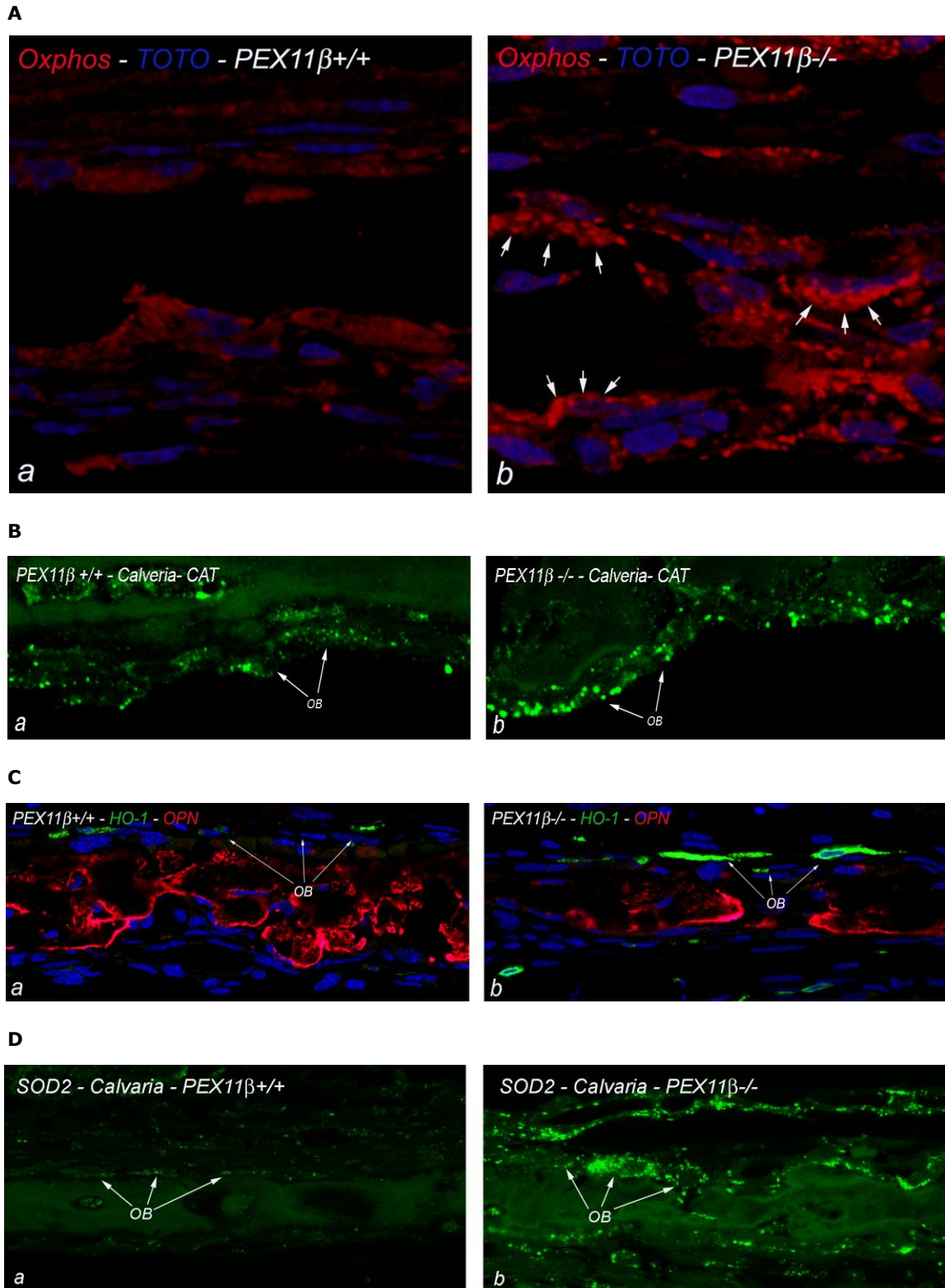


**Fig27.** Immunofluorescence preparation was performed to examine the protein levels of ROS producing enzyme and ROS scavenging enzymes in WT and PEX11β KO mice.

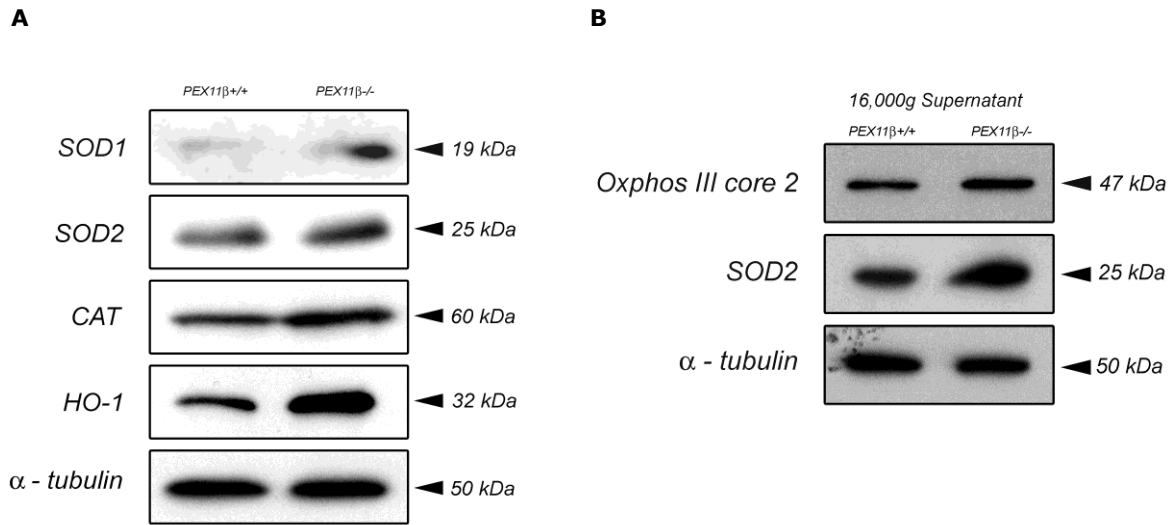


**Fig28.** Western blot analyses were performed to investigate the protein levels of antioxidant enzymes, including SOD1, SOD2, CAT, heme oxygenase 1 (HO-1), the complex III (core 2) of the mitochondrial respiratory chain (Oxphos III) in WT and PEX11β KO osteoblasts .

**A:** the whole cell lysate; **B:** 16,000g supernatant

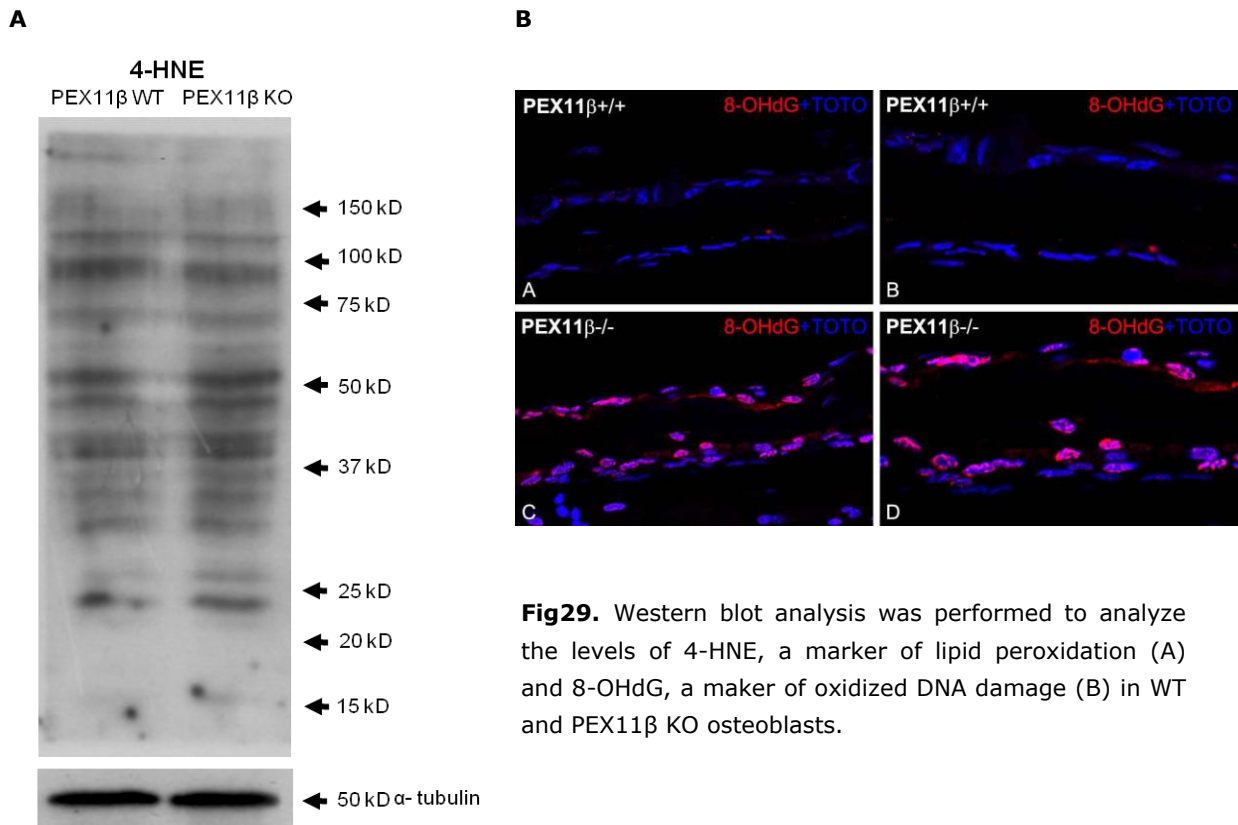


**Fig29.** Western blot analysis was performed to analyze the levels of 4-HNE, a marker of lipid peroxidation (A) and 8-OHdG, a maker of oxidized DNA damage (B) in WT and PEX11β KO osteoblasts.

#### ***4.2.7 PEX11 $\beta$ deficiency diminished Canonical Wnt signaling activity and increased PPAR $\gamma$ abundance***

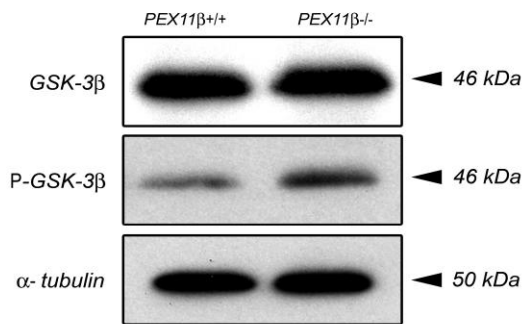
In the following, the potential mechanisms by which PEX11 $\beta$  deficiency could result in ossification defects were explored. For this purpose, Western blots and IF preparations of major transcription factors and proteins involved in the regulation of signaling cascades for osteoblast differentiation were analyzed. The protein level of p-GSK, the cytoplasmic binding partner of  $\beta$ -catenin, was enhanced in PEX11 $\beta$  KO osteoblasts (Fig30A). In contrast, a reduction in  $\beta$ -catenin was observed in KO osteoblasts using Western blot analysis (Fig30B). Furthermore, the translocation of  $\beta$ -catenin from the cytoplasm into the nucleus was attenuated in PEX11 $\beta$  deficiency osteoblasts compared with WT osteoblasts (Fig30B). Importantly, expression of the classical  $\beta$ -catenin/TCF target gene Cyclin D1 was also decreased in KO osteoblasts (Fig30C). These data indicate that canonical Wnt signaling is diminished in PEX11 $\beta$  KO osteoblasts.

In addition, the level of FoxO1, a crucial regulator of redox balance in osteoblasts, was reduced in PEX11 $\beta$  KO osteoblasts (Fig31A, B), suggesting an oxidative imbalance. Next we examined whether the pronounced expression of antioxidant genes in PEX11 $\beta$  KO osteoblasts is mediated via other transcriptional factors. Indeed, Nrf2 was increased in PEX11 $\beta$  KO osteoblasts (Fig31C). Moreover, the expression of I $\kappa$ B $\alpha$ , which is the inhibitor of NF- $\kappa$ B signaling, was found to be reduced in PEX11 $\beta$  KO mice (Fig31D, E), indicating the activation of NF- $\kappa$ B signaling.

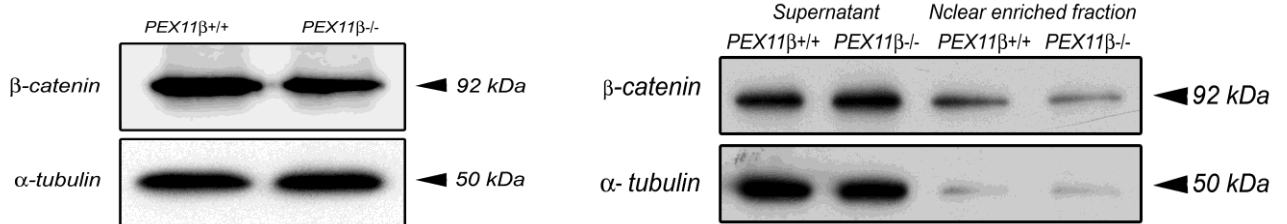
Interestingly, we observed that the expression level of PPAR $\gamma$  was increased in PEX11 $\beta$  KO osteoblasts (Fig32). Moreover, the protein level of the osteoblast transcription factor-Runx2 in IF preparations was reduced (Fig33A). Furthermore,

its distribution was also altered, showing a reduction of this protein in the nuclear area and a more prominent abundance in the cytoplasm (Fig33B). These data indicate that ROS triggered signaling pathways might partially contribute to the ossification defects in PEX11 $\beta$  KO mice.

**A**



**B**



**C**

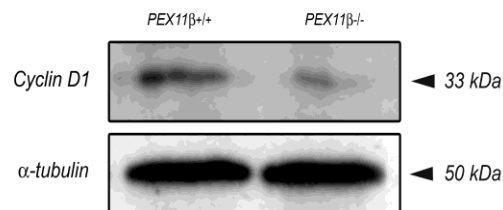


**Fig30.** The protein levels of GSK-3 $\beta$ , p-GSK-3 $\beta$ ,  $\beta$ -catenin and cyclin D1 were determined in WT and PEX11 $\beta$  KO mice.

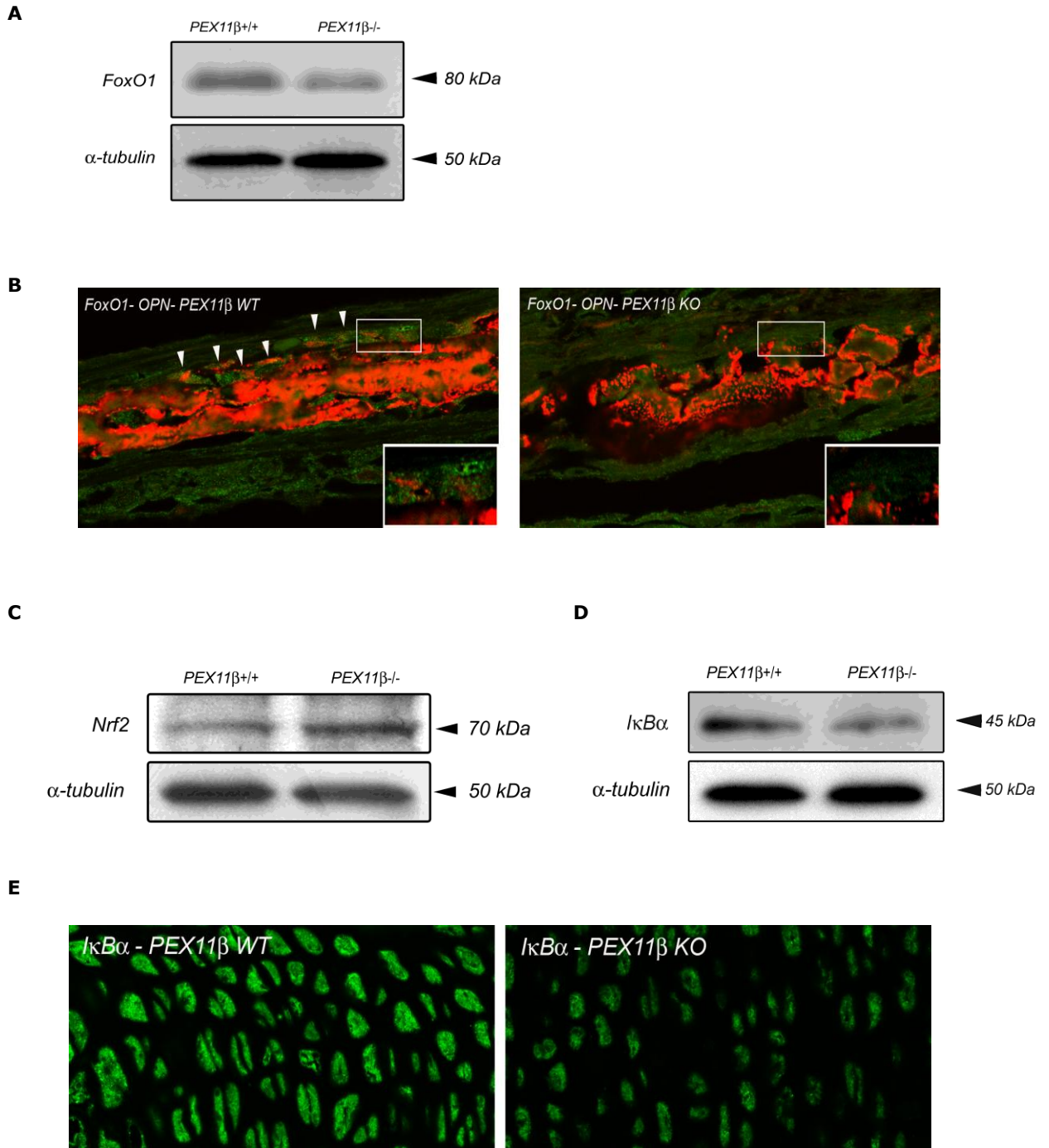


**Fig31.** The levels of FoxO1, Nrf2 and  $I\kappa B\alpha$  were examined by Western blot analyses and IF preparations. Arrow head: osteoblasts with FoxO1 positive labeling.

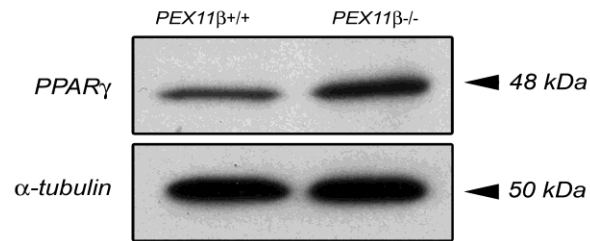
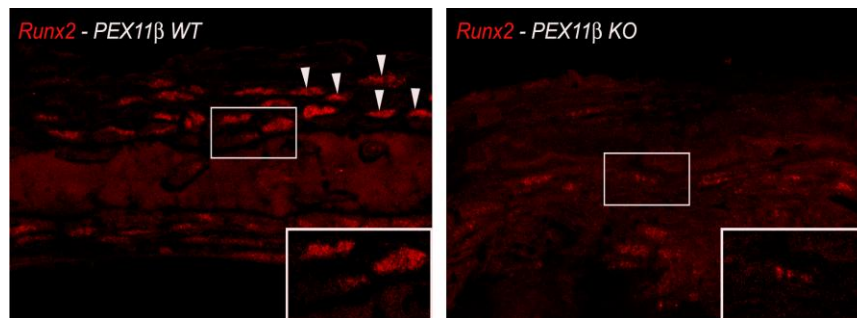


**Fig32.** Western blot analysis was performed to analyze the level of PPAR $\gamma$  in WT and PEX11 $\beta$  KO osteoblasts.

**A**



**B**

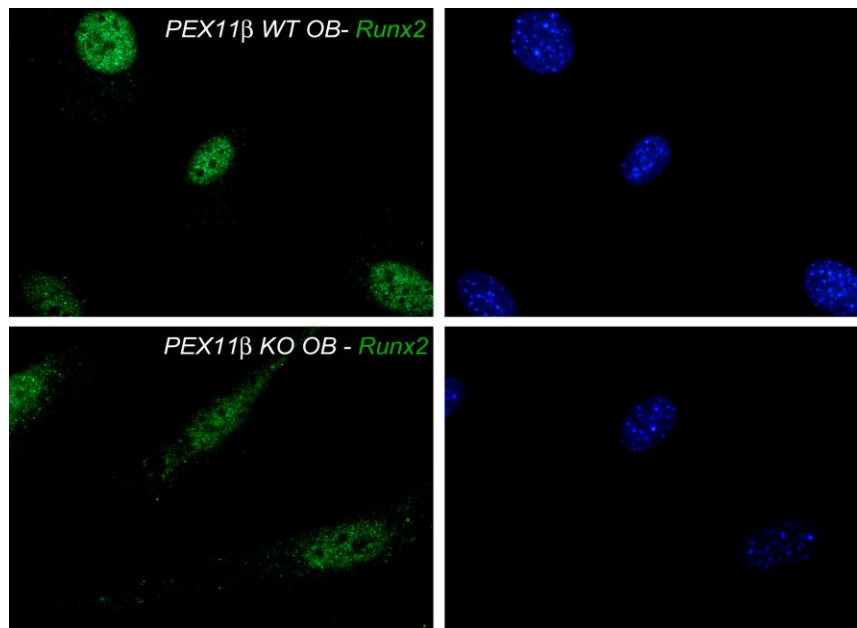


**Fig33.** Immunofluorescence analysis was used to detect Runx2 abundance and localization in WT and PEX11 $\beta$  KO osteoblasts. **(A)** The protein level of Runx2 was investigated in calvariae of WT and PEX11 $\beta$  KO mice. **(B)** Runx2 localization was examined in PEX11 $\beta$  KO osteoblasts, showing a shift of Runx2 into the cytoplasm.

## **5 Discussion**

### **5.1 Part 1**

In the present study, we characterized the peroxisomal compartment to achieve insights into its possible metabolic roles in distinct cell types of the skeleton and the process of osteoblast maturation. Our results revealed that peroxisomes were present in all cell types of skeleton, however, with heterogenous abundance and enzyme composition. Furthermore, clear differences were observed in their abundance and functions during osteoblast maturation.

#### **5.1.1 Peroxisomes are ubiquitous, however, with heterogeneous enzyme composition in different cell types of the skeleton**

Bone develops through two essential processes, intramembranous ossification and endochondral ossification. During intramembranous ossification, bone tissue is differentiated directly from mesenchyme and no cartilage is present. By contrast, the process of endochondral ossification is characterized by the formation of initial cartilage anlagen that is replaced by bone (Olsen et al., 2000). Endochondral ossification is a complex and tightly regulated process that involves programmed proliferation and maturation of chondrocytes, followed by terminal differentiation, hypertrophy and replacement of cartilage by bone.

Hypertrophic chondrocytes are localized at the end of growth plates of long bone prior to the ossification zones and are required for the process of endochondral ossification (Vu et al., 1998). Matrix vesicles play a key role in initiating mineralization. These vesicles are particles that are released from

plasma membrane of mineralizing cells, such as hypertrophic chondrocytes and are rich in lipids, such as cholesterol, free fatty acids, glycolipids and lysophospholipids (Wang and Kirsch, 2002; Wuthier, 1976). As shown in morphological stainings for Pex14p localization in this thesis, the highest numerical abundance of peroxisomes was present in hypertrophic chondrocytes, followed by osteoblasts. Pex14p is a biogenesis protein of the peroxisomal membrane in the docking complex, which facilitates inward transfer of targeted proteins. Since Pex14p is exposed to the cytoplasm and is present on each peroxisomal membrane surface, the anti-Pex14p antibody proved to be the best available marker for peroxisomes in morphological preparations, which stained peroxisomes ubiquitously in all cell types of the skeleton. Since peroxisomes are known to be involved in the synthesis of membrane lipids (cholesterol and etherlipids) (Singh et al., 1989; Wanders, 2004b), two lipid classes that strongly influence the physiological properties of membranes (Karnati and Baumgart-Vogt, 2008), they might function in facilitating the formation of phospholipid-rich matrix vesicles in hypertrophic chondrocytes and osteoblasts, thereby exerting an effect on the process of endochondral ossification. Interestingly, in PEX7 KO mice which exhibit a plasmalogen synthesis defect, the endochondral ossification process is strongly impaired (Brites et al., 2003). Furthermore, other extracellular free ligands, their receptors, and various downstream cytoplasmic and nuclear transducers regulate the processes of chondrocyte maturation, differentiation, and hypertrophy. Molecules like retinoids (De Luca et al., 2000; Takishita et al., 1990) and vitamin D (Boyan et al., 2002; Dean et al., 2001) as well as extracellular matrix proteins such as parathyroid-hormone-related peptide (Chung et al., 1998), bone morphogenic protein 6 (De Luca et al., 2001;

Grimsrud et al., 1999) and insulin-like growth factor I (Hunziker et al., 1994; Nilsson et al., 2005) have been implicated in the switch of reserve or proliferative stage to hypertrophic stage. In this respect, it is of interest that peroxisomes are involved in retinoid and most probably also in vitamin D precursor synthesis (Fransen et al., 1999). Moreover, in PEX5 KO animals it was shown that IGF-I signaling was impaired (Baes et al., 1997). In addition, inhibition of mevalonate pathway in cholesterol synthesis abrogated IGF-I signaling (Siddals et al., 2004). Interestingly, all the enzymes for cholesterol synthesis from mevalonate to farnesyldiphosphate are localized in peroxisomes (Kovacs et al., 2007). Additionally, several studies have provided evidences that growth plate chondrocytes accumulate large amounts of cytoplasmic calcium before the initiation of mineralization (Gunter et al., 1990; Iannotti et al., 1994) and alterations of  $\text{Ca}^{2+}$  homeostasis play a vital role in chondrocyte differentiation and mineralization. Lasorsa and his colleagues demonstrated that peroxisomes are also involved in intracellular  $\text{Ca}^{2+}$  homeostasis besides mitochondria and the smooth ER (Lasorsa et al., 2008), suggesting that peroxisomes might play an important role in regulating the mineralization process of the growth plate.

Osteoblasts are derived from pluripotent mesenchymal stem cells and are located on bony surfaces (Cohen, 2006). They are responsible for synthesizing matrix proteins that subsequently become mineralized during the process of bone formation. We observed that peroxisomes were more numerous in osteoblasts than in osteocytes. By affecting the synthesis of cholesterol and plasmalogens in lipid rafts, which are important platforms for signaling receptors and required for the osteoblast mineralization process (Anderson, 1995;

Babiychuk and Draeger, 2000; Brown and London, 1998; Genge et al., 1990; Pierini and Maxfield, 2001; Saslowsky et al., 2002), these organelles might also play an important role in the regulation of osteoblast signaling pathways and the osteoblast mineralization. Indeed, alterations of lipid rafts have been found in a mouse model with deficiency in plasmalogen synthesis (Rodemer et al., 2003). Moreover, since the vinyl ether bond in plasmalogens is more susceptible to oxidation than their 1-acyl analogues, this peroxisome-derived lipid class might scavenge ROS, thus 'protecting' plasma membrane phospholipids from oxidative damage and prevent protein modification by lipid peroxidation (Brites et al., 2004). In addition, catalase is also an important antioxidant enzyme, which possesses the highest capacity to degrade H<sub>2</sub>O<sub>2</sub> (Schrader and Fahimi, 2004). Catalase protein was highly enriched in hypertrophic chondrocytes and osteoblasts, wherefore both cell types might be more protected against oxidative stress than others of the skeletal tissues. Together, our data indicate that peroxisomes play a crucial role in protecting hypertrophic chondrocytes and osteoblasts against ROS and regulating the process of bone formation.

#### ***5.1.2 The abundance of peroxisomal enzymes is differently affected by osteoblast maturation and seems to be regulated by PPAR $\alpha$***

Immunofluorescence preparation (Fig12), RT-PCR (Fig14) and Western blot analyses (Fig15) revealed that peroxisomes and peroxisomal enzymes were present at lower abundance in 3 day-old osteoblasts in comparison to later time points, which is in agreement with the low mRNA levels of Pex11 $\alpha$  and Pex11 $\beta$  at this stage. Pex11-type proteins were suggested to be involved in the proliferation of peroxisomes, since the knockout of the PEX11 gene leads to an increase in size and a decrease in the number of peroxisomes and

overexpression of these proteins results in an increase in tubulation and peroxisome number (Li et al., 2002a; Schrader et al., 1998; Thoms and Erdmann, 2005). In addition, we observed that PPAR $\alpha$ , the nuclear receptor regulating Pex11 $\alpha$  transcription (Passreiter et al., 1998; Schrader et al., 1998), was also expressed at a very low level in 3 day-old osteoblasts. PPAR $\alpha$  is critical for peroxisomal protein induction and peroxisome proliferation after treatment with hypolipidemic substances (Isseemann and Green, 1990). For induction of peroxisome proliferation, lipid ligands bind to PPAR $\alpha$  and stimulate the heterodimerization of this transcription factor with RxR and its nuclear translocation (Keller et al., 2000). The activation of PPAR $\alpha$ /RxR leads to an increased peroxisome number. Osumi and his colleagues have shown that proliferation of peroxisomes not only takes place *in situ* in rodents, but also in cultured cells, such as H4IIEC3 rat hepatoma cells after treatment with ciprofibrate, a PPAR $\alpha$  agonist (Osumi et al., 1990). Taken together, our findings indicate that low levels of PPAR $\alpha$ , PEX11 $\alpha$  and PEX11 $\beta$  might contribute to the low number of peroxisomes in the early osteoblasts.

In addition to low levels of these three regulating proteins, catalase and 3-ketoacyl-CoA thiolase were also present in a lower level in the enriched peroxisomal fraction (P3) at day 3. This is in line with the low level of Pex5p, a cytoplasmic shuttling receptor involved in translocation of most peroxisomal matrix proteins containing PTS1 into peroxisomes (Dammai and Subramani, 2001), which might explain the reduced import of catalase. Pex5pL is involved in the translocation of both PTS1 and PTS2 proteins into the peroxisomes, since it binds the PTS2 receptor (Pex7p) prior to import of PTS2 proteins. In the absence of Pex5pL, the Pex7p/PTS2-protein complex is unable to dock at the peroxisomal

membrane (Wanders, 2004a). Thiolase is a PTS2 protein to which Pex7p binds directly before it is associated with Pex5pL for the process of its import. In PEX5 and PEX7 knockout mice, thiolase was present in its precursor form in the cytoplasm, whereas in extracts from wild type mice thiolase was detected in its mature form (Baes et al., 1997; Brites et al., 2003). Catalase and thiolase proteins reached a maximum at day 7 and thereafter decreased again. This pattern is also followed by Pex5p, suggesting that peroxisomal import goes down again at later time points. In this thesis, it was also observed that PPAR $\alpha$  protein shifted from the nucleus back to the cytoplasm at day 15 and this may probably attenuate the transcription of "peroxisomal" genes.

In contrast to catalase, thiolase was still present at higher levels in 15day-old osteoblasts cultivated with differentiation medium. It is noteworthy that primary mineralization area was observed at the same time using Alizarin red S staining, suggesting that the high thiolase level might maintain a high activity of peroxisomal  $\beta$ -oxidation for shuttling of acetyl-CoA units into the synthesis of cholesterol and plasmalogens (Karnati and Baumgart-Vogt, 2008; Kovacs et al., 2007), because intact lipid rafts are required for the osteoblast mineralization process (Gillette and Nielsen-Preiss, 2004).

### ***5.1.3 Treatment with PPAR $\alpha$ or PPAR $\gamma$ agonists alters the enzyme composition of the peroxisomal compartment in osteoblasts***

PPAR $\alpha$  is a member of the nuclear hormone receptor superfamily and plays an important role in lipid metabolism by regulating the genes involved in fatty acid oxidation. Our data exhibited an increase in the protein levels of Pex13p, Pex14p and thiolase in primary osteoblasts treated with the PPAR $\alpha$  agonist ciprofibrate, indicating that the activation of PPAR $\alpha$  increased peroxisome proliferation and

induced the transcriptional activation of the genes required for the peroxisomal fatty acid  $\beta$ -oxidation. Moreover, catalase was enhanced as well, but to a lower extent. This is in line with previous reports that the peroxisomal proliferation and  $\beta$ -oxidation enzymes might be induced at high levels in cell cultures of H4IIEC3 rat hepatoma cells (Osumi et al., 1990) and rat Fao cells (Duclos et al., 1997). Previous studies with whole animals (mostly rats) indeed demonstrated that the expression of the enzymes for the lipid  $\beta$ -oxidation, such as ACOX and thiolase is induced very strongly by PPAR $\alpha$  agonist, whereas the maximal induction of catalase does not exceed 1 or 2-fold (Fahimi et al., 1982; Rao and Reddy, 1987). In contrast to other cell types (Causeret et al., 1993; Colton et al., 2004; Gatica et al., 2007), treatment with ciprofibrate displayed a dose-dependent reduction of the ABCD3 protein in osteoblasts.

In contrast to PPAR $\alpha$ , PPAR $\gamma$  is implicated in adipogenesis and glucose homeostasis, and is recently considered as a negative regulator of osteogenesis (Jeon et al., 2003; Lecka-Czernik et al., 2002; Lin et al., 2007; Nuttall et al., 1998). PPAR $\gamma$  can be activated by a wide variety of substances including long chain fatty acids, 15-deoxy- $\Delta^{12,14}$ -prostaglandin J2 (15d-PGJ2), and thiazolidinedione compounds, such as troglitazone (Rosen and Spiegelman, 2001). Results of this study showed that troglitazone enhanced catalase expression in both homogenates and enriched peroxisomal fractions. This is in agreement with previous report that PPAR $\gamma$  agonists could significantly enhance catalase mRNA and activity in adipose tissue (Okuno et al., 2008). In comparison to catalase, the peroxisomal membrane protein Pex14p was only slightly elevated in homogenates during troglitazone treatment, indicating that PPAR $\gamma$  might not be associated with strong peroxisome proliferation (Thoms and

Erdmann, 2005). Interestingly, thiolase and ABCD3 exhibited an opposite expression pattern in individual peroxisomes and were also regulated in the opposite direction versus ciprofibrate treatment, suggesting that PPAR $\gamma$  and PPAR $\alpha$  agonists exert different effects on the peroxisomal compartment in osteoblasts cultures. In addition, the results of this thesis indicate that ABCD3 is differently regulated from  $\beta$ -oxidation enzymes, even though it is suggested to be involved in the transport of lipid metabolites across the peroxisomal membrane. However, its exact functions are still under debate.

In addition, ciprofibrate increased the expression of OPN, but troglitazone reduced the level of this bone matrix protein, suggesting that PPAR $\alpha$  induction leads to higher differentiation of osteoblasts and more bone matrix production, which is paralleled by peroxisomal enzyme induction.

## **5.2 Part 2**

PEX11 $\beta$  KO mice were generated and partially characterized by Li et al (Li et al., 2002b). Even though PEX11 $\beta$  KO mice show no apparent defect in peroxisomal protein import and exhibit only mild defects in peroxisomal metabolic functions in the brain and liver, they exhibit numerous pathological features of Zellweger syndrome, including the developmental delay, hypotonia, and neuronal migration defects. In addition to these defects, ossification impairment was also observed in PEX11 $\beta$  KO mice.

### ***5.2.1 Oxidative stress and lipid peroxidation might contribute to the impairment of bone ossification in PEX11 $\beta$ KO mice***

Bone development is regulated by two essential processes, intramembranous ossification and endochondral ossification. Intramembranous ossification refers to the process by which flat bones, including those of the cranial vault, some facial bones, and the lateral aspect of the clavicle, develop directly from the mesenchymal precursor cells (Mundlos, 1999). Whereas, endochondral ossification utilizes an intermediate step of cartilage formation for the development of long bones as well as other bones of the skeleton (Erlebacher et al., 1995). E19 PEX11 $\beta$  KO mice exhibit delayed ossification of bone elements in the cranial vault, sternum, coccygeal vertebrae and distal bone elements of fore- and hindlimbs. These data indicate that both intramembranous and endochondral ossification are impaired in PEX11 $\beta$  KO mice. Similar alterations in ossification were also reported in other mouse models for Zellweger syndrome or rhizomelic chondrodysplasia punctata (Baes et al., 1997; Brites et al., 2003; Faust and Hatten, 1997; Maxwell et al., 2003). However, the pathogenesis of the ossification impairment is not yet resolved.

Mammalian peroxisomes are normally found to be densely populated by enzymes that form ROS, such as acyl-CoA oxidases, urate oxidase, 2-hydroxyacid oxidase as well as D-amino acid and D-aspartate oxidases (Antonenkov et al., 2009; Baumgart, 1997; Fahimi and Baumgart, 1999). In recent years, it has become clear that in addition to catalase peroxisomes also harbour a variety of other enzymes involved in the decomposition of H<sub>2</sub>O<sub>2</sub> and O<sub>2</sub><sup>•-</sup>, such as Copper/Zinc superoxide dismutase (SOD1), glutathione peroxidase (GPx) and peroxiredoxin I (PrxI) (Immenschuh and Baumgart-Vogt, 2005;

Knoops et al., 1999; Morel et al., 2004; Oshino et al., 1973; Seo et al., 2000; Singh, 1996). Under normal conditions, there is an equilibrium distribution relationship between these enzymes. If the balance between the generation and scavenging of these ROS is disturbed, increased oxidative stress may develop, leading to oxidation of lipids in membranes, of thiol-containing proteins, and of mitochondrial DNA. In addition, even under physiological conditions, 2 to 3% of the consumed oxygen is converted to superoxide in mitochondria (Baumgart et al., 2001). Alterations in mitochondrial respiration might increase the ROS release, especially when mitochondrial antioxidant defense systems are overloaded or due to outer membrane damage and ROS leakage.

In this study, several antioxidant enzymes were elevated in PEX11 $\beta$  KO osteoblasts, such as catalase and HO-1, suggesting the occurrence of oxidative stress in PEX11 $\beta$  KO osteoblasts. An increase in catalase was also reported in other studies on cells with peroxisomal deficiency. Singh and colleagues observed higher catalase activity in cultured skin fibroblasts from Zellweger patients than in control fibroblasts (Singh et al., 1996). Recently, a Belgian group described the upregulation of the peroxisomal enzyme catalase in white matter areas of brain-specific PEX5 KO mice (Hulshagen et al., 2008). As mentioned above, the protein level of HO-1 was also enhanced in PEX11 $\beta$  KO osteoblasts. Interestingly, HO-1 is an enzyme that is thought to be increased for regulating cellular defense mechanisms against oxidative stress. Under stress conditions, HO-1 can be translocated to the plasma membrane (specifically to caveolae), most probably influencing cell surface signaling (Wang et al., 2009). In addition, HO-1 in the liver can generate biliverdin, which is converted by biliverdin reductase to bilirubin and bilirubin is a potent antioxidant (Vile et al.,

1994). A further sign of oxidative stress in PEX11 $\beta$  KO mice was the significant upregulation of SOD2, an important antioxidant enzyme in mitochondria for conversion of O<sub>2</sub><sup>·-</sup> into H<sub>2</sub>O<sub>2</sub>, which is further degraded by the mitochondrial glutathione peroxidase. A strong SOD2 increase was also described in PEX5 deficient mice, however, in other cell types (Baumgart et al., 2001). In addition to the SOD2 increase, a complex III induction was found in this thesis, indicating mitochondrial proliferation. Indeed, Li and coworkers did detect mitochondrial proliferation in some hepatocytes of PEX11 $\beta$  KO mice (Li et al., 2002b). However, this proliferation was much more pronounced in PEX5 KO hepatocytes (Baumgart et al., 2001).

Two possible mechanisms might be involved in the generation of strong oxidative stress in PEX11 $\beta$  KO animals: 1) a decrease in Forkhead box O1 (FoxO1) and 2) an increase in lipid peroxidation. Indeed, a significant reduction in FoxO1 was noted in PEX11 $\beta$  KO osteoblasts. FoxO1 belongs to the winged helix/forkhead family of transcription factors that is characterized by a 100-amino acid monomeric DNA-binding domain called the FOX domain. Rached and his colleagues observed increased levels of ROS and lipid peroxidation products as well as activation of the stress-evoked p53-dependent signaling cascade in the bones of FoxO1<sub>ob</sub> KO mice (Rached et al., 2010). Administration of the antioxidant NAC rescued the low bone formation phenotype of FoxO1<sub>ob</sub> KO mice and restored the redox balance in FoxO1-deficient osteoblasts (Rached et al., 2010). These studies revealed that FoxO1 is indeed an important regulator of redox balance in osteoblasts. In addition to the FoxO1 reduction, an increase in lipid peroxidation was observed in PEX11 $\beta$  KO osteoblasts as shown by staining of 4-HNE adducts on Western blots. Recently, it was shown that increased lipid

oxidation causes oxidative stress in the skeleton, resulting in an increase in the prevalence of apoptotic osteoblasts (Almeida et al., 2009).

Due to the strong reduction in the protein levels of ABCD3 and thiolase, the peroxisomal  $\beta$ -oxidation in the feedback loop of PPAR $\gamma$  ligand homeostasis is disturbed in PEX11 $\beta$  KO mice, leading to an increase of lipid ligands for PPAR $\gamma$  activation, which in combination with the increase of peroxidized lipids may strongly activate PPAR $\gamma$  (Almeida et al., 2009). In addition, several studies have provided the evidence that FoxO1 normally represses PPAR $\gamma$  activity *in vivo* and *in vitro* (Armoni et al., 2006; Armoni et al., 2007; Fan et al., 2009). Since FoxO1 is downregulated, this repression would be relieved, leading in combination with the above mentioned lipid increase to the strong activation of PPAR $\gamma$ . PPAR $\gamma$  activation would negatively promote the association with the Wnts, resulting in a decrease in  $\beta$ -catenin. Indeed, canonical Wnt signaling pathway was attenuated in PEX11 $\beta$  KO osteoblasts, since less activated- $\beta$ -catenin was translocated into the nucleus. Moreover, the protein level of Cyclin D1, a classical  $\beta$ -catenin/TCF target gene was reduced. The decreased canonical Wnt signal will negatively regulate the expression of its targeting genes, such as Runx2 (Dong et al., 2006; Gaur et al., 2005; Hamidouche et al., 2008). Indeed, this important osteoblast transcription factor was downregulated in PEX11 $\beta$  KO osteoblasts and was translocated from the nucleus to the cytoplasm. A less functional Runx2 signaling would lead to inefficient production of bone matrix proteins, such as OPN and BGP, which was definitely noted in PEX11 $\beta$  KO osteoblasts (Ducy et al., 1997; Fujiwara et al., 1999; Komori et al., 1997). In contrast to Runx2, decreased Wnt signaling would also increase PPAR $\gamma$  expression, resulting in a lower recruitment of mesenchymal stem cells into the osteoblast lineage and less osteoblast

differentiation (Kang et al., 2007; Lecka-Czernik et al., 1999; Takada et al., 2009). As mentioned already above, PPAR $\gamma$  was increased in PEX11 $\beta$  KO cells, which would automatically lead to a vicious cycle and further repress the bone formation. In addition to Wnt and PPAR $\gamma$ , most recently Rached and colleagues described that FoxO1 also plays a vital role in osteoblast proliferation and differentiation. FoxO1<sub>ob</sub> KO mice showed decreased osteoblast numbers, a diminished bone formation rate (BFR), and reduced bone volume (Rached et al., 2010). Moreover, it was demonstrated that FoxO1 is expressed during skeletogenesis in mouse embryos and that FoxO1 activity increased in the early hours of differentiation of mesenchymal cells into osteoblasts *in vitro*. Silencing of FoxO1 significantly disturbed skeletogenesis *in vivo* and *ex vivo* and prevented expression of osteoblast markers and subsequent matrix calcification (Teixeira et al., 2010). In addition, FoxO1 controls Runx2 expression and can directly interact with this transcription factor (Teixeira et al., 2010). These data suggest that a decrease in FoxO1 might at least in part contribute to the defect of ossification in PEX11 $\beta$  KO mice. The model shown in Fig34 summarizes a probable mechanism for the molecular pathogenesis of the ossification impairment in PEX11 $\beta$  KO mice.

Taken together, the data of this thesis revealed that PEX11 $\beta$  deficiency causes significant alterations of osteoblast signaling pathways involved in the regulation of ossification in PEX11 $\beta$  KO mice. Increased oxidative stress and lipid peroxidation due to the missing peroxisome proliferation capacity lead to the development of the ossification defects, wherefore, PEX11 $\beta$  mice might benefit by treatment with high levels of antioxidants. Further studies with different

treatment strategies of PEX11 $\beta$  KO mice might open new methods also for the therapies of patients with Zellweger syndrome.

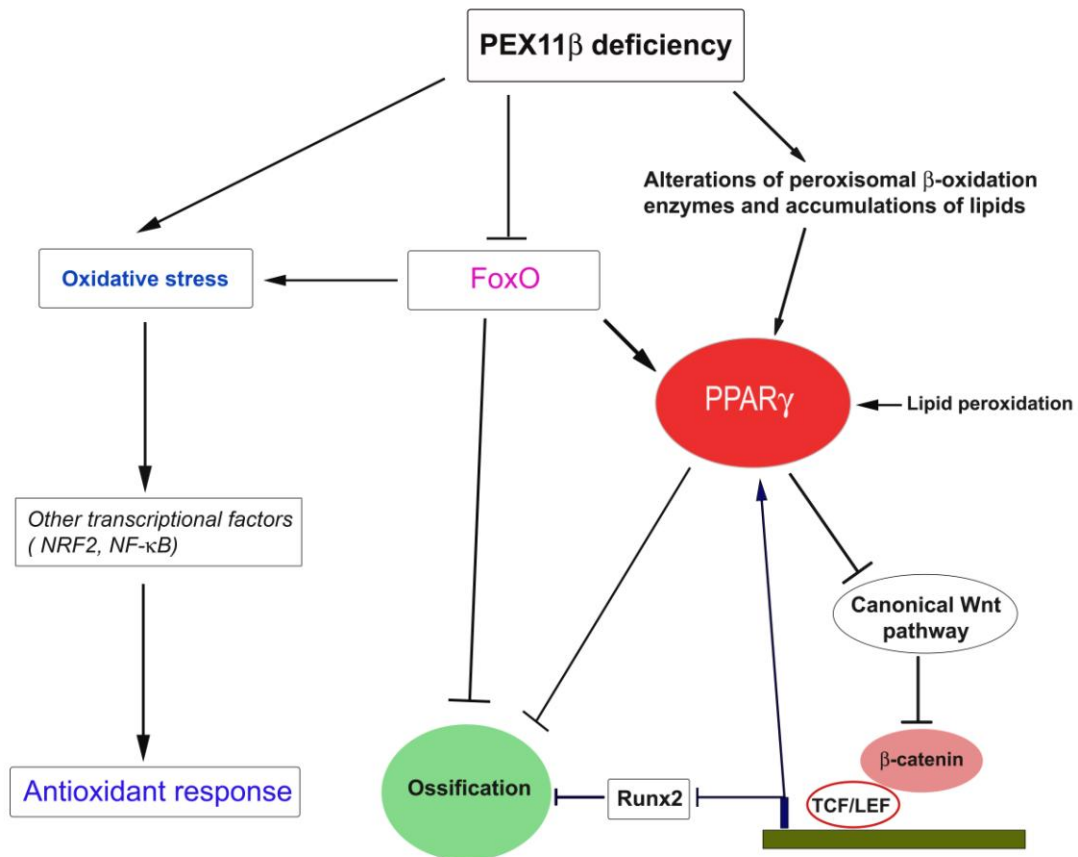


**Fig34.** Oxidative stress, abnormal lipid metabolism and lipid peroxidation might contribute to the impairment of bone ossification in PEX11 $\beta$  KO mice. PEX11 $\beta$  deficiency causes lipid abnormalities, leading to an increase in PPAR $\gamma$  activity. The increase in PPAR $\gamma$  activity attenuates canonical wnt signaling. Decreased canonical Wnt pathway will promote  $\beta$ -catenin accumulation in the cytoplasm and suppress its translocation to the nucleus, further affecting the expression of target genes. In addition, the FoxO1 protein was also reduced due to PEX11 $\beta$  deficiency, resulting in increased oxidative stress and further induction of PPAR $\gamma$ . Due to a decrease in FoxO1, enhanced NRF2 and NF- $\kappa$ B signaling would contribute to antioxidant response.

## **6 Summary**

Only sparse information is available in the literature on peroxisomes and their enzyme composition in different cell types of the mouse skeleton. However, the vital importance of peroxisomes in these tissues is accentuated by the strong ossification defects and growth retardation observed in children with peroxisomal biogenesis defects, such as the Zellweger syndrome, or corresponding knockout (KO) mouse models. Therefore, in the first part of this dissertation the peroxisomal compartment was characterized in different cell types of cartilage and bone, using a variety of morphological, biochemical as well as molecular biological techniques. In the second part of this dissertation, the pathological consequences of peroxisome dysfunction and the molecular pathogenesis of ossification defects were examined in PEX11 $\beta$  KO mice, a mouse model for Zellweger syndrome.

The results of this thesis revealed the presence of peroxisomes in all distinct cell types of the skeleton, however, with significant differences in their numerical abundance and enzyme composition. The peroxisomal biogenesis protein Pex14p proved to be the best marker for identification of the whole peroxisomal population in different cell types. The peroxisomal metabolic proteins catalase and the lipid transporter ABCD3 were strongly enriched in hypertrophic chondrocytes and osteoblasts, suggesting a close relationship of these proteins to ossification processes. In primary cell cultures, a low numerical abundance of peroxisomes was noted in 3d osteoblasts, whereas a constantly higher abundance of peroxisomes was observed in more mature osteoblasts at later time points (7d, 11d and 15d). In contrast, the protein levels of catalase and 3-ketoacyl-CoA thiolase, which were also low in 3d osteoblast reached their maximum at 7 days and declined thereafter. Interestingly, different members of the PPAR-family (peroxisome proliferation-activated receptors  $\alpha$ ,  $\beta$ ,  $\gamma$ ), transcription factors regulating peroxisomal  $\beta$ -oxidation genes, were altered in an individual pattern during osteoblast differentiation. PPAR $\alpha$  was regulated in a similar pattern as the peroxisomal metabolic proteins, whereas the expression of

PPAR $\gamma$  mRNA exhibited opposite regulation and the one for PPAR $\beta$  was not altered at all. Activation of PPAR $\alpha$  by treatment of primary osteoblasts with ciprofibrate for 6 days increased both peroxisomal number and metabolic enzymes, whereas treatment with the PPAR $\gamma$  agonist troglitazone altered the expressions of peroxisomal metabolic enzymes without a significant change in peroxisomal numerical abundance. Interestingly, thiolase and ABCD3 were differentially regulated by PPAR $\alpha$  or PPAR $\gamma$  agonists, indicating that different PPARs might indeed have distinct effects on the regulation of “peroxisomal” genes.

Analyses of PEX11 $\beta$  KO mice with flat-panel volumetric computer tomography or skeletal stainings revealed a strong reduction of bone volume, mass and density in comparison to their wildtype littermates. Comparative analyses of skeletal tissues and primary osteoblast cultures showed a significant decrease in the synthesis of osteoblast secretory marker proteins and a severe retardation in different ossification processes. Furthermore, increased oxidative stress and severe alterations of bone specific signaling pathways were detected in PEX11 $\beta$  KO osteoblasts. An increase in PPAR $\gamma$  was observed, which was accompanied by a decrease in canonical Wnt signaling and FoxO1 protein expression. In addition, the osteoblast transcription factor Runx2 was relocalized from the nucleus into the cytoplasm. All above mentioned alterations might contribute to the ossification defects observed in peroxisomal disorders.

Taken together, the results of this dissertation indicate that regular peroxisomal metabolic functions are required for intramembranous and endochondral ossification processes through protecting osteoblasts against ROS and lipid toxicity as well as the control of PPAR ligand homeostasis.

## ***7 Zusammenfassung***

Zum Thema Peroxisomen und Enzymzusammensetzung dieser Organellen im Stützgewebe sind aus der Literatur kaum Informationen erhältlich. Jedoch wird deren hoher Stellenwert für den Organismus durch die starken Ossifikationsdefekte und Wachstumsretardierung verdeutlicht, die bei Patienten mit peroxisomalen Biogenesestörungen oder entsprechenden Knockout-Mausmodellen auftreten. Deshalb wurde im ersten Teil dieser Dissertation das peroxisomale Kompartiment in unterschiedlichen Zelltypen von Knorpel und Knochen mithilfe einer großen Auswahl morphologischer, biochemischer und molekularbiologischer Methoden charakterisiert. Im zweiten Teil der Dissertation wurden die pathologischen Konsequenzen einer Peroxisomendysfunktion und die molekulare Pathogenese der Ossifikationsdefekte in PEX11 $\beta$ -Knockoutmäusen untersucht.

Die Resultate dieser Dissertation erbrachten den Nachweis von Peroxisomen in allen Zelltypen des Stützgewebes, jedoch mit unterschiedlicher numerischer Dichte und heterogener Enzymzusammensetzung der Organellen. Das peroxisomale Biogeneseprotein Pex14p stellte sich als bester Marker für die Identifikation der gesamte Peroxisomenpopulation unterschiedlicher Zelltypen heraus, während die metabolischen Proteine Katalase und der Lipidtransporter ABCD3 sehr stark in hypertrophischen Knorpelzellen und in Osteoblasten angereichert waren, was eine enge Beziehung zu Ossifikationsprozessen nahelegte. In primären Osteoblastenkulturen wurde im Frühstadium (3 Tage) eine geringe numerische Dichte der Peroxisomen nachgewiesen, während eine wesentlich höhere Anzahl dieser Organellen in mehr murenen Osteoblasten zu späteren Zeitpunkten aufgefunden wurden (7d, 11d, 15d). Im Unterschied zu der Peroxisomenverteilung erreichten die Proteinmengen für Katalase und 3-Ketoacyl-CoA-Thiolase, die in drei Tage alten Osteoblasten auch nur in geringer Menge vorhanden waren, ihr Maximum nach 7 Tagen und fielen danach wieder ab. Interessanterweise wurden unterschiedliche Mitglieder der PPAR-Familie (Peroxisomenproliferator-aktivierten Rezeptoren  $\alpha$ ,  $\beta$ ,  $\gamma$ ), Transkriptionsfaktoren für peroxisomale  $\beta$ -Oxidationsgene, individuell in unterschiedlicher Weise im

Verlauf der Osteoblastendifferenzierung verändert. PPAR $\alpha$  wurde in ähnlicher Weise wie die metabolischen peroxisomalen Proteine verändert, während die Expression der mRNA für PPAR $\gamma$  eine gegensätzliche Regulation aufwies und die für PPAR $\beta$  nicht verändert wurde. Aktivierung von PPAR $\alpha$  durch Behandlung primärer Osteoblasten für 6 Tage mit Ciprofibrat führte zur Erhöhung sowohl der Peroxisomenanzahl als auch der metabolischen Enzyme, während Behandlung mit dem PPAR $\gamma$ -Agonisten Troglitazon nur eine signifikante Veränderung metabolischer Enzyme bewirkte. Interessanterweise wurden Thiolase und ABCD3 durch die PPAR $\alpha$ -oder PPAR $\gamma$ -Agonisten in gegensätzlicher Weise verändert, was vermuten lässt, dass verschiedene PPARs unterschiedliche Wirkung auf die Regulation peroxisomaler Gene ausüben. Analysen von PEX11 $\beta$ -Knockoutmäusen mittels „flat-panel volumetric CT“ oder Skelettfärbungen erbrachten eine starke Verminderung des Volumens, der Masse und der Dichte der Knochen im Vergleich zu Kontrolltieren. Vergleichende Analysen der Stützgewebe und von primären Osteoblastenkulturen erbrachten eine signifikante Abnahme in der Synthese von osteoblastenspezifischen sekretorischen Markerproteinen (Osteopontin und Osteocalcin) und eine starke Retardierung der verschiedenen Ossifikationsprozesse. Weiterhin wurden oxidativer Stress und schwere Veränderungen von osteoblastenspezifischer Signaltransduktionswege in PEX11 $\beta$ <sup>-/-</sup>-Osteoblasten nachgewiesen. Die Erhöhung der PPAR $\gamma$  mRNA-Expression wurde gezeigt und die Verminderung des kanonischen Wnt-Signalweges sowie die Translokation von Runx2 aus dem Zellkern ins Cytoplasma nachgewiesen. Zusätzlich wurde eine Reduktion der Proteinmenge des FoxO1-Transkriptionsfaktors nachgewiesen, was zusammen mit den oben erwähnten Befunden zu einer Minderung der Ossifikationprozesse in peroxisomalen Krankheiten beitragen könnte.

Zusammenfassend lässt sich feststellen, dass reguläre peroxisomale Stoffwechselfunktionen für den normalen Ablauf desmalen und enchondraler Ossifikationsprozesse notwendig sind und sowohl für den Schutz der Osteoblasten gegen ROS- und Lipidtoxizität als auch zur Kontrolle der PPAR-Ligandenhomöostase unerlässlich sind.

## 8 References

- Abe, I., and Fujiki, Y. (1998). cDNA cloning and characterization of a constitutively expressed isoform of the human peroxin Pex11p. *Biochem Biophys Res Commun* 252, 529-533.
- Abe, I., Okumoto, K., Tamura, S., and Fujiki, Y. (1998). Clofibrate-inducible, 28-kDa peroxisomal integral membrane protein is encoded by PEX11. *FEBS Lett* 431, 468-472.
- Agamanolis, D.P., and Novak, R.W. (1995). Rhizomelic chondrodysplasia punctata: report of a case with review of the literature and correlation with other peroxisomal disorders. *Pediatr Pathol Lab Med* 15, 503-513.
- Akune, T., Ohba, S., Kamekura, S., Yamaguchi, M., Chung, U.I., Kubota, N., Terauchi, Y., Harada, Y., Azuma, Y., Nakamura, K., *et al.* (2004). PPARgamma insufficiency enhances osteogenesis through osteoblast formation from bone marrow progenitors. *J Clin Invest* 113, 846-855.
- Almeida, M., Ambrogini, E., Han, L., Manolagas, S.C., and Jilka, R.L. (2009). Increased lipid oxidation causes oxidative stress, increased peroxisome proliferator-activated receptor-gamma expression, and diminished pro-osteogenic Wnt signaling in the skeleton. *J Biol Chem* 284, 27438-27448.
- Almeida, M., Han, L., Martin-Millan, M., Plotkin, L.I., Stewart, S.A., Roberson, P.K., Kousteni, S., O'Brien, C.A., Bellido, T., Parfitt, A.M., *et al.* (2007). Skeletal involution by age-associated oxidative stress and its acceleration by loss of sex steroids. *J Biol Chem* 282, 27285-27297.
- Ambrogini, E., Almeida, M., Martin-Millan, M., Paik, J.H., Depinho, R.A., Han, L., Goellner, J., Weinstein, R.S., Jilka, R.L., O'Brien, C.A., *et al.* (2010). FoxO-mediated defense against oxidative stress in osteoblasts is indispensable for skeletal homeostasis in mice. *Cell Metab* 11, 136-146.
- Anderson, H.C. (1995). Molecular biology of matrix vesicles. *Clin Orthop Relat Res*, 266-280.
- Angermuller, S., Bruder, G., Volkl, A., Wesch, H., and Fahimi, H.D. (1987). Localization of xanthine oxidase in crystalline cores of peroxisomes. A cytochemical and biochemical study. *Eur J Cell Biol* 45, 137-144.
- Antonenkova, V., Grunau, S., Ohlmeier, S., and Hiltunen, K. (2009). Peroxisomes are oxidative organelles. *Antioxid Redox Signal*.
- Armoni, M., Harel, C., Karni, S., Chen, H., Bar-Yoseph, F., Ver, M.R., Quon, M.J., and Karnieli, E. (2006). FOXO1 represses peroxisome proliferator-activated receptor-gamma1 and -gamma2 gene promoters in primary adipocytes. A novel paradigm to increase insulin sensitivity. *J Biol Chem* 281, 19881-19891.
- Armoni, M., Harel, C., and Karnieli, E. (2007). Transcriptional regulation of the GLUT4 gene: from PPAR-gamma and FOXO1 to FFA and inflammation. *Trends Endocrinol Metab* 18, 100-107.

- Babij, P., Zhao, W., Small, C., Kharode, Y., Yaworsky, P.J., Bouxsein, M.L., Reddy, P.S., Bodine, P.V., Robinson, J.A., Bhat, B., *et al.* (2003). High bone mass in mice expressing a mutant LRP5 gene. *J Bone Miner Res* 18, 960-974.
- Babiychuk, E.B., and Draeger, A. (2000). Annexins in cell membrane dynamics. Ca(2+)-regulated association of lipid microdomains. *J Cell Biol* 150, 1113-1124.
- Baes, M., Gressens, P., Baumgart, E., Carmeliet, P., Casteels, M., Franssen, M., Evrard, P., Fahimi, D., Declercq, P.E., Collen, D., *et al.* (1997). A mouse model for Zellweger syndrome. *Nat Genet* 17, 49-57.
- Baudhuin, P., Beaufay, H., and De Duve, C. (1965). Combined biochemical and morphological study of particulate fractions from rat liver. Analysis of preparations enriched in lysosomes or in particles containing urate oxidase, D-amino acid oxidase, and catalase. *J Cell Biol* 26, 219-243.
- Baudhuin, P., Beaufay, H., Rahman-Li, Y., Sellinger, O.Z., Wattiaux, R., Jacques, P., and De Duve, C. (1964). Tissue fractionation studies. 17. Intracellular distribution of monoamine oxidase, aspartate aminotransferase, alanine aminotransferase, D-amino acid oxidase and catalase in rat-liver tissue. *Biochem J* 92, 179-184.
- Baumgart, E. (1997). Application of in situ hybridization, cytochemical and immunocytochemical techniques for the investigation of peroxisomes. A review including novel data. Robert Feulgen Prize Lecture 1997. *Histochem Cell Biol* 108, 185-210.
- Baumgart, E., Vanhooren, J.C., Franssen, M., Marynen, P., Puype, M., Vandekerckhove, J., Leunissen, J.A., Fahimi, H.D., Mannaerts, G.P., and van Veldhoven, P.P. (1996). Molecular characterization of the human peroxisomal branched-chain acyl-CoA oxidase: cDNA cloning, chromosomal assignment, tissue distribution, and evidence for the absence of the protein in Zellweger syndrome. *Proc Natl Acad Sci U S A* 93, 13748-13753.
- Baumgart, E., Vanhorebeek, I., Grabenbauer, M., Borgers, M., Declercq, P.E., Fahimi, H.D., and Baes, M. (2001). Mitochondrial alterations caused by defective peroxisomal biogenesis in a mouse model for Zellweger syndrome (PEX5 knockout mouse). *Am J Pathol* 159, 1477-1494.
- Bernhard, W., and Rouiller, C. (1956). Microbodies and the problem of mitochondrial regeneration in liver cells. *J Biophys Biochem Cytol* 2, 355-360.
- Boyan, B.D., Sylvia, V.L., Dean, D.D., Del Toro, F., and Schwartz, Z. (2002). Differential regulation of growth plate chondrocytes by 1 $\alpha$ ,25-(OH) $_2$ D $_3$  and 24R,25-(OH) $_2$ D $_3$  involves cell-maturation-specific membrane-receptor-activated phospholipid metabolism. *Crit Rev Oral Biol Med* 13, 143-154.
- Boyden, L.M., Mao, J., Belsky, J., Mitzner, L., Farhi, A., Mitnick, M.A., Wu, D., Insogna, K., and Lifton, R.P. (2002). High bone density due to a mutation in LDL-receptor-related protein 5. *N Engl J Med* 346, 1513-1521.
- Boyle, W.J., Simonet, W.S., and Lacey, D.L. (2003). Osteoclast differentiation and activation. *Nature* 423, 337-342.

- Bradford, M.M. (1976). A rapid and sensitive method for the quantitation of microgram quantities of protein utilizing the principle of protein-dye binding. *Anal Biochem* 72, 248-254.
- Braverman, N., Steel, G., Obie, C., Moser, A., Moser, H., Gould, S.J., and Valle, D. (1997). Human PEX7 encodes the peroxisomal PTS2 receptor and is responsible for rhizomelic chondrodysplasia punctata. *Nat Genet* 15, 369-376.
- Braverman, N., Zhang, R., Chen, L., Nimmo, G., Scheper, S., Tran, T., Chaudhury, R., Moser, A., and Steinberg, S. A Pex7 hypomorphic mouse model for plasmalogen deficiency affecting the lens and skeleton. *Mol Genet Metab* 99, 408-416.
- Brighton, C.T., Sugioka, Y., and Hunt, R.M. (1973). Cytoplasmic structures of epiphyseal plate chondrocytes. Quantitative evaluation using electron micrographs of rat costochondral junctions with special reference to the fate of hypertrophic cells. *J Bone Joint Surg Am* 55, 771-784.
- Brites, P., Motley, A.M., Gressens, P., Mooyer, P.A., Ploegaert, I., Everts, V., Evrard, P., Carmeliet, P., Dewerchin, M., Schoonjans, L., *et al.* (2003). Impaired neuronal migration and endochondral ossification in Pex7 knockout mice: a model for rhizomelic chondrodysplasia punctata. *Hum Mol Genet* 12, 2255-2267.
- Brites, P., Waterham, H.R., and Wanders, R.J. (2004). Functions and biosynthesis of plasmalogens in health and disease. *Biochim Biophys Acta* 1636, 219-231.
- Brown, D.A., and London, E. (1998). Functions of lipid rafts in biological membranes. *Annu Rev Cell Dev Biol* 14, 111-136.
- Caetano-Lopes, J., Canhao, H., and Fonseca, J.E. (2007). Osteoblasts and bone formation. *Acta Reumatol Port* 32, 103-110.
- Caplan, A.I. (1988). Bone development. *Ciba Found Symp* 136, 3-21.
- Causeret, C., Bentejac, M., and Bugaut, M. (1993). Proteins and enzymes of the peroxisomal membrane in mammals. *Biol Cell* 77, 89-104.
- Chung, U.I., Lanske, B., Lee, K., Li, E., and Kronenberg, H. (1998). The parathyroid hormone/parathyroid hormone-related peptide receptor coordinates endochondral bone development by directly controlling chondrocyte differentiation. *Proc Natl Acad Sci U S A* 95, 13030-13035.
- Cohen, M.M., Jr. (2006). The new bone biology: pathologic, molecular, and clinical correlates. *Am J Med Genet A* 140, 2646-2706.
- Colton, H.M., Falls, J.G., Ni, H., Kwanyuen, P., Creech, D., McNeil, E., Casey, W.M., Hamilton, G., and Cariello, N.F. (2004). Visualization and quantitation of peroxisomes using fluorescent nanocrystals: treatment of rats and monkeys with fibrates and detection in the liver. *Toxicol Sci* 80, 183-192.
- Cooper, T.G., and Beevers, H. (1969). Beta oxidation in glyoxysomes from castor bean endosperm. *J Biol Chem* 244, 3514-3520.

- Dammai, V., and Subramani, S. (2001). The human peroxisomal targeting signal receptor, Pex5p, is translocated into the peroxisomal matrix and recycled to the cytosol. *Cell* *105*, 187-196.
- Danino, D., and Hinshaw, J.E. (2001). Dynamin family of mechanoenzymes. *Curr Opin Cell Biol* *13*, 454-460.
- De Duve, C., and Baudhuin, P. (1966). Peroxisomes (microbodies and related particles). *Physiol Rev* *46*, 323-357.
- De Luca, F., Barnes, K.M., Uyeda, J.A., De-Levi, S., Abad, V., Palese, T., Mericq, V., and Baron, J. (2001). Regulation of growth plate chondrogenesis by bone morphogenetic protein-2. *Endocrinology* *142*, 430-436.
- De Luca, F., Uyeda, J.A., Mericq, V., Mancilla, E.E., Yanovski, J.A., Barnes, K.M., Zile, M.H., and Baron, J. (2000). Retinoic acid is a potent regulator of growth plate chondrogenesis. *Endocrinology* *141*, 346-353.
- Dean, D.D., Boyan, B.D., Schwart, Z., Muniz, O.E., Carreno, M.R., Maeda, S., and Howell, D.S. (2001). Effect of 1alpha,25-dihydroxyvitamin D3 and 24R,25-dihydroxyvitamin D3 on metalloproteinase activity and cell maturation in growth plate cartilage in vivo. *Endocrine* *14*, 311-323.
- Dieuaide-Noubhani, M., Asselberghs, S., Mannaerts, G.P., and Van Veldhoven, P.P. (1997). Evidence that multifunctional protein 2, and not multifunctional protein 1, is involved in the peroxisomal beta-oxidation of pristanic acid. *Biochem J* *325 ( Pt 2)*, 367-373.
- Dong, Y.F., Soung do, Y., Schwarz, E.M., O'Keefe, R.J., and Drissi, H. (2006). Wnt induction of chondrocyte hypertrophy through the Runx2 transcription factor. *J Cell Physiol* *208*, 77-86.
- Duclos, S., Bride, J., Ramirez, L.C., and Bournot, P. (1997). Peroxisome proliferation and beta-oxidation in Fao and MH1C1 rat hepatoma cells, HepG2 human hepatoblastoma cells and cultured human hepatocytes: effect of ciprofibrate. *Eur J Cell Biol* *72*, 314-323.
- Ducy, P., Zhang, R., Geoffroy, V., Ridall, A.L., and Karsenty, G. (1997). *Osf2/Cbfa1*: a transcriptional activator of osteoblast differentiation. *Cell* *89*, 747-754.
- Eckert, J.H., and Erdmann, R. (2003). Peroxisome biogenesis. *Rev Physiol Biochem Pharmacol* *147*, 75-121.
- Ellies, D.L., Viviano, B., McCarthy, J., Rey, J.P., Itasaki, N., Saunders, S., and Krumlauf, R. (2006). Bone density ligand, Sclerostin, directly interacts with LRP5 but not LRP5G171V to modulate Wnt activity. *J Bone Miner Res* *21*, 1738-1749.
- Erdmann, R., and Blobel, G. (1995). Giant peroxisomes in oleic acid-induced *Saccharomyces cerevisiae* lacking the peroxisomal membrane protein Pmp27p. *J Cell Biol* *128*, 509-523.
- Erlebacher, A., Filvaroff, E.H., Gitelman, S.E., and Derynck, R. (1995). Toward a molecular understanding of skeletal development. *Cell* *80*, 371-378.
- Fahimi, H.D. (1968). Cytochemical localization of peroxidase activity in rat hepatic microbodies (peroxisomes). *J Histochem Cytochem* *16*, 547-550.

- Fahimi, H.D. (1969). Cytochemical localization of peroxidatic activity of catalase in rat hepatic microbodies (peroxisomes). *J Cell Biol* 43, 275-288.
- Fahimi, H.D., and Baumgart, E. (1999). Current cytochemical techniques for the investigation of peroxisomes. A review. *J Histochem Cytochem* 47, 1219-1232.
- Fahimi, H.D., Reinicke, A., Sujatta, M., Yokota, S., Ozel, M., Hartig, F., and Stegmeier, K. (1982). The short- and long-term effects of bezafibrate in the rat. *Ann N Y Acad Sci* 386, 111-135.
- Fan, W., Imamura, T., Sonoda, N., Sears, D.D., Patsouris, D., Kim, J.J., and Olefsky, J.M. (2009). FOXO1 transrepresses peroxisome proliferator-activated receptor gamma transactivation, coordinating an insulin-induced feed-forward response in adipocytes. *J Biol Chem* 284, 12188-12197.
- Fang, Y., Morrell, J.C., Jones, J.M., and Gould, S.J. (2004). PEX3 functions as a PEX19 docking factor in the import of class I peroxisomal membrane proteins. *J Cell Biol* 164, 863-875.
- Faust, P.L., and Hatten, M.E. (1997). Targeted deletion of the PEX2 peroxisome assembly gene in mice provides a model for Zellweger syndrome, a human neuronal migration disorder. *J Cell Biol* 139, 1293-1305.
- Fransen, M., Van Veldhoven, P.P., and Subramani, S. (1999). Identification of peroxisomal proteins by using M13 phage protein VI phage display: molecular evidence that mammalian peroxisomes contain a 2,4-dienoyl-CoA reductase. *Biochem J* 340 ( Pt 2), 561-568.
- Fujiwara, M., Tagashira, S., Harada, H., Ogawa, S., Katsumata, T., Nakatsuka, M., Komori, T., and Takada, H. (1999). Isolation and characterization of the distal promoter region of mouse *Cbfa1*. *Biochim Biophys Acta* 1446, 265-272.
- Gatica, A., Aguilera, M.C., Contador, D., Loyola, G., Pinto, C.O., Amigo, L., Tichauer, J.E., Zanlungo, S., and Bronfman, M. (2007). P450 CYP2C epoxygenase and CYP4A omega-hydroxylase mediate ciprofibrate-induced PPARalpha-dependent peroxisomal proliferation. *J Lipid Res* 48, 924-934.
- Gaur, T., Lengner, C.J., Hovhannisyan, H., Bhat, R.A., Bodine, P.V., Komm, B.S., Javed, A., van Wijnen, A.J., Stein, J.L., Stein, G.S., *et al.* (2005). Canonical WNT signaling promotes osteogenesis by directly stimulating Runx2 gene expression. *J Biol Chem* 280, 33132-33140.
- Genge, B.R., Wu, L.N., and Wuthier, R.E. (1990). Differential fractionation of matrix vesicle proteins. Further characterization of the acidic phospholipid-dependent Ca<sup>2+</sup>(+)-binding proteins. *J Biol Chem* 265, 4703-4710.
- Ghaedi, K., Tamura, S., Okumoto, K., Matsuzono, Y., and Fujiki, Y. (2000). The peroxin pex3p initiates membrane assembly in peroxisome biogenesis. *Mol Biol Cell* 11, 2085-2102.
- Ghys, K., Fransen, M., Mannaerts, G.P., and Van Veldhoven, P.P. (2002). Functional studies on human Pex7p: subcellular localization and interaction with proteins containing a peroxisome-targeting signal type 2 and other peroxins. *Biochem J* 365, 41-50.
- Gilbert, S.F. (2000). *Developmental biology*, 6th (Sunderland, USA: Sinauer Associates, Inc.)

- Gillette, J.M., and Nielsen-Preiss, S.M. (2004). The role of annexin 2 in osteoblastic mineralization. *J Cell Sci* *117*, 441-449.
- Goldfischer, S., Moore, C.L., Johnson, A.B., Spiro, A.J., Valsamis, M.P., Wisniewski, H.K., Ritch, R.H., Norton, W.T., Rapin, I., and Gartner, L.M. (1973). Peroxisomal and mitochondrial defects in the cerebro-hepato-renal syndrome. *Science* *182*, 62-64.
- Gong, Y., Slee, R.B., Fukai, N., Rawadi, G., Roman-Roman, S., Reginato, A.M., Wang, H., Cundy, T., Glorieux, F.H., Lev, D., *et al.* (2001). LDL receptor-related protein 5 (LRP5) affects bone accrual and eye development. *Cell* *107*, 513-523.
- Gould, S.J., Kalish, J.E., Morrell, J.C., Bjorkman, J., Urquhart, A.J., and Crane, D.I. (1996). Pex13p is an SH3 protein of the peroxisome membrane and a docking factor for the predominantly cytoplasmic PTs1 receptor. *J Cell Biol* *135*, 85-95.
- Grimsrud, C.D., Romano, P.R., D'Souza, M., Puzas, J.E., Reynolds, P.R., Rosier, R.N., and O'Keefe, R.J. (1999). BMP-6 is an autocrine stimulator of chondrocyte differentiation. *J Bone Miner Res* *14*, 475-482.
- Gunter, T.E., Zuscik, M.J., Puzas, J.E., Gunter, K.K., and Rosier, R.N. (1990). Cytosolic free calcium concentrations in avian growth plate chondrocytes. *Cell Calcium* *11*, 445-457.
- Hajra, A.K., Burke, C.L., and Jones, C.L. (1979). Subcellular localization of acyl coenzyme A: dihydroxyacetone phosphate acyltransferase in rat liver peroxisomes (microbodies). *J Biol Chem* *254*, 10896-10900.
- Hamidouche, Z., Hay, E., Vaudin, P., Charbord, P., Schule, R., Marie, P.J., and Fromigue, O. (2008). FHL2 mediates dexamethasone-induced mesenchymal cell differentiation into osteoblasts by activating Wnt/beta-catenin signaling-dependent Runx2 expression. *FASEB J* *22*, 3813-3822.
- Harada, S., and Rodan, G.A. (2003). Control of osteoblast function and regulation of bone mass. *Nature* *423*, 349-355.
- He, X., Semenov, M., Tamai, K., and Zeng, X. (2004). LDL receptor-related proteins 5 and 6 in Wnt/beta-catenin signaling: arrows point the way. *Development* *131*, 1663-1677.
- Heiland, I., and Erdmann, R. (2005). Biogenesis of peroxisomes. Topogenesis of the peroxisomal membrane and matrix proteins. *FEBS J* *272*, 2362-2372.
- Heymans, H.S., Oorthuys, J.W., Nelck, G., Wanders, R.J., and Schutgens, R.B. (1985). Rhizomelic chondrodysplasia punctata: another peroxisomal disorder. *N Engl J Med* *313*, 187-188.
- Hirai, K.I. (1969). Light microscopic study of the peroxidatic activity of catalase in formaldehyde-fixed rat liver. *J Histochem Cytochem* *17*, 585-590.
- Hoepfner, D., van den Berg, M., Philippsen, P., Tabak, H.F., and Hetteema, E.H. (2001). A role for Vps1p, actin, and the Myo2p motor in peroxisome abundance and inheritance in *Saccharomyces cerevisiae*. *J Cell Biol* *155*, 979-990.

- Honsho, M., Hiroshige, T., and Fujiki, Y. (2002). The membrane biogenesis peroxin Pex16p. Topogenesis and functional roles in peroxisomal membrane assembly. *J Biol Chem* 277, 44513-44524.
- Hruban, Z., Vigil, E.L., Slesers, A., and Hopkins, E. (1972). Microbodies: constituent organelles of animal cells. *Lab Invest* 27, 184-191.
- Hulshagen, L., Krysko, O., Bottelbergs, A., Huyghe, S., Klein, R., Van Veldhoven, P.P., De Deyn, P.P., D'Hooge, R., Hartmann, D., and Baes, M. (2008). Absence of functional peroxisomes from mouse CNS causes dysmyelination and axon degeneration. *J Neurosci* 28, 4015-4027.
- Hunziker, E.B., Wagner, J., and Zapf, J. (1994). Differential effects of insulin-like growth factor I and growth hormone on developmental stages of rat growth plate chondrocytes in vivo. *J Clin Invest* 93, 1078-1086.
- Iannotti, J.P., Naidu, S., Noguchi, Y., Hunt, R.M., and Brighton, C.T. (1994). Growth plate matrix vesicle biogenesis. The role of intracellular calcium. *Clin Orthop Relat Res*, 222-229.
- Immenschuh, S., and Baumgart-Vogt, E. (2005). Peroxiredoxins, oxidative stress, and cell proliferation. *Antioxid Redox Signal* 7, 768-777.
- Islinger, M., Luers, G.H., Li, K.W., Loos, M., and Volkl, A. (2007). Rat liver peroxisomes after fibrate treatment. A survey using quantitative mass spectrometry. *J Biol Chem* 282, 23055-23069.
- Issemann, I., and Green, S. (1990). Activation of a member of the steroid hormone receptor superfamily by peroxisome proliferators. *Nature* 347, 645-650.
- Jagger, C.J., Lean, J.M., Davies, J.T., and Chambers, T.J. (2005). Tumor necrosis factor- $\alpha$  mediates osteopenia caused by depletion of antioxidants. *Endocrinology* 146, 113-118.
- Jeon, M.J., Kim, J.A., Kwon, S.H., Kim, S.W., Park, K.S., Park, S.W., Kim, S.Y., and Shin, C.S. (2003). Activation of peroxisome proliferator-activated receptor- $\gamma$  inhibits the Runx2-mediated transcription of osteocalcin in osteoblasts. *J Biol Chem* 278, 23270-23277.
- Jones, J.M., Morrell, J.C., and Gould, S.J. (2004). PEX19 is a predominantly cytosolic chaperone and import receptor for class 1 peroxisomal membrane proteins. *J Cell Biol* 164, 57-67.
- Kang, S., Bennett, C.N., Gerin, I., Rapp, L.A., Hankenson, K.D., and Macdougald, O.A. (2007). Wnt signaling stimulates osteoblastogenesis of mesenchymal precursors by suppressing CCAAT/enhancer-binding protein  $\alpha$  and peroxisome proliferator-activated receptor  $\gamma$ . *J Biol Chem* 282, 14515-14524.
- Karnati, S., and Baumgart-Vogt, E. (2008). Peroxisomes in mouse and human lung: their involvement in pulmonary lipid metabolism. *Histochem Cell Biol* 130, 719-740.
- Kashiwayama, Y., Asahina, K., Shibata, H., Morita, M., Muntau, A.C., Roscher, A.A., Wanders, R.J., Shimozaawa, N., Sakaguchi, M., Kato, H., *et al.* (2005). Role of Pex19p in the targeting of PMP70 to peroxisome. *Biochim Biophys Acta* 1746, 116-128.

- Kato, M., Patel, M.S., Levasseur, R., Lobov, I., Chang, B.H., Glass, D.A., 2nd, Hartmann, C., Li, L., Hwang, T.H., Brayton, C.F., *et al.* (2002). Cbfa1-independent decrease in osteoblast proliferation, osteopenia, and persistent embryonic eye vascularization in mice deficient in Lrp5, a Wnt coreceptor. *J Cell Biol* 157, 303-314.
- Keller, G.A., Barton, M.C., Shapiro, D.J., and Singer, S.J. (1985). 3-Hydroxy-3-methylglutaryl-coenzyme A reductase is present in peroxisomes in normal rat liver cells. *Proc Natl Acad Sci U S A* 82, 770-774.
- Keller, J.M., Collet, P., Bianchi, A., Huin, C., Bouillaud-Kremerik, P., Becuwe, P., Schohn, H., Domenjoud, L., and Dauca, M. (2000). Implications of peroxisome proliferator-activated receptors (PPARS) in development, cell life status and disease. *Int J Dev Biol* 44, 429-442.
- Knoops, B., Clippe, A., Bogard, C., Arsalane, K., Wattiez, R., Hermans, C., Duconseille, E., Falmagne, P., and Bernard, A. (1999). Cloning and characterization of AOEB166, a novel mammalian antioxidant enzyme of the peroxiredoxin family. *J Biol Chem* 274, 30451-30458.
- Koch, A., Schneider, G., Luers, G.H., and Schrader, M. (2004). Peroxisome elongation and constriction but not fission can occur independently of dynamin-like protein 1. *J Cell Sci* 117, 3995-4006.
- Koch, A., Thiemann, M., Grabenbauer, M., Yoon, Y., McNiven, M.A., and Schrader, M. (2003). Dynamin-like protein 1 is involved in peroxisomal fission. *J Biol Chem* 278, 8597-8605.
- Komori, T., Yagi, H., Nomura, S., Yamaguchi, A., Sasaki, K., Deguchi, K., Shimizu, Y., Bronson, R.T., Gao, Y.H., Inada, M., *et al.* (1997). Targeted disruption of Cbfa1 results in a complete lack of bone formation owing to maturational arrest of osteoblasts. *Cell* 89, 755-764.
- Kovacs, W.J., Olivier, L.M., and Krisans, S.K. (2002). Central role of peroxisomes in isoprenoid biosynthesis. *Prog Lipid Res* 41, 369-391.
- Kovacs, W.J., Shackelford, J.E., Tape, K.N., Richards, M.J., Faust, P.L., Fliesler, S.J., and Krisans, S.K. (2004). Disturbed cholesterol homeostasis in a peroxisome-deficient PEX2 knockout mouse model. *Mol Cell Biol* 24, 1-13.
- Kovacs, W.J., Tape, K.N., Shackelford, J.E., Duan, X., Kasumov, T., Kelleher, J.K., Brunengraber, H., and Krisans, S.K. (2007). Localization of the pre-squalene segment of the isoprenoid biosynthetic pathway in mammalian peroxisomes. *Histochem Cell Biol* 127, 273-290.
- Kovacs, W.J., Tape, K.N., Shackelford, J.E., Wikander, T.M., Richards, M.J., Fliesler, S.J., Krisans, S.K., and Faust, P.L. (2009). Peroxisome deficiency causes a complex phenotype because of hepatic SREBP/Insig dysregulation associated with endoplasmic reticulum stress. *J Biol Chem* 284, 7232-7245.
- Lasorsa, F.M., Pinton, P., Palmieri, L., Scarcia, P., Rottensteiner, H., Rizzuto, R., and Palmieri, F. (2008). Peroxisomes as novel players in cell calcium homeostasis. *J Biol Chem* 283, 15300-15308.

- Lazarow, P.B., and De Duve, C. (1976). A fatty acyl-CoA oxidizing system in rat liver peroxisomes; enhancement by clofibrate, a hypolipidemic drug. *Proc Natl Acad Sci U S A* *73*, 2043-2046.
- Lazarow, P.B., and Fujiki, Y. (1985). Biogenesis of peroxisomes. *Annu Rev Cell Biol* *1*, 489-530.
- Lean, J.M., Davies, J.T., Fuller, K., Jagger, C.J., Kirstein, B., Partington, G.A., Urry, Z.L., and Chambers, T.J. (2003). A crucial role for thiol antioxidants in estrogen-deficiency bone loss. *J Clin Invest* *112*, 915-923.
- Lecka-Czernik, B., Gubrij, I., Moerman, E.J., Kajkenova, O., Lipschitz, D.A., Manolagas, S.C., and Jilka, R.L. (1999). Inhibition of *Osf2/Cbfa1* expression and terminal osteoblast differentiation by PPARgamma2. *J Cell Biochem* *74*, 357-371.
- Lecka-Czernik, B., Moerman, E.J., Grant, D.F., Lehmann, J.M., Manolagas, S.C., and Jilka, R.L. (2002). Divergent effects of selective peroxisome proliferator-activated receptor-gamma 2 ligands on adipocyte versus osteoblast differentiation. *Endocrinology* *143*, 2376-2384.
- Li, X., Baumgart, E., Dong, G.X., Morrell, J.C., Jimenez-Sanchez, G., Valle, D., Smith, K.D., and Gould, S.J. (2002a). PEX11alpha is required for peroxisome proliferation in response to 4-phenylbutyrate but is dispensable for peroxisome proliferator-activated receptor alpha-mediated peroxisome proliferation. *Mol Cell Biol* *22*, 8226-8240.
- Li, X., Baumgart, E., Morrell, J.C., Jimenez-Sanchez, G., Valle, D., and Gould, S.J. (2002b). PEX11 beta deficiency is lethal and impairs neuronal migration but does not abrogate peroxisome function. *Mol Cell Biol* *22*, 4358-4365.
- Li, X., and Gould, S.J. (2002). PEX11 promotes peroxisome division independently of peroxisome metabolism. *J Cell Biol* *156*, 643-651.
- Li, X., and Gould, S.J. (2003). The dynamin-like GTPase DLP1 is essential for peroxisome division and is recruited to peroxisomes in part by PEX11. *J Biol Chem* *278*, 17012-17020.
- Li, X., Zhang, Y., Kang, H., Liu, W., Liu, P., Zhang, J., Harris, S.E., and Wu, D. (2005). Sclerostin binds to LRP5/6 and antagonizes canonical Wnt signaling. *J Biol Chem* *280*, 19883-19887.
- Lin, T.H., Yang, R.S., Tang, C.H., Lin, C.P., and Fu, W.M. (2007). PPARgamma inhibits osteogenesis via the down-regulation of the expression of COX-2 and iNOS in rats. *Bone* *41*, 562-574.
- Little, R.D., Carulli, J.P., Del Mastro, R.G., Dupuis, J., Osborne, M., Folz, C., Manning, S.P., Swain, P.M., Zhao, S.C., Eustace, B., et al. (2002). A mutation in the LDL receptor-related protein 5 gene results in the autosomal dominant high-bone-mass trait. *Am J Hum Genet* *70*, 11-19.
- Liu, C., Li, Y., Semenov, M., Han, C., Baeg, G.H., Tan, Y., Zhang, Z., Lin, X., and He, X. (2002). Control of beta-catenin phosphorylation/degradation by a dual-kinase mechanism. *Cell* *108*, 837-847.

- Loughran, P.A., Stolz, D.B., Vodovotz, Y., Watkins, S.C., Simmons, R.L., and Billiar, T.R. (2005). Monomeric inducible nitric oxide synthase localizes to peroxisomes in hepatocytes. *Proc Natl Acad Sci U S A* 102, 13837-13842.
- Mani, A., Radhakrishnan, J., Wang, H., Mani, M.A., Nelson-Williams, C., Carew, K.S., Mane, S., Najmabadi, H., Wu, D., and Lifton, R.P. (2007). LRP6 mutation in a family with early coronary disease and metabolic risk factors. *Science* 315, 1278-1282.
- Mannaerts, G.P., and Van Veldhoven, P.P. (1993). Metabolic pathways in mammalian peroxisomes. *Biochimie* 75, 147-158.
- Marshall, P.A., Krimkevich, Y.I., Lark, R.H., Dyer, J.M., Veenhuis, M., and Goodman, J.M. (1995). Pmp27 promotes peroxisomal proliferation. *J Cell Biol* 129, 345-355.
- Masters, C., and Crane, D. (1984). On the role of peroxisomes in the metabolism of lipids--evidence from studies on mammalian tissues in vivo. *Mol Cell Biochem* 65, 23-35.
- Matsuzaki, T., and Fujiki, Y. (2008). The peroxisomal membrane protein import receptor Pex3p is directly transported to peroxisomes by a novel Pex19p- and Pex16p-dependent pathway. *J Cell Biol* 183, 1275-1286.
- Maxwell, M., Bjorkman, J., Nguyen, T., Sharp, P., Finnie, J., Paterson, C., Tonks, I., Paton, B.C., Kay, G.F., and Crane, D.I. (2003). Pex13 inactivation in the mouse disrupts peroxisome biogenesis and leads to a Zellweger syndrome phenotype. *Mol Cell Biol* 23, 5947-5957.
- Mbalaviele, G., Abu-Amer, Y., Meng, A., Jaiswal, R., Beck, S., Pittenger, M.F., Thiede, M.A., and Marshak, D.R. (2000). Activation of peroxisome proliferator-activated receptor-gamma pathway inhibits osteoclast differentiation. *J Biol Chem* 275, 14388-14393.
- McNiven, M.A. (1998). Dynamin: a molecular motor with pinchase action. *Cell* 94, 151-154.
- Morel, F., Rauch, C., Petit, E., Piton, A., Theret, N., Coles, B., and Guillouzo, A. (2004). Gene and protein characterization of the human glutathione S-transferase kappa and evidence for a peroxisomal localization. *J Biol Chem* 279, 16246-16253.
- Moser, H.W. (1993). Peroxisomal diseases. *Adv Hum Genet* 21, 1-106, 443-151.
- Motley, A.M., Hettema, E.H., Hogenhout, E.M., Brites, P., ten Asbroek, A.L., Wijburg, F.A., Baas, F., Heijmans, H.S., Tabak, H.F., Wanders, R.J., *et al.* (1997). Rhizomelic chondrodysplasia punctata is a peroxisomal protein targeting disease caused by a non-functional PTS2 receptor. *Nat Genet* 15, 377-380.
- Mukai, S., Ghaedi, K., and Fujiki, Y. (2002). Intracellular localization, function, and dysfunction of the peroxisome-targeting signal type 2 receptor, Pex7p, in mammalian cells. *J Biol Chem* 277, 9548-9561.
- Mundlos, S. (1999). Cleidocranial dysplasia: clinical and molecular genetics. *J Med Genet* 36, 177-182.
- Nenicu, A., Luers, G.H., Kovacs, W., David, M., Zimmer, A., Bergmann, M., and Baumgart-Vogt, E. (2007). Peroxisomes in human and mouse testis: differential expression of peroxisomal proteins in germ cells and distinct somatic cell types of the testis. *Biol Reprod* 77, 1060-1072.

- Neuberger, G., Maurer-Stroh, S., Eisenhaber, B., Hartig, A., and Eisenhaber, F. (2003). Motif refinement of the peroxisomal targeting signal 1 and evaluation of taxon-specific differences. *J Mol Biol* 328, 567-579.
- Nilsson, O., Marino, R., De Luca, F., Phillip, M., and Baron, J. (2005). Endocrine regulation of the growth plate. *Horm Res* 64, 157-165.
- Novikoff, A.B., and Goldfischer, S. (1969). Visualization of peroxisomes (microbodies) and mitochondria with diaminobenzidine. *J Histochem Cytochem* 17, 675-680.
- Nuttall, M.E., Patton, A.J., Olivera, D.L., Nadeau, D.P., and Gowen, M. (1998). Human trabecular bone cells are able to express both osteoblastic and adipocytic phenotype: implications for osteopenic disorders. *J Bone Miner Res* 13, 371-382.
- Obert, M., Ahlemeyer, B., Baumgart-Vogt, E., and Traupe, H. (2005). Flat-panel volumetric computed tomography: a new method for visualizing fine bone detail in living mice. *J Comput Assist Tomogr* 29, 560-565.
- Okuno, Y., Matsuda, M., Kobayashi, H., Morita, K., Suzuki, E., Fukuhara, A., Komuro, R., Shimabukuro, M., and Shimomura, I. (2008). Adipose expression of catalase is regulated via a novel remote PPARgamma-responsive region. *Biochem Biophys Res Commun* 366, 698-704.
- Olsen, B.R., Reginato, A.M., and Wang, W. (2000). Bone development. *Annu Rev Cell Dev Biol* 16, 191-220.
- Oshino, N., Chance, B., Sies, H., and Bucher, T. (1973). The role of H<sub>2</sub>O<sub>2</sub> generation in perfused rat liver and the reaction of catalase compound I and hydrogen donors. *Arch Biochem Biophys* 154, 117-131.
- Osumi, T., Yokota, S., and Hashimoto, T. (1990). Proliferation of peroxisomes and induction of peroxisomal beta-oxidation enzymes in rat hepatoma H4IIEC3 by ciprofibrate. *J Biochem* 108, 614-621.
- Passreiter, M., Anton, M., Lay, D., Frank, R., Harter, C., Wieland, F.T., Gorgas, K., and Just, W.W. (1998). Peroxisome biogenesis: involvement of ARF and coatomer. *J Cell Biol* 141, 373-383.
- Pierini, L.M., and Maxfield, F.R. (2001). Flotillas of lipid rafts fore and aft. *Proc Natl Acad Sci U S A* 98, 9471-9473.
- Piters, E., Boudin, E., and Van Hul, W. (2008). Wnt signaling: a win for bone. *Arch Biochem Biophys* 473, 112-116.
- Purdue, P.E., Skoneczny, M., Yang, X., Zhang, J.W., and Lazarow, P.B. (1999). Rhizomelic chondrodysplasia punctata, a peroxisomal biogenesis disorder caused by defects in Pex7p, a peroxisomal protein import receptor: a minireview. *Neurochem Res* 24, 581-586.
- Purdue, P.E., Zhang, J.W., Skoneczny, M., and Lazarow, P.B. (1997). Rhizomelic chondrodysplasia punctata is caused by deficiency of human PEX7, a homologue of the yeast PTS2 receptor. *Nat Genet* 15, 381-384.

- Rached, M.T., Kode, A., Xu, L., Yoshikawa, Y., Paik, J.H., Depinho, R.A., and Kousteni, S. (2010). FoxO1 is a positive regulator of bone formation by favoring protein synthesis and resistance to oxidative stress in osteoblasts. *Cell Metab* 11, 147-160.
- Rachubinski, R.A., and Subramani, S. (1995). How proteins penetrate peroxisomes. *Cell* 83, 525-528.
- Raisz, L.G. (2005). Clinical practice. Screening for osteoporosis. *N Engl J Med* 353, 164-171.
- Rao, M.S., and Reddy, J.K. (1987). Peroxisome proliferation and hepatocarcinogenesis. *Carcinogenesis* 8, 631-636.
- Rhodin, J. (1954) Correlation of ultrastructural organization and function in normal and experimentally changing convoluted tubule cells of the mouse kidney. Doctorate Thesis. Karolinska Institutet, Aktiebolaget Godvil, Stockholm.
- Ricote, M., Li, A.C., Willson, T.M., Kelly, C.J., and Glass, C.K. (1998). The peroxisome proliferator-activated receptor-gamma is a negative regulator of macrophage activation. *Nature* 391, 79-82.
- Rodan, G.A., and Martin, T.J. (2000). Therapeutic approaches to bone diseases. *Science* 289, 1508-1514.
- Rodemer, C., Thai, T.P., Brugger, B., Kaercher, T., Werner, H., Nave, K.A., Wieland, F., Gorgas, K., and Just, W.W. (2003). Inactivation of ether lipid biosynthesis causes male infertility, defects in eye development and optic nerve hypoplasia in mice. *Hum Mol Genet* 12, 1881-1895.
- Rosen, E.D., and Spiegelman, B.M. (2001). PPARgamma : a nuclear regulator of metabolism, differentiation, and cell growth. *J Biol Chem* 276, 37731-37734.
- Ruel, L., Stambolic, V., Ali, A., Manoukian, A.S., and Woodgett, J.R. (1999). Regulation of the protein kinase activity of Shaggy(Zeste-white3) by components of the wingless pathway in *Drosophila* cells and embryos. *J Biol Chem* 274, 21790-21796.
- Sacksteder, K.A., and Gould, S.J. (2000). The genetics of peroxisome biogenesis. *Annu Rev Genet* 34, 623-652.
- Sacksteder, K.A., Jones, J.M., South, S.T., Li, X., Liu, Y., and Gould, S.J. (2000). PEX19 binds multiple peroxisomal membrane proteins, is predominantly cytoplasmic, and is required for peroxisome membrane synthesis. *J Cell Biol* 148, 931-944.
- Santos, M.J., Imanaka, T., Shio, H., Small, G.M., and Lazarow, P.B. (1988). Peroxisomal membrane ghosts in Zellweger syndrome--aberrant organelle assembly. *Science* 239, 1536-1538.
- Saslowsky, D.E., Lawrence, J., Ren, X., Brown, D.A., Henderson, R.M., and Edwardson, J.M. (2002). Placental alkaline phosphatase is efficiently targeted to rafts in supported lipid bilayers. *J Biol Chem* 277, 26966-26970.
- Schrader, M., and Fahimi, H.D. (2004). Mammalian peroxisomes and reactive oxygen species. *Histochem Cell Biol* 122, 383-393.

- Schrader, M., Reuber, B.E., Morrell, J.C., Jimenez-Sanchez, G., Obie, C., Stroh, T.A., Valle, D., Schroer, T.A., and Gould, S.J. (1998). Expression of PEX11beta mediates peroxisome proliferation in the absence of extracellular stimuli. *J Biol Chem* 273, 29607-29614.
- Seedorf, U., Brysch, P., Engel, T., Schrage, K., and Assmann, G. (1994). Sterol carrier protein X is peroxisomal 3-oxoacyl coenzyme A thiolase with intrinsic sterol carrier and lipid transfer activity. *J Biol Chem* 269, 21277-21283.
- Semenov, M., Tamai, K., and He, X. (2005). SOST is a ligand for LRP5/LRP6 and a Wnt signaling inhibitor. *J Biol Chem* 280, 26770-26775.
- Seo, M.S., Kang, S.W., Kim, K., Baines, I.C., Lee, T.H., and Rhee, S.G. (2000). Identification of a new type of mammalian peroxiredoxin that forms an intramolecular disulfide as a reaction intermediate. *J Biol Chem* 275, 20346-20354.
- Shimozawa, N. (2007). Molecular and clinical aspects of peroxisomal diseases. *J Inherit Metab Dis* 30, 193-197.
- Siddals, K.W., Marshman, E., Westwood, M., and Gibson, J.M. (2004). Abrogation of insulin-like growth factor-I (IGF-I) and insulin action by mevalonic acid depletion: synergy between protein prenylation and receptor glycosylation pathways. *J Biol Chem* 279, 38353-38359.
- Singh, H., Usher, S., and Poulos, A. (1989). Dihydroxyacetone phosphate acyltransferase and alkyldihydroxyacetone phosphate synthase activities in rat liver subcellular fractions and human skin fibroblasts. *Arch Biochem Biophys* 268, 676-686.
- Singh, I. (1996). Mammalian peroxisomes: metabolism of oxygen and reactive oxygen species. *Ann N Y Acad Sci* 804, 612-627.
- Singh, I., Kremser, K., Ghosh, B., Singh, A.K., and Pai, S. (1996). Abnormality in translational regulation of catalase expression in disorders of peroxisomal biogenesis. *J Neurochem* 67, 2373-2378.
- Steinberg, S.J., Dodt, G., Raymond, G.V., Braverman, N.E., Moser, A.B., and Moser, H.W. (2006). Peroxisome biogenesis disorders. *Biochim Biophys Acta* 1763, 1733-1748.
- Still, K., Grabowski, P., Mackie, I., Perry, M., and Bishop, N. (2008). The peroxisome proliferator activator receptor alpha/delta agonists linoleic acid and bezafibrate upregulate osteoblast differentiation and induce periosteal bone formation in vivo. *Calcif Tissue Int* 83, 285-292.
- Subramani, S. (1993). Protein import into peroxisomes and biogenesis of the organelle. *Annu Rev Cell Biol* 9, 445-478.
- Takada, I., Kouzmenko, A.P., and Kato, S. (2009). Wnt and PPARgamma signaling in osteoblastogenesis and adipogenesis. *Nat Rev Rheumatol* 5, 442-447.
- Takishita, Y., Hiraiwa, K., and Nagayama, M. (1990). Effect of retinoic acid on proliferation and differentiation of cultured chondrocytes in terminal differentiation. *J Biochem* 107, 592-596.
- Tamai, K., Semenov, M., Kato, Y., Spokony, R., Liu, C., Katsuyama, Y., Hess, F., Saint-Jeannet, J.P., and He, X. (2000). LDL-receptor-related proteins in Wnt signal transduction. *Nature* 407, 530-535.

- Teixeira, C.C., Liu, Y., Thant, L.M., Pang, J.T., Palmer, G., and Alikhani, M. (2010). FOXO1, a novel regulator of osteoblast differentiation and skeletogenesis. *J Biol Chem*.
- Terlecky, S.R., and Fransen, M. (2000). How peroxisomes arise. *Traffic* 1, 465-473.
- Tetsu, O., and McCormick, F. (1999). Beta-catenin regulates expression of cyclin D1 in colon carcinoma cells. *Nature* 398, 422-426.
- Thoms, S., and Erdmann, R. (2005). Dynamin-related proteins and Pex11 proteins in peroxisome division and proliferation. *FEBS J* 272, 5169-5181.
- Van Veldhoven, P.P. Biochemistry and genetics of inherited disorders of peroxisomal fatty acid metabolism. *J Lipid Res*.
- Vile, G.F., Basu-Modak, S., Waltner, C., and Tyrrell, R.M. (1994). Heme oxygenase 1 mediates an adaptive response to oxidative stress in human skin fibroblasts. *Proc Natl Acad Sci U S A* 91, 2607-2610.
- Vu, T.H., Shipley, J.M., Bergers, G., Berger, J.E., Helms, J.A., Hanahan, D., Shapiro, S.D., Senior, R.M., and Werb, Z. (1998). MMP-9/gelatinase B is a key regulator of growth plate angiogenesis and apoptosis of hypertrophic chondrocytes. *Cell* 93, 411-422.
- Wanders, R.J. (2004a). Metabolic and molecular basis of peroxisomal disorders: a review. *Am J Med Genet A* 126A, 355-375.
- Wanders, R.J. (2004b). Peroxisomes, lipid metabolism, and peroxisomal disorders. *Mol Genet Metab* 83, 16-27.
- Wanders, R.J., Ferdinandusse, S., Brites, P., and Kemp, S. Peroxisomes, lipid metabolism and lipotoxicity. *Biochim Biophys Acta* 1801, 272-280.
- Wang, W., and Kirsch, T. (2002). Retinoic acid stimulates annexin-mediated growth plate chondrocyte mineralization. *J Cell Biol* 157, 1061-1069.
- Wang, X.M., Kim, H.P., Nakahira, K., Ryter, S.W., and Choi, A.M. (2009). The heme oxygenase-1/carbon monoxide pathway suppresses TLR4 signaling by regulating the interaction of TLR4 with caveolin-1. *J Immunol* 182, 3809-3818.
- Wiese, S., Gronemeyer, T., Ofman, R., Kunze, M., Grou, C.P., Almeida, J.A., Eisenacher, M., Stephan, C., Hayen, H., Schollenberger, L., *et al.* (2007). Proteomics characterization of mouse kidney peroxisomes by tandem mass spectrometry and protein correlation profiling. *Mol Cell Proteomics* 6, 2045-2057.
- Wilson, G.N., Holmes, R.G., Custer, J., Lipkowitz, J.L., Stover, J., Datta, N., and Hajra, A. (1986). Zellweger syndrome: diagnostic assays, syndrome delineation, and potential therapy. *Am J Med Genet* 24, 69-82.
- Wuthier, R.E. (1976). Lipids of matrix vesicles. *Fed Proc* 35, 117-121.
- Yan, D., Wiesmann, M., Rohan, M., Chan, V., Jefferson, A.B., Guo, L., Sakamoto, D., Caothien, R.H., Fuller, J.H., Reinhard, C., *et al.* (2001). Elevated expression of axin2 and hnk4 mRNA provides evidence that Wnt/beta -catenin signaling is activated in human colon tumors. *Proc Natl Acad Sci U S A* 98, 14973-14978.

## 9. Index of abbreviations

For abbreviations of enzyme and chemical names see page 28, 29 and 30.

APS	Ammonium persulfate
BLAST	Basic Local Alignment Search Tool
cDNA	Complementary deoxyribonucleic acid
°C	Degree Celcius
DNA	Deoxyribonucleic acid
DTT	1,4-dithio-DL-threitol
h	Hour(s)
IgG	Immunoglobulin G
min	Minute(s)
M	Molar
mg	Milligram
ml	Millilitre
µg	Microgram
µl	Microliter
µm	Micrometer
NCBI	National Centre for Biotechnology Information
ng	Nanogram
%	Percentage
PBD	Peroxisome biogenesis disorder
PBS	Phosphate-buffered saline
PBST	Phosphate-buffered saline with Tween
PCR	Polymerase chain reaction
PEX	Gene encoding a peroxin (peroxisome biogenesis protein)
PMP	Peroxisomal membrane protein
PPAR	Peroxisomal proliferator-activated receptor
PTS	Peroxisomal targeting signal
RNA	Ribonucleic acid
RT	Room temperature
s	Second(s)
NaCl	Sodium chloride
SDS-PAGE	Sodium dodecyl sulfate polyacrylamide gel electrophoresis
NaOH	Sodium hydroxide
TBS	Tris-buffered saline
v/v	Volume/volume
w/v	Weight/volume

## ***10 Acknowledgement***

First of all, I take this opportunity to express my deepest gratitude to my supervisor, Prof. Dr. Eveline Baumgart-Vogt, whose encouragement, guidance and support from the initial to the final level enabled me to develop an understanding of the subject. Her perpetual energy and enthusiasm in research have motivated all her doctoral students, including me. In addition, she is always accessible and willing to help her students with their research. As a result, my research life became smooth and rewarding for me. She will always remain the best example in my research life.

I also want to thank PD Dr. Barbara Ahlemeyer for her kind help during my doctoral study. Special warm-hearted thanks to Dr. Wieland Stöckmann for his frequent help at all times without any hesitation. I would like to express my gratitude to Dr. Dr. Klaus-Peter Valerius for his expertise and guidance in animal experiments. This thesis would never have taken shape without the help of technical staff and I am very grateful to Gabriele Thiele, Magdalene Gottwald, Elke Richter and Andrea Textor for their excellent technical assistance. In addition, I want to heartily thank those people who spent their time and shared their knowledge for helping me to complete my thesis with the best possible results: Dr. Srikanth Karnati and Vijith Vijayan. Further thanks also go to our secretaries-Erike Hellmann and Silvia Heller and all members in the Department of Anatomy and Cell Biology II for their warm and friendly nature.

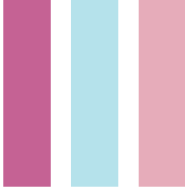
Friends have always been my strength and it is a delight to acknowledge all those who have been with me for various periods: Bo Liang, Zhongfang Wang, Lei Wang, Benpeng Gong, Jin Li, Chunguang Chen, Yu Xiao, Dilin Liu, Zhiguo Zhang, Wei Fan, Huihua Xiao, Puyan Zhao, and Xia Tian.

My further gratitude goes to my family for their unflagging love and support throughout my life and this dissertation would have simply been impossible without them. I am indebted to my father, Wujiu Qian, for his care and love. During my study, he caught a severe disease and passed away in April, 2010. Although he is no longer with us, he is forever remembered. I am sure that he shares our joy and happiness in the heaven. I cannot ask for more from my mother, Fengying Yu, as she is simply perfect. I have no suitable word that can fully describe her everlasting love to me. Additionally, I also would like to thank my brother-Guojun Qian and my older sister in law-Shujuan Li for patience, support and encouragement.

Finally, special thanks to the PhD program of the Medical Faculty of the Justus Liebig University, Giessen for giving me the opportunity to be a part of this prestigious educational unit.

**Der Lebenslauf wurde aus der elektronischen  
Version der Arbeit entfernt.**

**The curriculum vitae was removed from the  
electronic version of the paper.**



*édition scientifique*  
**VVB LAUFERSWEILER VERLAG**

VVB LAUFERSWEILER VERLAG  
STAUFENBERGRING 15  
D-35396 GIESSEN

Tel: 0641-5599888 Fax: -5599890  
redaktion@doktorverlag.de  
www.doktorverlag.de

ISBN: 978-3-8359-5698-8



9 783835 195698